

Technical Publication SJ2025-04

**LONG-TERM DYNAMICS OF SUBMERGED AQUATIC VEGETATION
ABUNDANCE AND OBSTACLES TO RECOVERY IN THE LOWER ST. JOHNS
RIVER, FLORIDA**

Riley Timbs¹

Randy Fink¹

Samantha Ehnert-Russo¹

Justin J. Solomon²

R.B. Brodie²



¹St. Johns River Water Management District

Palatka, Florida

²Florida Fish and Wildlife Conservation Commission

Fish and Wildlife Research Institute

St. Petersburg, Florida

Long-Term Dynamics of Submerged Aquatic Vegetation Abundance and Obstacles to Recovery in the Lower St. Johns River, Florida



The St. Johns River Water Management District was created in 1972 by passage of the Florida Water Resources Act, which created five regional water management districts. The St. Johns District includes all or part of 18 counties in northeast and east-central Florida. Its mission is to preserve and manage the region's water resources, focusing on core missions of water supply, flood protection, water quality and natural systems protection and improvement. In its daily operations, the district conducts research, collects data, manages land, restores and protects water above and below the ground, and preserves natural areas.

This document is published to disseminate information collected by the district in pursuit of its mission. Electronic copies are available at www.sjrwm.com/documents/technical-reports or by calling the district at the number below.

Scientific Reference Center
St. Johns River Water Management District
4049 Reid Street/P.O. Box 1429
Palatka, FL 32178-1429 (32177 for street deliveries)
386-329-4500

EXECUTIVE SUMMARY

The Lower St. Johns River (LSJR) is a subtropical, estuarine river system in northeast Florida characterized by northward flow, long hydrological residence times, dark water, and strong salinity gradients driven by tidal forcing and freshwater inflows. Submerged aquatic vegetation (SAV), primarily *Vallisneria americana*, plays a critical role in stabilizing sediments, supporting trophic interactions, and mediating nutrient cycling in the LSJR.

The geographic extent of SAV and the size of individual beds vary depending on multiple stressors, but salinity and light are key factors. Salinity concentrations over 2 can stress *V. americana* and sustained concentrations over 5 can be lethal. Light is critical for SAV, and plants that receive more light have increased growth rates, colonization depths, and resistance to stressors such as salinity and hydrogen sulfide. Generally, die-offs in the northern sections are caused by sustained or acute saltwater intrusions from droughts and tides while die-offs in the southern sections are caused by light reductions brought on by elevated water levels and decreased water clarity from rainfall and river discharge. Hurricanes contribute to die-offs throughout the entire system by spiking salinity via storm surge, limiting light with severe rainfall, and physically tearing up SAV beds with excessive winds and wave action.

The decline of SAV in the LSJR following Hurricane Irma in 2017 surpassed prior die-offs in both scale and persistence. Post-Irma recovery has been slower than previous die-offs and canopy heights remain at near study period (2002 - 2023) lows. While *V. americana* remains ubiquitous in the river mainstem and some estuarine sections show partial recovery of bed widths, freshwater bed widths are volatile and have exhibited more recent declines. Historical patterns suggest that robust bed widths are a precursor to canopy height recovery, but the slow post-Irma expansion of SAV beds has potentially delayed vertical growth and canopy height improvement.

To identify potential factors limiting post-Irma recovery we used the St. Johns River Water Management District (SJRWMD) annual SAV monitoring dataset to examine long-term trends in SAV abundance and identify periods of successful SAV recovery. We then used SJRWMD Water Quality, United States Geological Survey (USGS) continuous monitoring, and Florida Fish and Wildlife Conservation Commission (FWC) nekton data to compare water quality, hydrological conditions, and herbivore abundance between the successful recovery and the post-Irma periods.

Estuarine SAV beds in the post-Irma period were exposed to more severe salinity maximums and greater overall salinity stress than from 2002 - 2004 when the system recovered from a die-off caused by drought-induced high salinity. However, this analysis is based on monthly ambient data which may not be sufficient to capture daily salinity fluctuations from tidal forcing. Data with improved temporal resolution are critical to understanding salinity dynamics in the river.

Freshwater SAV beds recovered from 2006 - 2008 following a die-off triggered by prolonged low light conditions associated with the passage of three hurricanes in 2004. During the recovery, SAV benefited from the highest sustained light availability observed in the study period, driven by low water levels and low water color. In contrast, light availability in the post-Irma period has been approximately 40% lower. This reduction is primarily due to persistently higher water levels and the absence of the unusually low color conditions that supported recovery during 2006–2008. Other factors that affect light attenuation such as total suspended solids (TSS) and phytoplankton (Chlorophyll *a*) did not emerge as differentiating factors between the successful recovery and post-Irma periods.

Previous studies documented the negative effect of herbivory on post-Irma SAV recovery. Populations of generalist grazers (white shrimp, blue crab, gizzard shad, threadfin shad, and tilapia) remained stable over the study period. These species have little effect on the biomass of robust SAV beds but may suppress canopy heights in the extremely low-biomass beds of the post-Irma LSJR given the less favorable salinity and light environment. However, the dataset used in this report did not contain data on the two species suspected to apply the most grazing pressure, manatees (*Trichechus manatus latirostris*) and turtles (*Pseudemys sp.*). Without these data, we are unable to make conclusive comparisons of grazing pressure between the recovery and post-Irma periods.

KEY FINDINGS

- Hurricane Irma caused the most severe SAV die-off of the 2002-2023 study period and recovery of SAV abundance has been slow.
- Salinity intrusions in the estuarine sections have been more stressful to SAV during the post-Irma recovery than during the successful 2002-2004 recovery period.
- Light availability in the fresh sections during the post-Irma period is lower than during the successful 2006-2008 recovery period, driven by deeper water and higher color.
- Populations of generalist nekton species that graze on SAV have remained stable over the study period, but more data are needed to determine the biomass of SAV consumed.
- The dataset did not contain enough observations of manatees and turtles for robust analyses of these species of interest.
- Overall, water quality and hydrological conditions in the wake of Hurricane Irma are less conducive to SAV recovery than during previous periods of successful recovery after less severe die-offs.

CONTENTS

Executive Summary	iii
Key Findings	v
Contents	vi
List of Figures	viii
List of Tables	xiv
Introduction	1
Section 1 Long-Term Temporal Dynamics of SAV Abundance	4
Methods.....	4
Data Collection	4
Delineation of Spatial Zones	4
Temporal Analysis.....	5
Results	7
Section 2 Assessment of Relationships Between SAV Recovery Periods and Environmental Conditions	12
Introduction	12
Methods.....	12
Data Collection	12
Analysis	12
Results	16
Light Attenuation.....	16
Chlorophyll <i>a</i>	19
Salinity.....	30
Nutrients	39
Discussion	45
Section 3 Assessment of Relationships Between SAV Recovery Periods and Abundances of Selected Fish And Macroinvertebrates	47
Methods.....	47
Survey Design.....	47
Analysis	49
Results	52

White Shrimp, <i>Litopenaeus setiferus</i>	53
Blue Crab, <i>Callinectes sapidus</i>	56
Gizzard Shad, <i>Dorosoma cepedianum</i>	59
Threadfin Shad, <i>Dorosoma petenense</i>	62
Golden Shiner, <i>Notemigonus crysoleucas</i>	65
Rainwater Killifish, <i>Lucania parva</i>	68
Eastern Mosquitofish, <i>Gambusia holbrooki</i>	71
Bluefin Killifish, <i>Lucania goodei</i>	74
Seminole Killifish, <i>Fundulus seminolis</i>	77
Least Killifish, <i>Heterandria formosa</i>	80
Sailfin Molly, <i>Poecilia latipinna</i>	83
Pinfish, <i>Lagodon rhomboides</i>	86
Tilapia, <i>Oreochromis/Sarotherodon</i> complex.....	89
Discussion	93
Conclusions.....	94
Severity of Post-Irma Die-off.....	94
Light Availability in Freshwater Zones	94
Salinity Stress in Estuarine Zones.....	94
Limited Role Chlorophyll and Nutrients.....	95
Nekton Community Dynamics and Herbivory	95
Acknowledgements	96
Appendix A Annual Variability of SAV Abundance by Zone.....	97
Zone 1	97
Zone 2	102
Zone 3	106
Zone 4	110
Zone 5	114
Zone 6	118
References.....	123

LIST OF FIGURES

Figure 1.1 SAV sites by Zone throughout the estuarine, transitional, and freshwater regions.	6
Figure 1.2 Time series of annual mean SAV bed width, and canopy height within all Zones of the Lower St. Johns River from 2002–2023	9
Figure 1.3 Maps of annual SAV canopy height at each transect over the study period.	10
Figure 1.4 Maps of annual SAV bed width at each transect over the study period.....	11
Figure 2.1 Map of SAV Zones, associated ambient water quality sites (blue), and USGS continuous monitoring stations (yellow).	14
Figure 2.2 Changepoint analysis from 2002–2023 (left) and boxplots with results of Bonferroni-corrected Dunn’s tests (right) comparing water color among the recovery (green), background (grey), and recent (brown) periods in each Zone of the study area.	18
Figure 2.3 Changepoint analysis from 2002–2023 (left) and boxplots with results of Bonferroni-corrected Dunn’s tests (right) comparing pheophytin-corrected chlorophyll <i>a</i> among the recovery (green), background (grey), and recent (brown) periods in each Zone of the study area.	20
Figure 2.4 Changepoint analysis from 2002–2023 (left) and boxplots with results of Bonferroni-corrected Dunn’s tests (right) comparing total suspended solids among the recovery (green), background (grey), and recent (brown) periods in each Zone of the study area.	22
Figure 2.5 Changepoint analysis from 2002–2023 (left) and boxplots with results of Bonferroni-corrected Dunn’s tests (right) comparing the diffuse attenuation coefficient among the recovery (green), background (grey), and recent (brown) periods in each Zone of the study area.	24
Figure 2.6 Changepoint analysis from 2002–2023 (left) and boxplots with results of Bonferroni-corrected Dunn’s tests (right) comparing water elevation among the recovery (green), background (grey), and recent (brown) periods at the Jacksonville (Estuarine) and Buffalo Bluff (Fresh) USGS NWIS monitoring stations.	26
Figure 2.7 Changepoint analysis from 2002–2023 (left) and boxplots with results of Bonferroni-corrected Dunn’s tests (right) comparing percent surface irradiance at a fixed reference point among the recovery (green), background (grey), and recent (brown) periods in the estuarine and fresh sections of the study area.	28

Figure 2.8 Changepoint analysis from 2002–2023 (left) and boxplots with results of Bonferroni-corrected Dunn’s tests (right) comparing monthly salinity among the recovery (green), background (grey), and recent (brown) periods in each Zone of the study area. 32

Figure 2.9 Line graphs of SSI calculated with salinity values from the daily salinity model (black) and interpolated ambient data (black) in the estuarine Zones of the study area..... 35

Figure 2.10 Time series from 2002–2023 (left) and boxplots with results of one-inflated beta models (right) comparing salinity suitability index among the recovery (green), background (grey), and recent (brown) periods in Zones 1–4 of the study area. 36

Figure 2.11 Bar graphs displaying the percent of days during the recovery (green), background (grey), and recent (brown) periods spent in each stress category of the SSI. 37

Figure 2.12 Changepoint analysis from 2002–2023 (left) and boxplots with results of Bonferroni-corrected Dunn’s tests (right) comparing total phosphorus among the recovery (green), background (grey), and recent (brown) periods in each Zone of the study area. 41

Figure 2.13 Changepoint analysis from 2002–2023 (left) and boxplots with results of Bonferroni-corrected Dunn’s tests (right) comparing total nitrogen among the recovery (green), background (grey), and recent (brown) periods in each Zone of the study area.. 43

Figure 3.1 Fisheries-Independent Monitoring program 21.3 m seine sampling sites in the lower St. Johns River, September 2005 through August 2022 by Zone. Sampling Universe was post stratified into seven collection Zones (Zones 1–7) to match SJRWMD sampling water bodies. 48

Figure 3.2 Relative abundance of white shrimp collected with 21.3 m seines (water depths ≤ 1.8 m) in the lower St. Johns River. Box: average relative abundance; error bars: 95% CI. 54

Figure 3.3 Relative abundance with standard error of white shrimp collected with 21.3 m seines (water depths ≤ 1.8 m) within the estuarine, transitional, and freshwater regions of the lower St. Johns River throughout long-term temporal periods of SAV abundance (recovery, recent, and other)..... 55

Figure 3.4 Relative abundance of blue crab collected with 21.3 m seines (water depths ≤ 1.8 m) in the lower St. Johns River. Box: average relative abundance; error bars: 95% CI..... 57

Figure 3.5 Relative abundance with standard error of blue crab collected with 21.3 m seines (water depths ≤ 1.8 m) within the estuarine, transitional, and freshwater regions of the lower St. Johns River throughout long-term temporal periods of SAV abundance (recovery, recent, and other)..... 58

Figure 3.6 Relative abundance of gizzard shad collected with 21.3 m seines (water depths \leq 1.8 m) in the lower St. Johns River. Box: average relative abundance; error bars: 95% CI.	60
Figure 3.7 Relative abundance with standard error of gizzard shad collected with 21.3 m seines (water depths \leq 1.8 m) within the estuarine, transitional, and freshwater regions of the lower St. Johns River throughout long-term temporal periods of SAV abundance (recovery, recent, and other).....	61
Figure 3.8 Relative abundance of threadfin shad collected with 21.3 m seines (water depths \leq 1.8 m) in the lower St. Johns River. Box: average relative abundance; error bars: 95% CI.	63
Figure 3.9 Relative abundance with standard error of threadfin shad collected with 21.3 m seines (water depths \leq 1.8 m) within the estuarine, transitional, and freshwater regions of the lower St. Johns River throughout long-term temporal periods of SAV abundance (recovery, recent, and other).....	64
Figure 3.10 Relative abundance of golden shiner collected with 21.3 m seines (water depths \leq 1.8 m) in the lower St. Johns River. Box: average relative abundance; error bars: 95% CI.	66
Figure 3.11 Relative abundance with standard error of golden shiner collected with 21.3 m seines (water depths \leq 1.8 m) within the estuarine, transitional, and freshwater regions of the lower St. Johns River throughout long-term temporal periods of SAV abundance (recovery, recent, and other).....	67
Figure 3.12 Relative abundance of rainwater killifish collected with 21.3 m seines (water depths \leq 1.8 m) in the lower St. Johns River. Box: average relative abundance; error bars: 95% CI.	69
Figure 3.13 Relative abundance with standard error of rainwater killifish collected with 21.3 m seines (water depths \leq 1.8 m) within the estuarine, transitional, and freshwater regions of the lower St. Johns River throughout long-term temporal periods of SAV abundance (recovery, recent, and other).	70
Figure 3.14 Relative abundance of Mosquitofish collected with 21.3 m seines (water depths \leq 1.8 m) in the lower St. Johns River. Box: average relative abundance; error bars: 95% CI.	72
Figure 3.15 Relative abundance with standard error of eastern mosquitofish collected with 21.3 m seines (water depths \leq 1.8 m) within the estuarine, transitional, and freshwater regions of the lower St. Johns River throughout long-term temporal periods of SAV abundance (recovery, recent, and other).	73

Figure 3.16 Relative abundance of bluefin killifish collected with 21.3 m seines (water depths \leq 1.8 m) in the lower St. Johns River. Box: average relative abundance; error bars: 95% CI. 75

Figure 3.17 Relative abundance with standard error of bluefin killifish collected with 21.3 m seines (water depths \leq 1.8 m) within the estuarine, transitional, and freshwater regions of the lower St. Johns River throughout long-term temporal periods of SAV abundance (recovery, recent, and other) 76

Figure 3.18 Relative abundance of seminole killifish collected with 21.3 m seines (water depths \leq 1.8 m) in the lower St. Johns River. Box: average relative abundance; error bars: 95% CI. 78

Figure 3.19 Relative abundance with standard error of seminole killifish collected with 21.3 m seines (water depths \leq 1.8 m) within the estuarine, transitional, and freshwater regions of the lower St. Johns River throughout long-term temporal periods of SAV abundance (recovery, recent, and other) 79

Figure 3.20 Relative abundance of least killifish collected with 21.3 m seines (water depths \leq 1.8 m) in the lower St. Johns River. Box: average relative abundance; error bars: 95% CI. 81

Figure 3.21 Relative abundance with standard error of least killifish collected with 21.3 m seines (water depths \leq 1.8 m) within the estuarine, transitional, and freshwater regions of the lower St. Johns River throughout long-term temporal periods of SAV abundance (recovery, recent, and other). 82

Figure 3.22 Relative abundance of sailfin molly collected with 21.3 m seines (water depths \leq 1.8 m) in the lower St. Johns River. Box: average relative abundance; error bars: 95% CI. 84

Figure 3.23 Relative abundance with standard error of sailfin molly collected with 21.3 m seines (water depths \leq 1.8 m) within the estuarine, transitional, and freshwater regions of the lower St. Johns River throughout long-term temporal periods of SAV abundance (recovery, recent, and other) 85

Figure 3.24 Relative abundance of pinfish collected with 21.3 m seines (water depths \leq 1.8 m) in the lower St. Johns River. Box: average relative abundance; error bars: 95% CI. 87

Figure 3.25 Relative abundance with standard error of pinfish collected with 21.3 m seines (water depths \leq 1.8 m) within the estuarine, transitional, and freshwater regions of the lower St. Johns River throughout long-term temporal periods of SAV abundance (recovery, recent, and other). 88

Figure 3.26 Relative abundance of tilapia collected with 21.3 m seines (water depths ≤ 1.8 m) in the lower St. Johns River. Box: average relative abundance; error bars: 95% CI. 90

Figure 3.27 Relative abundance with standard error of tilapia collected with 21.3 m seines (water depths ≤ 1.8 m) within the estuarine, transitional, and freshwater regions of the lower St. Johns River throughout long-term temporal periods of SAV abundance (recovery, recent, and other) 91

Figure A.1 Time series of annual mean SAV canopy height, bed width, and percent occurrence within Zone 1 of the Lower St. Johns River from 2002–2023 99

Figure A.2 Map of SAV canopy height at each transect over the study period in Zone 1. 100

Figure A.3 Map of SAV bed width at each transect over the study period in Zone 1..... 101

Figure A.4 Time series of annual mean SAV canopy height, bed width, and percent occurrence within Zone 2 of the Lower St. Johns River from 2002–2023 103

Figure A.5 Map of SAV canopy height at each transect over the study period in Zone 2. 104

Figure A.6 Map of SAV bed width at each transect over the study period in Zone 2..... 105

Figure A.7 Time series of annual mean SAV canopy height, bed width, and percent occurrence within Zone 3 of the Lower St. Johns River from 2002–2023. 107

Figure A.8 Map of SAV canopy height at each transect over the study period in Zone 3. 108

Figure A.9 Map of SAV bed width at each transect over the study period in Zone 3..... 109

Figure A.10 Time series of annual mean SAV canopy height, bed width, and percent occurrence within Zone 4 of the Lower St. Johns River from 2002–2023 111

Figure A.11 Map of SAV canopy height at each transect over the study period in Zone 4. 112

Figure A.12 Map of SAV bed width at each transect over the study period in Zone 4..... 113

Figure A.13 Time series of annual mean SAV canopy height, bed width, and percent occurrence within Zone 5 of the Lower St. Johns River from 2002–2023 115

Figure A.14 Map of SAV canopy height at each transect over the study period in Zone 5. 116

Figure A.15 Map of SAV bed width at each transect over the study period in Zone 5..... 117

Figure A.16 Time series of annual mean SAV canopy height, bed width, and percent occurrence within Zone 6 of the Lower St. Johns River from 2002–2023 120

Figure A.17 Map of SAV canopy height at each transect over the study period in Zone 6. 121

Figure A.18 Map of SAV bed width at each transect over the study period in Zone 6..... 122

LIST OF TABLES

Table 1.1	Details of Zones used for analysis of SAV and WQ trends.....	4
Table 2.1	List of time periods determined in Section 1 to be used for groupwise comparison of water quality parameters.....	15
Table 2.2	Maximum monthly salinity of ambient samples during each monitoring period in each Zone of the study area	31
Table 2.3	Matrix of SSI values produced by combinations of salinity and exposure times and the level of stress associated with SSI values (from Chamberlain 2012)	33
Table 3.1	P values of Bonferroni-corrected Dunn’s tests of relative abundance between groups for each species of the study. P values below the alpha of 0.05 are in bold.	92

INTRODUCTION

The Lower St. Johns River (LSJR) in the northeastern part of the Florida peninsula is the final 100 mile stretch of the St. Johns River. It begins north of Lake George at the convergence of the Ocklawaha and Middle St. Johns Rivers and extends through Jacksonville where the mouth of the river opens into the Atlantic Ocean. The basin covers 2,750 square miles with a mix of land use, transitioning from agricultural land in the south to an urbanized city with one of Florida's largest ports in the north. The LSJR is a slow-flowing, dark water river that transitions from a freshwater riverine system in its upper reaches to a brackish and marine-influenced estuarine system near its mouth. This gradient is controlled by freshwater inflows from the Upper and Middle St. Johns Rivers and tidal forcing of the Atlantic Ocean. Salinity exhibits diel, seasonal, and event-driven variability creating volatile salinity regime. This spatial and temporal heterogeneity supports diverse habitats and biological assemblages (Hendrickson and Konwinski 1998).

Submerged aquatic vegetation (SAV) inhabit the shallow (< 1 m) littoral Zones of the LSJR from Lake George to the Ortega River. Although the river has supported diverse SAV beds, the freshwater species *Vallisneria americana* has been the most abundant and widespread macrophyte in the LSJR. Other species in the LSJR include: *Eleocharis spp.*, *Ceratophyllum spp.*, *Chara spp.*, *Hydrilla verticillata*, *Potamogeton spp.*, *Rupia maritima*, and *Zannichellia palustris* (Dobberfuhl 2007, Sagan 2007b, a, Morris and Dobberfuhl 2009). Due to the estuarine characteristics of the river, SAV habitat has been historically classified based on salinity regime and water residence time with an oligohaline-mesohaline (0.5–18.0) ecozone from the Ortega River to Julington Creek and two freshwater ecozones extending upstream through the remainder of the mainstem (Sagan 2007b, Magley and Joyner 2008).

SAV in the LSJR has a history of die-off and recovery. Changes in salinity, temperature, and light availability, as well as hurricanes, contribute to seasonal and interannual variation of the geographic extent, biomass, and community composition of SAV in the river (Lacoul and Freedman 2006, Bornette and Puijalon 2011, Moore 2012, Goldberg and Trent 2020). The response to varying conditions often differs between the estuarine and freshwater sections. For example, salinity intrusions caused by an extended drought from 1999–2001 resulted in a die-off in the lower, mesohaline/oligohaline, river but had no negative effect in the upper, freshwater region. By contrast, in 2004, prolonged conditions of low light resulting from depth and color increases from three major hurricanes (Charley, Frances, and Jeanne) were followed by SAV loss throughout the freshwater region, but the lower reach was less affected. In both cases SAV recovered to pre-die-off abundance within three years (Sagan 2002, Sagan 2007b, Sagan 2009). In addition to water quality and hydrologic factors, herbivory limits SAV in other Floridian ecosystems and enclosure studies have observed grazing impacts on *V. americana* in the LSJR (Harwell and Havens 2003, Adler et al. 2018, Timbs and Kolterman 2023). However, the identities and temporal patterns of abundance of the primary herbivore species are unknown.

In September 2017, Hurricane Irma produced extremely high river elevations, elevated salinity, increased water color, and wind-driven physical disturbance throughout the LSJR. This caused the most severe decline in SAV since our study dataset began in 2002 with canopy heights and bed widths falling by 80% basin wide. Post-Irma recovery has been slower than after past die-offs. Six years after the storm, SAV bed widths have moderately improved, but canopy heights have remained very low (<5 cm) (Goldberg and Trent 2020, Juárez et al. 2022, Timbs and Russo 2023). The cause of the stunted recovery has yet to be determined as there has not been a robust comparison of SAV stressors between past recoveries and the post-Irma period.

Multiple long-term datasets are available to assess SAV stressors in the LSJR. As one of its core missions, the SJRWMD maintains long-term monthly ambient water quality monitoring at many sites in the LSJR with a variety of parameters relevant to the temporal dynamics of SAV abundance. Additionally, the USGS National Water Information System (NWIS) has multiple continuous monitoring stations within the LSJR that record salinity and water elevation. The Florida Fish and Wildlife Conservation Commission's (FWC) northeast Florida Fisheries-Independent Monitoring (FIM) program was established in 2001 to assess nekton (finfish and macro-invertebrate) populations in Northeast Florida estuaries. The survey data allow for the investigation of the distribution and abundance of individual species that may be contributing to herbivory over time in the littoral areas where SAV is present in the LSJR. In addition, the survey data enable investigation of relationships between the distribution and abundance of these herbivorous species and variations in season, habitat, salinity, and water quality.

We used the SJRWMD annual SAV monitoring dataset to examine long-term trends in SAV abundance and identify times of successful SAV recovery. We then leveraged the SJRWMD Water Quality, NWIS, and FWC FIM datasets to compare water quality, hydrological conditions, and herbivore abundance between the successful recovery and the post-Irma periods and identify potential factors limiting post-Irma recovery.

This report contains three sections and an Appendix:

- Section 1: Long-term Temporal Dynamics of Submerged Aquatic Vegetation Abundance
 - Delineates spatial zones based on salinity and determines year-to-year changes in SAV canopy height, bed width, and percent occurrence within each spatial Zone. These changes are used to identify periods of SAV recovery.
- Section 2: Relationships Between Submerged Aquatic Vegetation Recovery Periods and Water Quality / Hydrological Conditions
 - Compares parameters relevant to SAV recovery among the successful recovery periods identified in Section 1, the recent post-Irma period, and the rest of the study period within each Zone.

- Section 3: Assessment of Relationships Between Submerged Aquatic Vegetation Recovery Periods and Abundances of Selected Fish and Macroinvertebrates
 - Examines trends in abundance of potential grazers and compares their abundance among the successful recovery periods identified in Section 1, the recent post-Irma period, and the rest of the study period within each spatial Zone.
- Appendix A: Annual Variability of Submerged Aquatic Vegetation Abundance by Zone
 - Year-to-year statistical analysis with detailed figures and maps of SAV abundance within each zone used to make recovery period delineations in Section 1.

SECTION 1 LONG-TERM TEMPORAL DYNAMICS OF SAV ABUNDANCE

Methods

Data Collection

The St. Johns River Water Management District performed annual summer (June – August) monitoring at approximately 200 fixed transects in the LSJR from 2002–2011 and 2015–2023 (Figure 1.1). Multiple monitoring methods were used over the study period, but all iterations used 5–10 evenly spaced 0.25 m² quadrats along a single transect placed perpendicular to shore at each site, beginning at the shoreline and extending to the deep edge of the SAV bed. To create the most consistent long-term dataset, only metrics that were recorded as, or could be derived from quadrat data for every monitoring year were used. This limited analysis to annual canopy height, bed width, and percent occurrence. These metrics are defined below:

Bed Width (m) – Linear distance in meters between the closest quadrat to shore containing SAV and the furthest quadrat from shore containing SAV at each transect. Bed width at transects with no SAV present were recorded as zero.

Canopy Height (cm) – Mean canopy height in centimeters of quadrats where SAV was present at each transect. Transects and quadrats with no SAV present were excluded.

Percent Occurrence (%) – Percent of sites within a zone where SAV was observed each year.

Delineation of Spatial Zones

Transects were grouped into Zones based on FDEP Water Body IDs (WBIDS) and SJRWMD ambient water quality sites (Figure 1.1). To identify the geographical extent that saltwater intrusion from tidal forcing affects SAV temporal patterns, smaller Zones were created in river sections where salinity at the ambient WQ site exceeded 5 at least once during the study period (Zones 1–4). Consistently low salinity WBIDS were grouped to maintain large sample size for analyses (Zones 5–6). The Zones, WBIDS, and accompanying SJRWMD ambient water quality sites are listed in Table 1.1. Doctors Lake (Zone 7) had too few observations over the study period for robust analyses and therefore was not included.

Table 1.1 Details of Zones used for analysis of SAV and WQ trends.

Zone	Salinity Range	FDEP WBIDS	Number of Transects	SJRWMD WQ Sites
1	0.2 - 33.7	2213E, 2213F	19	JAXSJR40
2	0.2 - 18.5	2213G	13	MP72
3	0.1 - 11.0	2213H	13	SJRHBP
4	0.2 - 8.5	2213I	11	20030157
5	0.2 - 3.1	2213J, 2213K	32	SJWSIL, SRP
6	0.1 - 0.8	2213L, 2213M	42	SJRCC, SJP

Temporal Analysis

Initial, basin-wide statistical models yielded large residuals after Hurricane Irma and in years with large-scale die-off events due to overestimation of bed width and canopy height. Thus, to analyze temporal variation we created separate Poisson-family generalized linear mixed models for each zone. Models predicted bed width and canopy height as a function of year with site as a random factor using the lme4 package (Bates et al. 2015) in the R statistical software (R Development Core Team). Individual year to year comparisons were made by performing post-hoc Bonferroni-corrected Dunn's tests with the emmeans package (Lenth 2023). Statistical significance was determined using an alpha level of 0.05. Annual means are presented as the mean \pm standard error.

Interannual changes in SAV were analyzed to identify periods of successful recovery. Water quality and herbivore abundance were then compared between these recovery periods and the post-Irma period in Sections 2 and 3. Recovery periods were defined as at least two consecutive years of increasing canopy height and/or bed width, with no declines in either metric. Zone-by-Zone analysis of SAV temporal patterns and identification of SAV recovery periods are presented in Appendix A.

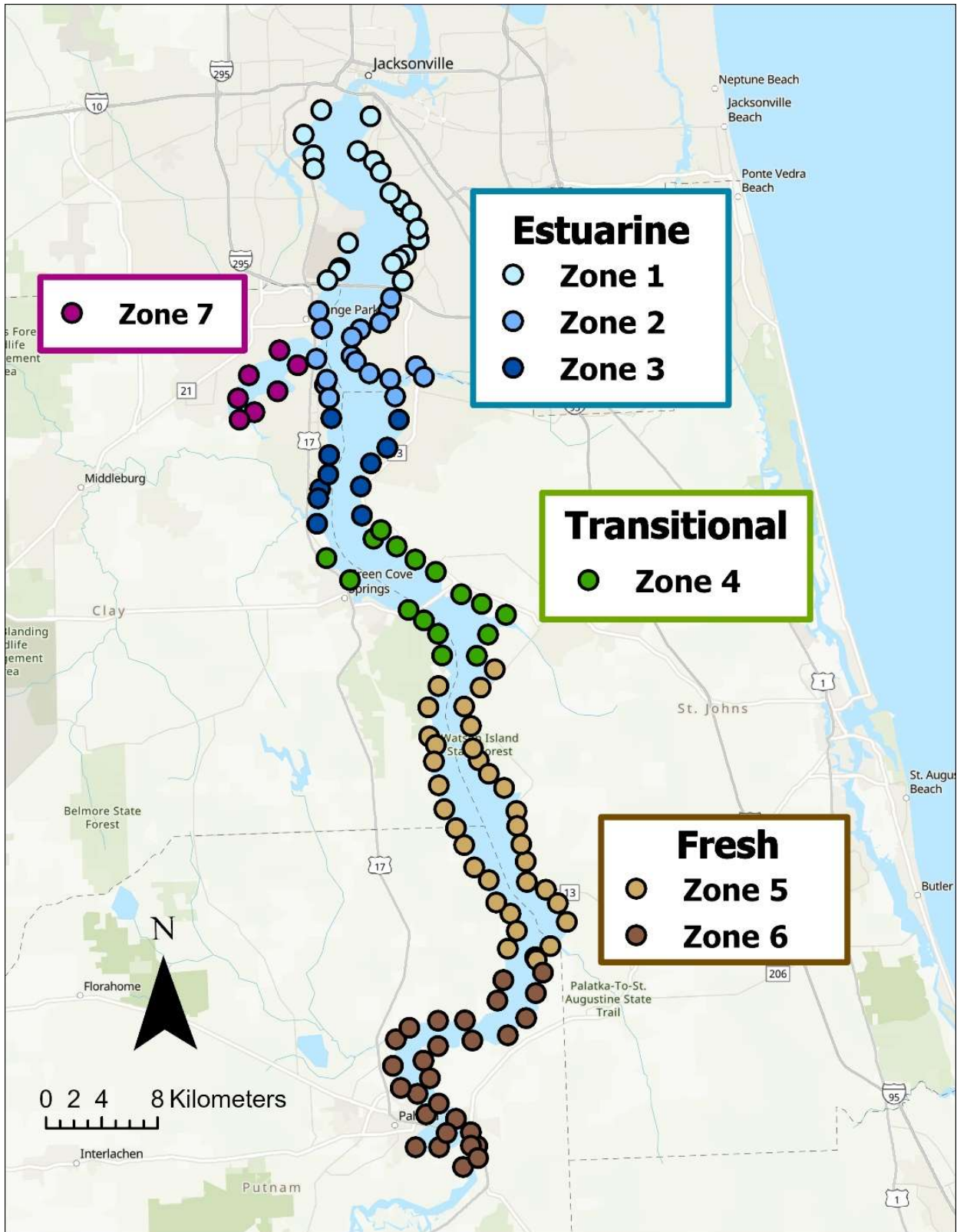


Figure 1.1 SAV sites by Zone throughout the estuarine, transitional, and freshwater regions.

Results

Zones 1, 2, and 3, the most estuarine parts of the Lower St. Johns River that sustain SAV, underwent a common recovery phase between 2002 and 2004 (Figure 1.2) following a die-off caused by the severe drought from 1998-2001 (Verdi et al. 2006, Sagan 2007b). During this period, canopy height and bed width increased in all three sections. Throughout the rest of the study period, Zones 2 and 3 demonstrated similar trends in bed width and canopy height that departed from Zone 1. Zones 2 and 3 had longer mean bed widths, more variable canopy heights, and had less pronounced decline from 2006 to 2009 and from 2016 to 2017. Zones 1 and 2 are considered part of the oligohaline-mesohaline ecozone in previous studies of the LSJR while Zone 3, the section of the river from Black Creek to Julington Creek, is not (Sagan 2007b, Magley and Joyner 2008). However, the temporal pattern of abundance in Zone 3 indicates that the SAV in this Zone varies in response to the same factors as the SAV Zones 1 and 2. Following Hurricane Irma in 2017, Zones 2 and 3 experienced a greater proportional loss in bed width compared to 1, which was already nearing minimal values. Subsequently, 2 and 3 successfully restored bed widths to pre-Irma levels between 2018 and 2023, whereas bed widths in Zone 1 did not increase. Across all three sections, canopy heights remained consistently low in the post-Irma period. There were indications of decline in all three sections from 2016 to 2017, a year preceding the landfall of Hurricane Irma, indicating potential salinity intrusion prior to the storm.

Zone 4 is in the transitional Zone between the estuarine and freshwater regions of the mainstem. As a result, the temporal pattern of bed width and canopy height in Zone 4 diverge from those in either region but were most similar to Zone 3. Similar to Zones 1-3, canopy height in Zone 4 increased between 2002 and 2004, but there was no change in bed width. Zone 4 also had consecutive increases in canopy height from 2009–2011 when no other Zone did. Thus, we designated 2009-2011 as the recovery period for SAV in this Zone. Zone 4 canopy height also did not increase during the 2006–2008 freshwater recovery. There are sparse data from 2015–2023 for the freshwater sections, but the Zone 4 patterns appear to more closely reflect these sections than the estuarine sections, given the delay of the decline to post-Irma and the lack of bed width recovery.

The freshwater Zones 5 and 6 have similar trends in bed width and, to a lesser extent, canopy height from 2002–2011. Both exhibited consecutive increases in canopy height from 2006–2008 and an increase in bed width from 2006–2007. Thus, we designated the years 2006-2008 as the recovery period for these Zones. There are sparse data for comparison after 2011 but based on the similarities in the first half of the study period, it is likely that Zone 6 exhibited similar post-Irma decline to Zones 5 and 4.

SAV varied differently over time depending on salinity regime, consistent with past studies (Dobberfuhl 2007, Sagan 2007a, b). SAV in the estuarine region expanded from 2002–2004, a time when SAV biomass in the fresh region was either unchanged or in decline. The inverse occurred during 2006–2008 when the freshwater SAV recovered, while SAV in the

estuarine section stagnated or declined. There has been a decline in SAV throughout the LSJR since Hurricane Irma in 2017. While both bed width and canopy height have exhibited considerable interannual variability, bed widths were approximately twice as large at the beginning of the recovery period than at the beginning of the recent post-Irma period in Zones 2–5, indicating that the 2017 die-off was more severe than any previously observed in the study period.

Long-Term Temporal Dynamics of SAV Abundance

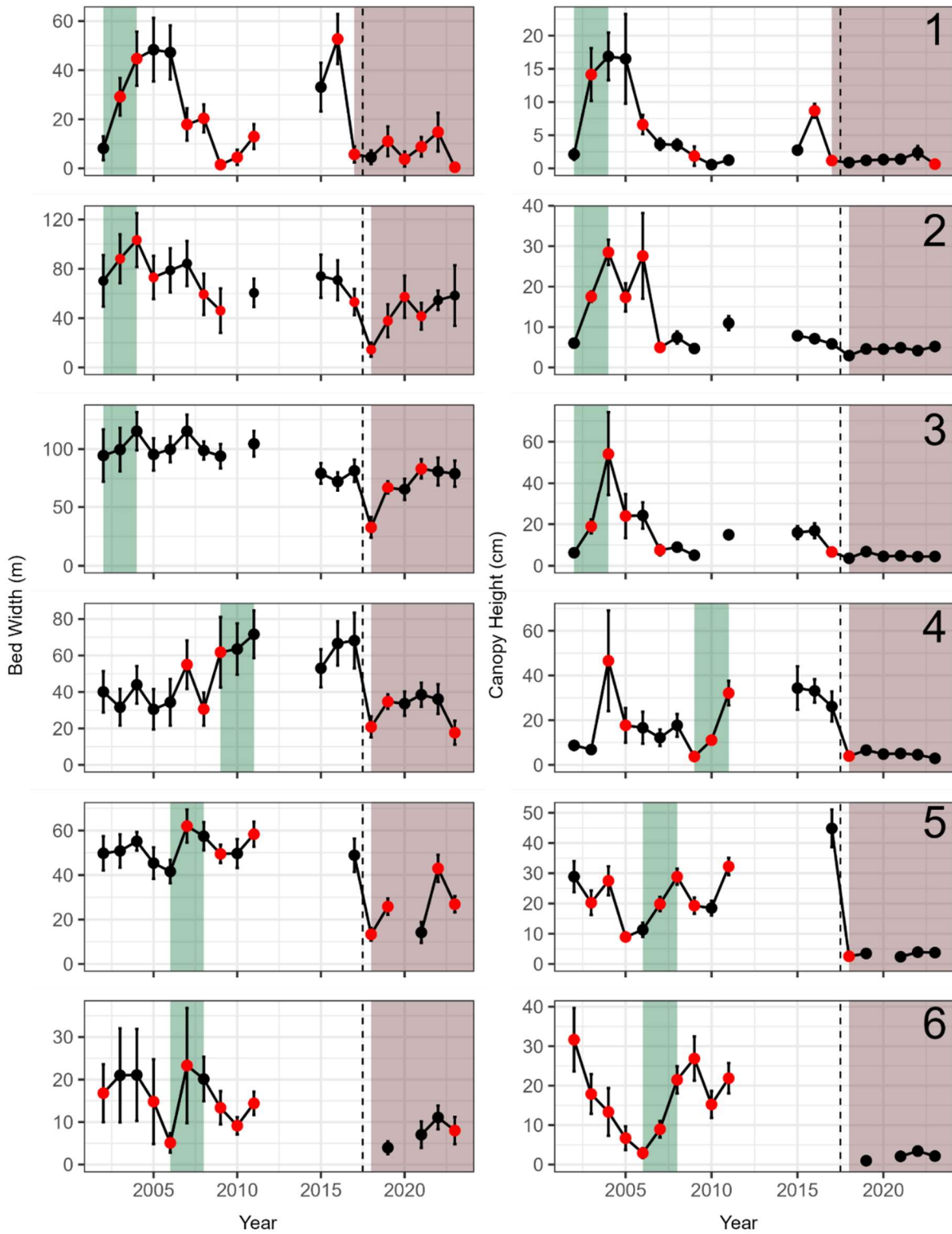


Figure 1.2 Time series of annual mean SAV bed width, and canopy height within all Zones of the Lower St. Johns River from 2002–2023. Error bars depict the standard error, and red points indicate a statistically significant change ($p < 0.05$) from the previous year. The background colors represent the selected periods for groupwise comparisons (Recovery Period = green, Recent Period = brown).

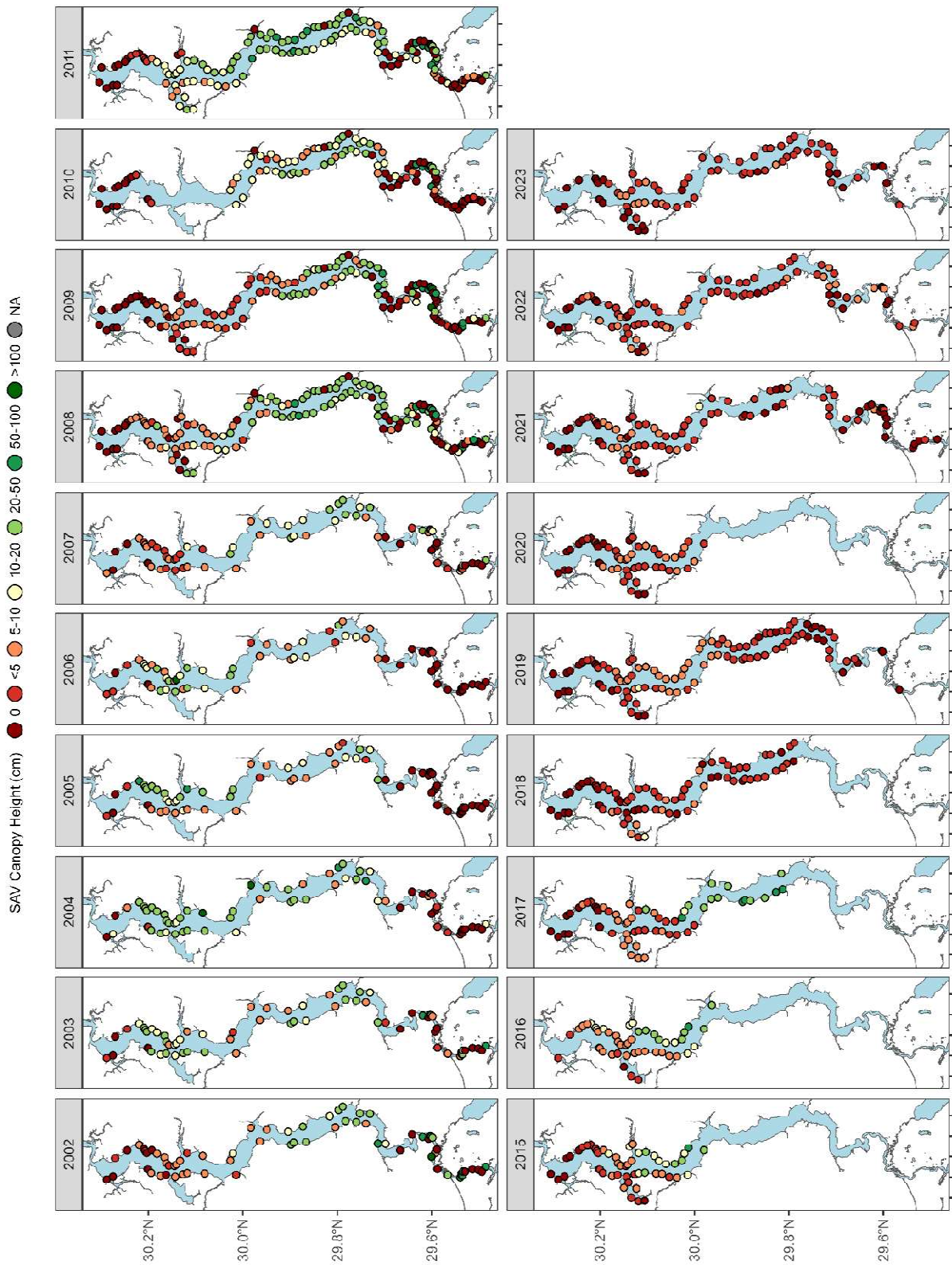


Figure 1.3 Maps of annual SAV canopy height at each transect over the study period.

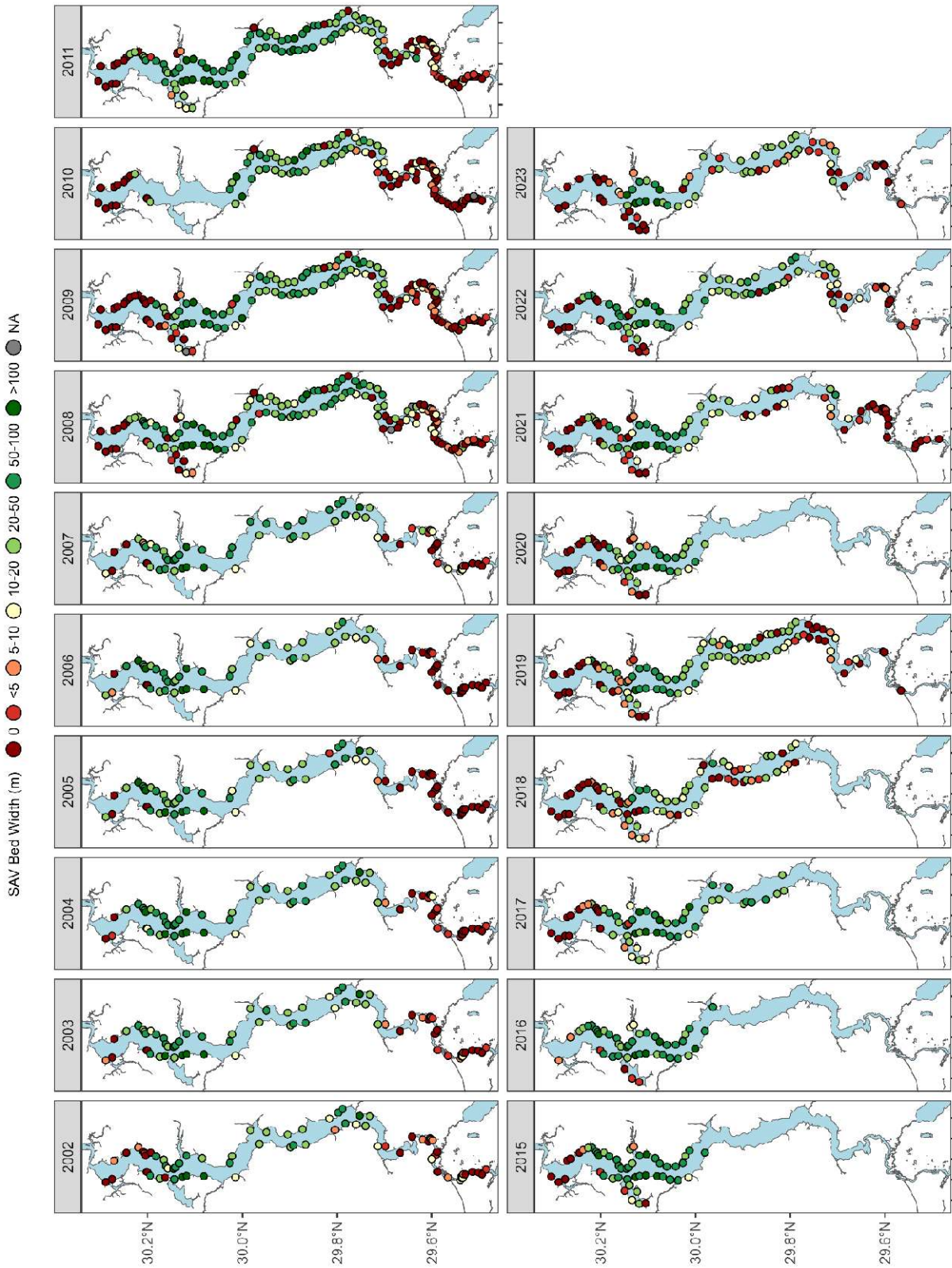


Figure 1.4 Maps of annual SAV bed width at each transect over the study period.

SECTION 2 ASSESSMENT OF RELATIONSHIPS BETWEEN SAV RECOVERY PERIODS AND ENVIRONMENTAL CONDITIONS

Introduction

In the year following Irma, water color remained exceptionally high throughout the Lower St. Johns River (LSJR), approximately double the pre-Irma mean (Unpublished SJRWMD Data), reducing light availability and contributing to the most severe SAV die-off of the study period (Section 1). Several years after Hurricane Irma, water quality conditions have returned to ranges comparable to pre-storm levels. However, SAV has not exhibited the regrowth observed after previous disturbances. Given the persistent lack of regrowth, we compared recent water conditions not only to long-term background levels but also to periods of successful SAV recovery as identified in Section 1. This approach allows for a more targeted assessment of specific water quality and hydrological parameters, including light availability, salinity, and nutrient dynamics, that may be impeding SAV restoration in the LSJR.

Methods

Data Collection

Salinity, water color, total suspended solids (TSS), Chlorophyll *a*, total nitrogen (TN), and total phosphorus (TP) data from January 2002 to December 2023 at 8 SJRWMD monthly and bimonthly ambient water quality sites were used for analysis. Samples flagged with lab codes indicating potential quality concerns were excluded from analysis. Within each Zone, we calculated the monthly median of each parameter. In Zones 5 and 6 these medians were calculated from two stations to provide a spatially representative value. Figure 2.1 shows the stations and sections used in analysis.

Daily water elevation values from the Jacksonville (USGS 02246500) and Buffalo Bluff (USGS 02244040) USGS NWIS monitoring stations were downloaded using the DataRetrieval package in R statistical software (R Development Core Team 2010, De Cicco et al. 2023). Data gaps for the Jacksonville station were filled with predictions from a linear model based on the Buffalo Bluff gage height, month, and year ($R^2 = 0.920$). The Jacksonville and Buffalo Bluff stations are at the approximate downstream and upstream limits of SAV colonization in the LSJR, respectively.

Analysis

To visualize temporal patterns in each parameter we performed nonparametric changepoint analysis on the monthly data with the `cpt.np` function from the `changepoint.np` package using the PELT method (Haynes 2017). Minimum segment length was set to 12 months to avoid fitting intra-annual variation. To meet the requirements of the test, a monthly time series with no missing values was created by imputing NA values with the study period median of the

missing month. When multiple data points were present for a month, the median of the available data was calculated. The COVID-19 pandemic prevented water quality sampling from July 2020 to December 2020 so the datapoints for this time are all imputations. Change point analysis of the daily USGS elevation data used a minimum segment length of 365 days.

The change point analyses for each parameter are displayed on the left side of the corresponding figure. The grey lines depict the raw and imputed data. Superimposed on these lines are horizontal black segments, which represent the mean value within the intervals defined by detected change points. These change points mark periods where the mean shifted, suggesting possible ecological changes. The green and brown shaded areas denote the recovery and recent periods identified in Section 1, respectively. The unshaded area represents the background (other) period.

To determine differences in potential stressors between times of successful SAV recovery and the recent scenario, monthly median water quality data for each Zone were grouped into three monitoring periods based on the temporal dynamics of SAV bed width, canopy height, and percent occurrence. Periods begin the month after a complete monitoring season (September) and end in the final month of a following season (July). The details and rationale of these selections can be found in Section 1. Doctors Lake (Zone 7) had too few SAV observations over the study period for identification of recovery periods so was not included.

The three periods are generally defined below:

- Recovery period – Samples before and during annual summer SAV monitoring when canopy height, bed width, and/or percent occurrence increased.
- Recent period – Samples after 2016–2018 die-off.
- Background (other) period – All other samples during the 2001–2023 study period.

Data were often non-normally distributed, and monitoring period sample sizes were not equal, so Kruskal-Wallis and Bonferroni-corrected pairwise Dunn's tests were used to detect among-group differences within each section. Alpha was set at 0.05. The salinity suitability index data (SSI) ranged from 0-1 and were one-inflated so we used one-inflated beta models with the *gamlss* package instead of Kruskal-Wallis tests (Rigby and Stasinopoulos 2005). Imputed data were not used for any groupwise analyses. No data were collected from July 2020 to December 2020, eliminating all fall water quality samples between the 2020 and 2021 SAV monitoring seasons. To avoid bias, the rest of the water quality samples between the 2020 and 2021 monitoring seasons were removed (January 2021 – August 2021).

Box plots on the right side of each figure present these comparisons across the predefined periods (Recovery, Other, and Recent). Each plot displays the raw data within each period as points and median and interquartile range as the boxes. Statistical significance between periods is indicated with asterisks (* = $p < 0.05$, ** = $p < 0.01$, *** = $p < 0.001$, ns = $p > 0.05$).

Assessment of Relationships Between SAV Recovery Periods and Environmental Conditions

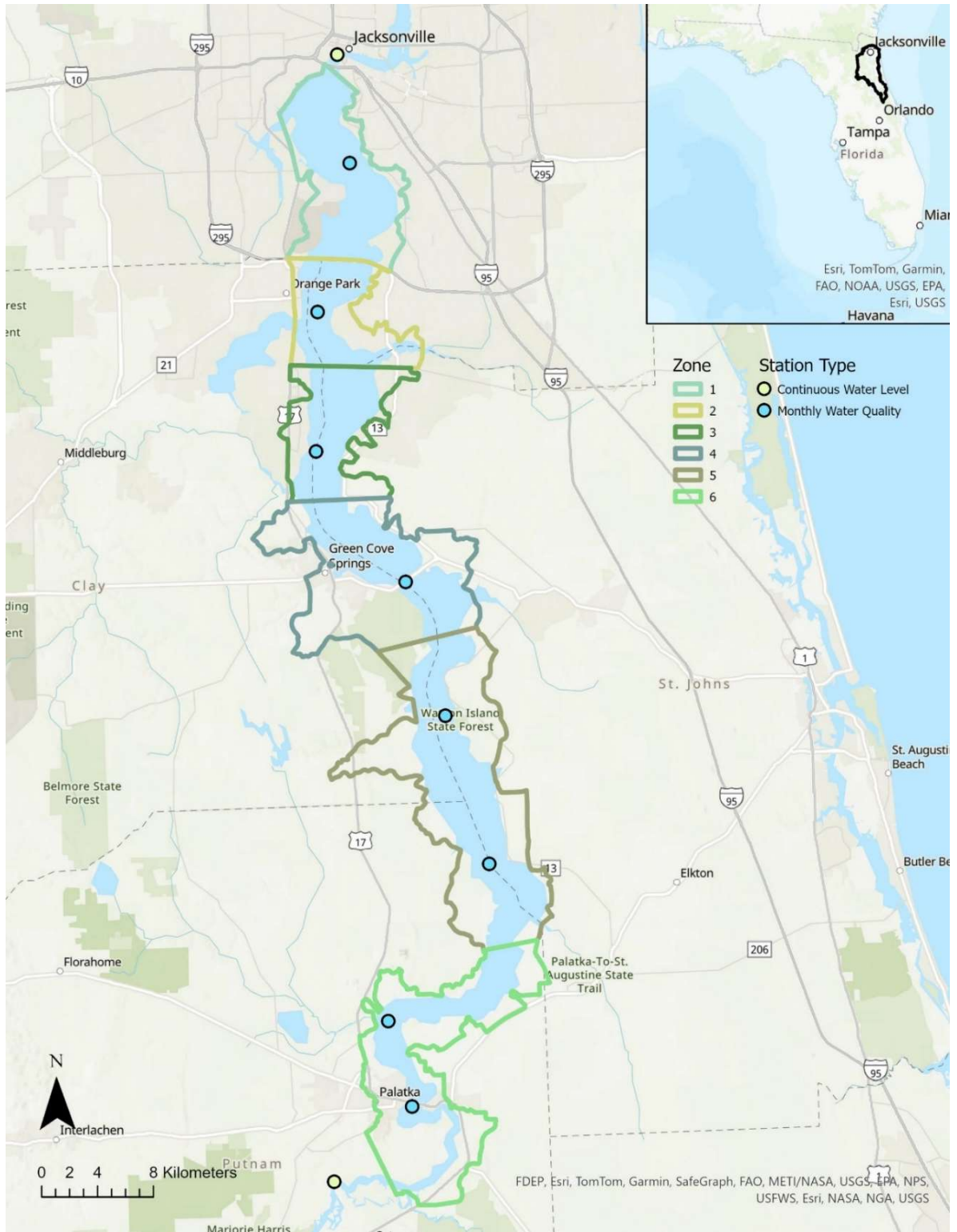


Figure 2.1 Map of SAV Zones, associated ambient water quality sites (blue), and USGS continuous monitoring stations (yellow).

Assessment of Relationships Between SAV Recovery Periods and Environmental Conditions

Table 2.1: List of time periods determined in Section 1 to be used for groupwise comparison of water quality parameters.

Zone	Recovery Period	Background Period	Recent Period
1	9/2002 – 8/2004	9/2001 – 8/2002, 9/2004 – 8/2017	9/2017 – 8/2020, 9/2021 – 8/2023
2	9/2002 – 8/2004	9/2001 – 8/2002, 9/2004 – 8/2018	9/2018 – 8/2020, 9/2021 – 8/2023
3	9/2002 – 8/2004	9/2001 – 8/2002, 9/2004 – 8/2018	9/2018 – 8/2020, 9/2021 – 8/2023
4	9/2009 – 8/2011	9/2001 – 8/2009, 9/2011 – 8/2018	9/2018 – 8/2020, 9/2021 – 8/2023
5	9/2006 – 8/2008	9/2001 – 8/2006, 9/2008 – 8/2018	9/2018 – 8/2020, 9/2021 – 8/2023
6	9/2006 – 8/2008	9/2001 – 8/2006, 9/2008 – 8/2018	9/2018 – 8/2020, 9/2021 – 8/2023

Results

Light Attenuation

Background

Light availability is a fundamental factor affecting SAV growth, reproduction, and survival (Dennison et al. 1993, Kirk 2010). Light limitation sets the maximum depth at which SAV can grow, and attenuation of light in overlying water varies with colored dissolved organic matter (i.e., color), suspended particles, and phytoplankton (Zimmerman 2003, Gallegos 2005). Reduced light availability has been linked to SAV declines worldwide (Orth et al. 2006).

SAV growth typically occurs when bottom light availability is 10–35% of surface irradiance, though the requirement may vary by species and environmental stressors such as salinity (Kemp et al. 2004). In the LSJR, colored dissolved organic matter (CDOM, assessed as water color) is the most dominant factor affecting light absorption, particularly upstream, while nutrient inputs can cause algal blooms that further absorb light (Gallegos 2005). During dry periods lower color, caused by reduced runoff from areas rich in organic matter, allows for greater light penetration, which can support SAV growth. In the mesohaline and oligohaline areas of the LSJR, SAV requires nearly 50% more light to maintain similar growth as in fresh Zones, underscoring the compound stress of salinity and light limitation (French and Moore 2003, Dobberfuhl 2007).

The amount of light available for SAV on the benthos is primarily determined by two factors: water depth (Z) and the diffuse attenuation coefficient (K_d), following the Lambert-Beer law:

$$\% \text{ Surface Irradiance} = 100 \times e^{-K_d \times Z}$$

As water depth increases, light must travel a greater distance through the water column, increasing the amount that gets absorbed or scattered before reaching the bottom. As such, light availability decreases exponentially as water depth increases. K_d accounts for the effects of water clarity on the amount of light absorbed and scattered by the water column, including absorption by color and scattering by suspended inorganic and organic matter such as sediments and algae. Higher K_d values indicate greater light attenuation and reduced light penetration.

This section examines the factors contributing to light attenuation in each Zone: colored dissolved matter (water color), limnetic algae (Chlorophyll a), suspended solids (TSS), the diffuse attenuation coefficient (K_d), and water depth. Then, they are compiled into a single metric (Percent Irradiance at Reference Point) that estimates light available to SAV at a fixed reference point in the estuarine and fresh sections of the river.

Water Color

Background

The LSJR is a blackwater system. As such, the intrinsic color of the water as determined by dissolved matter is a dominant factor influencing the light available for photosynthesis by submerged macrophytes. The expansive floodplain wetlands of the Middle and Upper St. Johns River Basin yield tannin-rich, high color runoff that darkens the river as rainfall and water elevation increase. Variation in rainfall patterns often cause severe (3 to 4-fold) changes in color that affect photic conditions for months or years at a time (Gallegos 2005).

Results

In Zone 1 mean color did not vary between the recovery and recent periods ($p = 1.00$) but both periods were greater than the background period ($p_{\text{Recovery}} = 0.035$, $p_{\text{Recent}} = 0.039$). The difference between the recent period and background period is largely driven by the high color from Hurricane Irma in September 2017, coinciding with the start of the recent period for this Zone (Figure 2.2). This difference is not observed if the recent period window is changed to September 2018 ($p = 0.803$). Water color did not vary among any periods in Zones 2 and 3, the other two estuarine sections ($p_2 = 0.628$, $p_3 = 0.782$).

The only among-group difference in the transitional Zone 4 was between the recovery period mean of 102.0 ± 18.2 PCU, and the background period mean of 131.1 ± 7.4 PCU ($p = 0.030$). Although the overall recovery period mean was not different than the recent period mean, the changepoint detected an approximately 75% decrease in color during the first year of the recovery to a study-period-low that was sustained through the remainder of the period (Figure 2.2).

The largest among-group difference in mean color occurred in the freshwater Zones. The recovery period mean in Zone 5 was 64.6 ± 6.5 PCU, approximately half the background period (141.4 ± 7.3 PCU, $p < 0.001$) and recent period (121.2 ± 8.6 PCU, $p < 0.001$) means. The recent and background period means were not different ($p = 1.00$). A near identical pattern also occurs in Zone 6 with the recovery mean roughly half of the background ($p < 0.001$) and the recent means ($p < 0.001$).

The pattern of temporal variation in color was consistent across all Zones and the differences among groups were largely due to differences in recovery timing between the fresh and estuarine sections. Color during the recent and background periods of the freshwater Zones was roughly twice as high as during the recovery period, and the estuarine Zones exhibited no differences between the recovery and recent periods. Results could be affected by a change in collection methods. The SJRWMD laboratory adopted a more precise color measurement method in 2010, prior to which color was recorded in increments of 5 PCU for observations below 100 PCU, and 25 PCU for those above 100 PCU.

Assessment of Relationships Between SAV Recovery Periods and Environmental Conditions

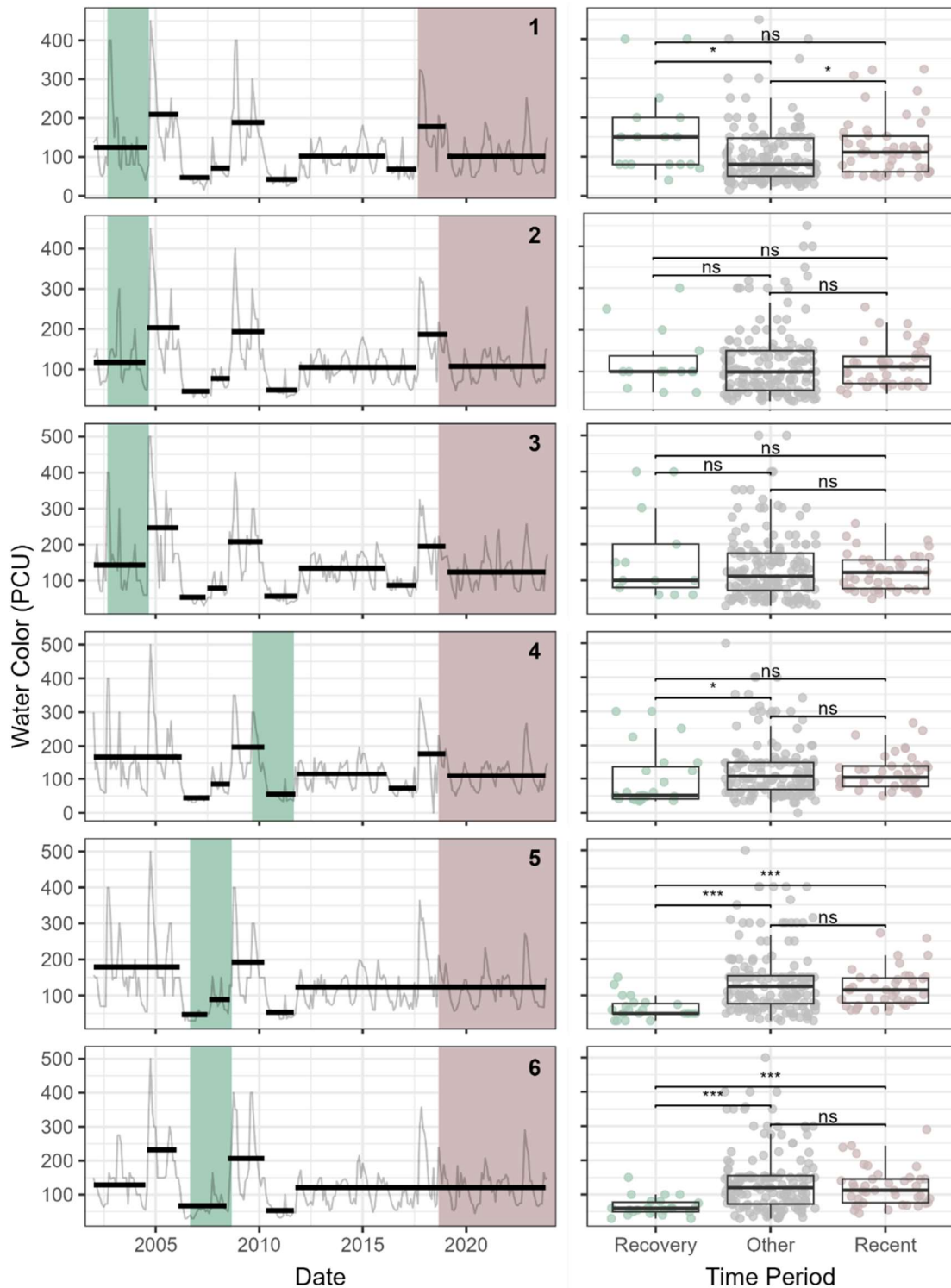


Figure 2.2 Changepoint analysis from 2002–2023 (left) and boxplots with results of Bonferroni-corrected Dunn’s tests (right) comparing water color among the recovery (green), background (grey), and recent (brown) periods in each Zone of the study area. Statistical significance between monitoring periods is indicated with asterisks (* = $p < 0.05$, ** = $p < 0.01$, *** = $p < 0.001$, ns = $p > 0.05$).

Chlorophyll *a*

Background

Pheophytin-corrected chlorophyll *a* (measured in $\mu\text{g/L}$) is a measurement of the concentration of living algae in the water column. Shading of submerged macrophytes by elevated concentrations of limnetic algae is commonly implicated in SAV declines worldwide (Dennison et al. 1993, Orth et al. 2006). In the intrinsically dark water of the LSJR, limnetic algae do not receive enough light to grow as dense as in other systems and contributes less to light attenuation than factors such as water color (Gallegos 2005). However, severe, prolonged blooms can be driven by wind and waves to form dense mats on the surface of littoral waters above SAV beds, blocking light. Additionally, algal mats can contribute to water column anoxia during decomposition which increases SAV vulnerability to stressors such as sediment sulfide and elevated salinities (Koch et al. 2007, Magley and Joyner 2008).

Results

Of the three estuarine Zones, Zone 1 was the only one where chlorophyll *a* varied among periods (Figure 2.3). Mean chlorophyll *a* during both the recovery period and the recent period were lower than during the background period ($p_{\text{Recovery}} = 0.004$, $p_{\text{Recent}} = 0.005$) though they were not different from each other ($p = 0.900$). Zone 4 did not vary among monitoring periods ($p = 0.179$).

The only difference among monitoring periods in the freshwater Zone 5 was the mean chlorophyll *a* during the recent period of $27.0 \pm 3.1 \mu\text{g/L}$ was higher than the background period mean of $17.8 \pm 1.1 \mu\text{g/L}$ ($p = 0.008$). However, the recent period was not different than the recovery period ($p = 0.459$). The Zone 6 mean during the recovery period of $28.9 \pm 3.8 \mu\text{g/L}$ was also greater than the background mean of $19.7 \pm 1.1 \mu\text{g/L}$ ($p = 0.019$) but was not different than the recent period ($p = 0.250$).

Chlorophyll *a* was highly variable from month to month and generally increased moving upstream from Zone 1 with mean annual concentrations in the estuarine Zones from 5–10 $\mu\text{g/L}$ and 15–30 $\mu\text{g/L}$ in the freshwater Zones. Among group differences in mean chlorophyll *a* were rare and the recovery and recent period means did not differ from each other in any Zone of the river (Figure 2.3).

Assessment of Relationships Between SAV Recovery Periods and Environmental Conditions

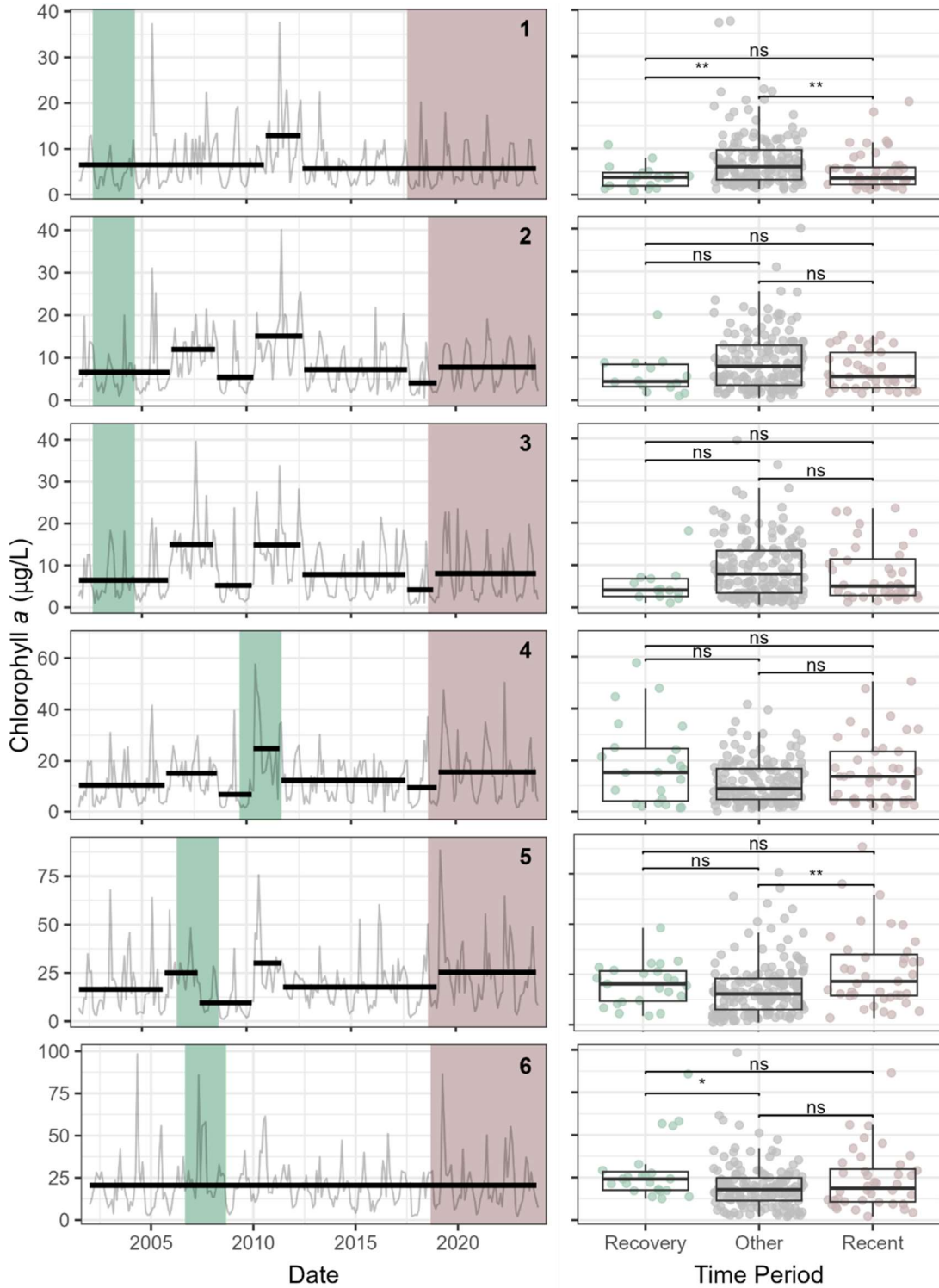


Figure 2.3 Changepoint analysis from 2002–2023 (left) and boxplots with results of Bonferroni-corrected Dunn’s tests (right) comparing pheophytin-corrected chlorophyll *a* among the recovery (green), background (grey), and recent (brown) periods in each Zone of the study area. Statistical significance between monitoring periods is indicated with asterisks (* = $p < 0.05$, ** = $p < 0.01$, *** = $p < 0.001$, ns = $p > 0.05$).

Total Suspended Solids

Background

Total suspended solids (TSS) consist of both organic and inorganic undissolved particles, including detritus, silt, and algae, which absorb downwelling light as well as increase the effective path length by scattering light, thereby reducing its penetration through the water column. High TSS can also indicate risk of SAV burial by sediment (Moore et al. 1997).

In the LSJR, TSS concentrations are often elevated due to nutrient runoff, urban stormwater, and tidal resuspension of sediments. The river receives substantial input from agriculture, which increases nutrient loading and contributes to high concentrations of organic and inorganic particles, especially during periods of high river flow or following storm events when physical forces resuspend river sediments (Dobberfuhl 2007, Magley and Joyner 2008). These conditions may exacerbate the challenges for SAV, which rely on sufficient light for photosynthesis and growth.

Results

There was only one difference among monitoring periods in the three estuarine sections (Figure 2.4). The Zone 1 recent period mean was 11.6 ± 1.0 mg/L, 35% lower than the background period mean of 15.6 ± 0.8 mg/L ($p = 0.015$).

In Zone 4, mean TSS during the recent period was 9.3 ± 0.7 mg/L. This was lower than background mean of 11.7 ± 0.4 mg/L ($p = 0.027$) and 40% lower than the recovery mean of 14.8 ± 1.3 mg/L ($p < 0.001$). The background and recovery means did not differ ($p = 0.060$).

Among group variation was inconsistent between the two freshwater regions. In Zone 5, the recent period mean was higher than the background period (10.8 ± 0.6 mg/L vs 9.4 ± 0.3 mg/L, $p = 0.040$) but not different than the recovery period ($p = 1.000$). There was a different pattern in Zone 6, where the recovery period mean of 10.7 ± 0.6 mg/L was greater than both the recent period mean of 7.9 ± 0.6 mg/L ($p = 0.003$) and the background period mean of 8.6 ± 0.3 mg/L ($p = 0.006$).

Among-group variation in TSS was inconsistent across and within the estuarine, transitional, and freshwater regions. TSS alone does not appear to be a definitive factor dividing the recovery, recent, and background periods.

Assessment of Relationships Between SAV Recovery Periods and Environmental Conditions

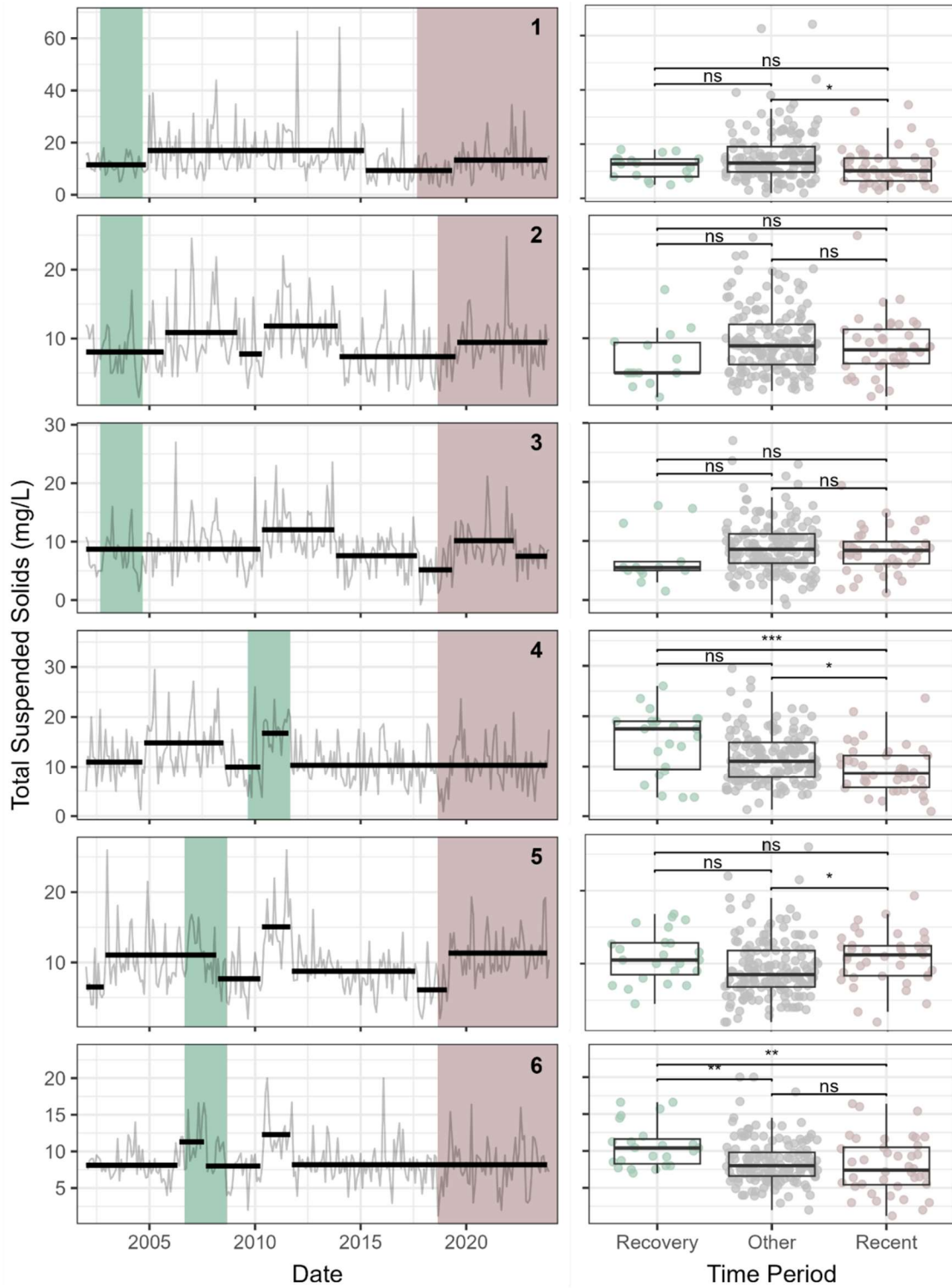


Figure 2.4 Changepoint analysis from 2002–2023 (left) and boxplots with results of Bonferroni-corrected Dunn’s tests (right) comparing total suspended solids among the recovery (green), background (grey), and recent (brown) periods in each Zone of the study area. Statistical significance between monitoring periods is indicated with asterisks (* = $p < 0.05$, ** = $p < 0.01$, *** = $p < 0.001$, ns = $p > 0.05$).

Diffuse Attenuation Coefficient (K_d)

Background

Water color, TSS, and chlorophyll *a* each individually influence light attenuation in the water column. The diffuse attenuation coefficient (K_d) integrates these parameters to provide a comprehensive measure of the reduction in light intensity with depth in the water column. This study uses a formula specifically developed for the LSJR by Gallegos 2005 to calculate K_d based on date, time, water color, TSS, chlorophyll *a*, and salinity for the study period.

Results

K_d did not vary among any groups in the estuarine or transitional Zones ($p_1 = 0.502$, $p_2 = 0.845$, $p_3 = 0.638$, $p_4 = 0.208$) (Figure 2.5).

Recovery period mean K_d in Zone 5 was $1.97 \pm 0.06 \text{ m}^{-1}$, approximately 25% lower than the background period mean of $2.48 \pm 0.35 \text{ m}^{-1}$ ($p < 0.001$) and recovery period mean of $2.50 \pm 0.08 \text{ m}^{-1}$ ($p < 0.001$). There was a similar pattern in Zone 6, though the recovery period mean was only lower than the background period mean ($p = 0.020$) and not the recent period mean ($p = 0.136$).

K_d only differed among monitoring periods in the fresh sections of the river where K_d was low during the recovery period, indicating that light availability was high during this time.

Assessment of Relationships Between SAV Recovery Periods and Environmental Conditions

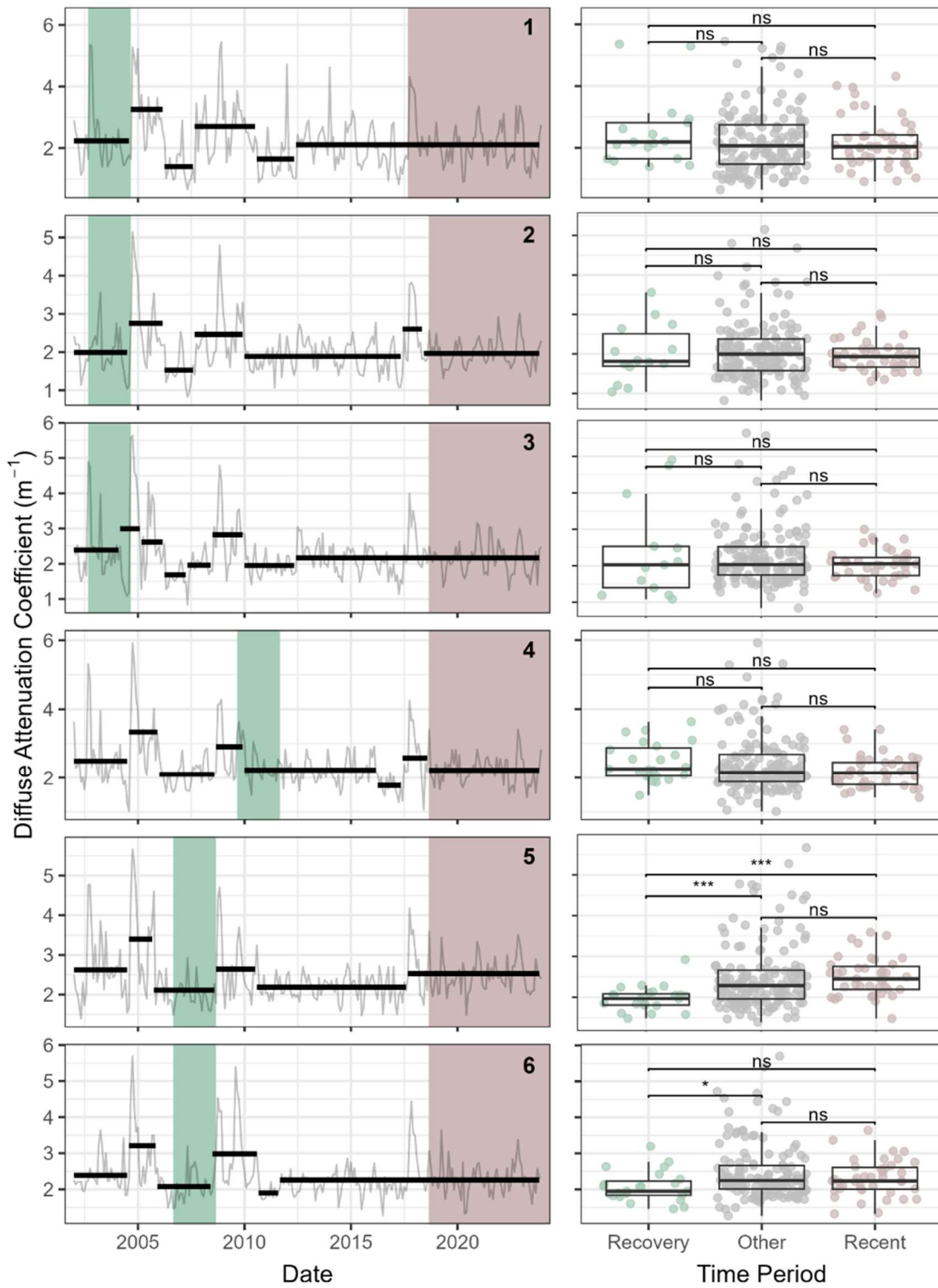


Figure 2.5 Changepoint analysis from 2002–2023 (left) and boxplots with results of Bonferroni-corrected Dunn’s tests (right) comparing the diffuse attenuation coefficient among the recovery (green), background (grey), and recent (brown) periods in each Zone of the study area. Statistical significance between monitoring periods is indicated with asterisks (* = $p < 0.05$, ** = $p < 0.01$, *** = $p < 0.001$, ns = $p > 0.05$).

Water Elevation

Background

Light attenuation increases exponentially with water depth and the naturally colored water of the LSJR limits SAV beds to littoral Zones with depths less than 1 meter, shallower than many SAV habitats (Gallegos 2005, Orth et al. 2006, Sagan 2009). Thus, small changes in water depth have disproportionately large influence on light availability. Increased water elevations may also enable large aquatic herbivores such as manatees to forage greater areas of SAV beds for longer periods of time (Smith 1993, Takoukam et al. 2021). This section includes daily water elevation data from the Jacksonville and Buffalo Bluff USGS continuous monitoring stations. The Jacksonville and Buffalo Bluff stations are roughly located at the downstream (estuarine) and upstream (fresh) limits of SAV colonization in the LSJR, respectively.

Results

Water elevations generally increased over the study period at both gages and were consistently higher during the recent period than the recovery period (Figure 2.6). The estuarine recovery period mean was 0.09 ± 0.01 m, 6 cm lower than the background period ($p < 0.001$) and 14 cm lower than the recent period ($p < 0.001$). Additionally, 85% of recent period values were greater than the recovery period mean, reflecting consistently higher water levels.

Similarly, mean water elevation in the fresh section during recovery was 8 cm lower than the background mean ($p < 0.001$) and 18 cm lower than the recent period ($p < 0.001$).

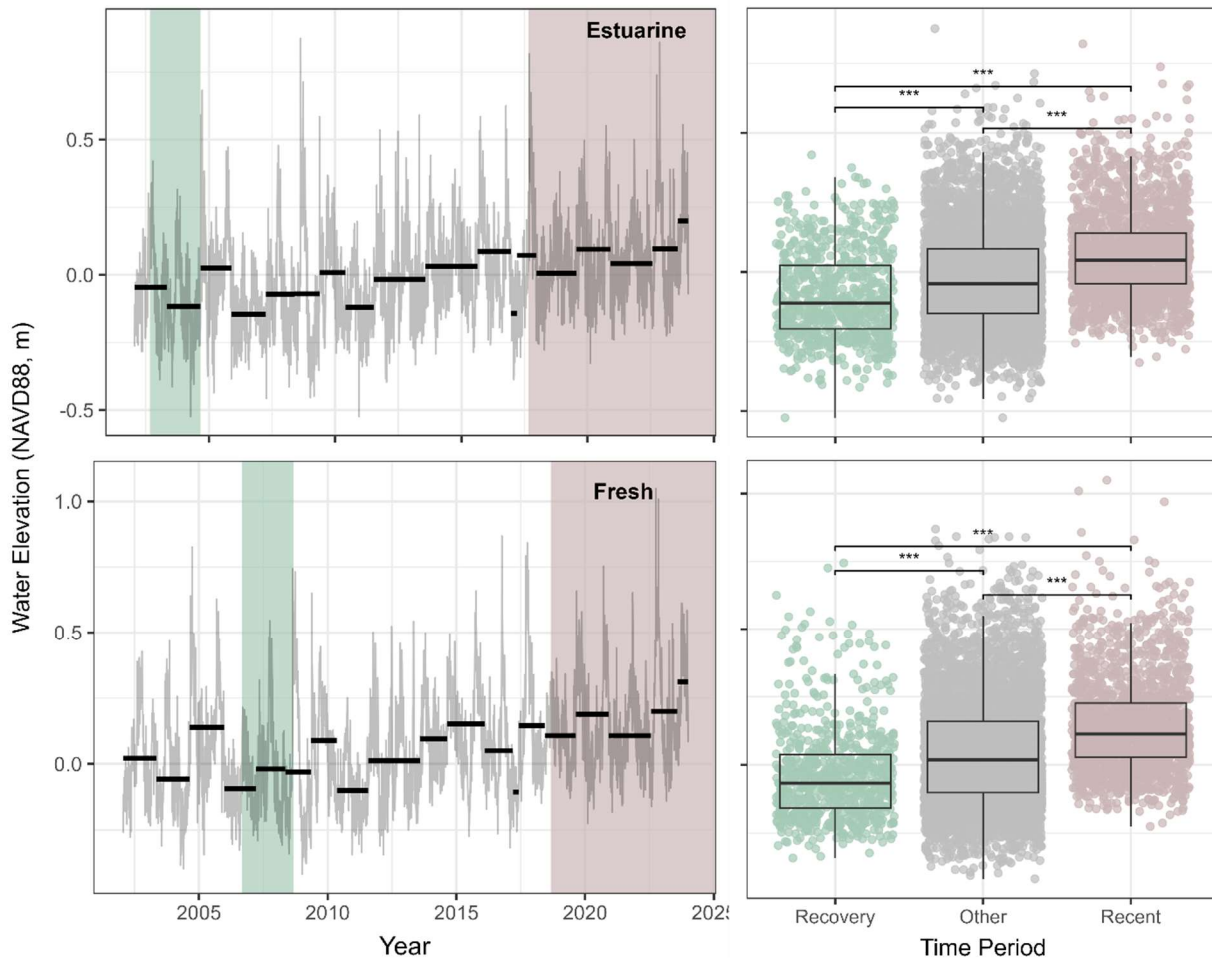


Figure 2.6 Changepoint analysis from 2002–2023 (left) and boxplots with results of Bonferroni-corrected Dunn’s tests (right) comparing water elevation among the recovery (green), background (grey), and recent (brown) periods at the Jacksonville (Estuarine) and Buffalo Bluff (Fresh) USGS NWIS monitoring stations. Statistical significance between monitoring periods is indicated with asterisks (* = $p < 0.05$, ** = $p < 0.01$, *** = $p < 0.001$, ns = $p > 0.05$).

Percent Irradiance at Reference Point

Background

Light availability at a given depth can be directly calculated as the percent of surface irradiance inputting K_d and water depth into the Beer-Lambert equation:

$$\% \text{ Irradiance} = 100 \times e^{-K_d \times \text{Depth}}$$

Monthly mean water elevation data from the Jacksonville and Buffalo Bluff USGS stations were paired with monthly K_d from the nearest river Zones, 1 and 6, respectively. These areas are the approximate downstream (estuarine) and upstream (fresh) limits of SAV colonization in the LSJR mainstem. To account for changes in water elevation over time, the depth variable in the equation is derived from a theoretical fixed reference point that was 1 meter deep during 2002, the start of the study period. This is calculated by subtracting the 2002 mean water depth from the monthly mean water depth and adding the difference to 1.

$$\text{Reference Point Depth} = 1 + (\text{Depth}_t - \text{Depth}_{2002})$$

The result is a time series of the percentage of sunlight reaching the bottom at a fixed point that was one meter deep during the start of the study period. One meter is the approximate maximum depth that SAV inhabits in the LSJR (Sagan 2007b, Moore 2012).

Results

Although irradiance varied widely over the study period, there were no differences among monitoring periods in the estuarine section ($p = 0.278$) (Figure 2.7). However, in the fresh section, mean percent irradiance during the recovery period was 16.8%, almost 70% higher than the recent period mean of 9.9% ($p < 0.001$). Recovery period irradiance was also greater than the background period ($p = 0.006$), which did not differ from the recent period ($p = 0.352$).

Assessment of Relationships Between SAV Recovery Periods and Environmental Conditions

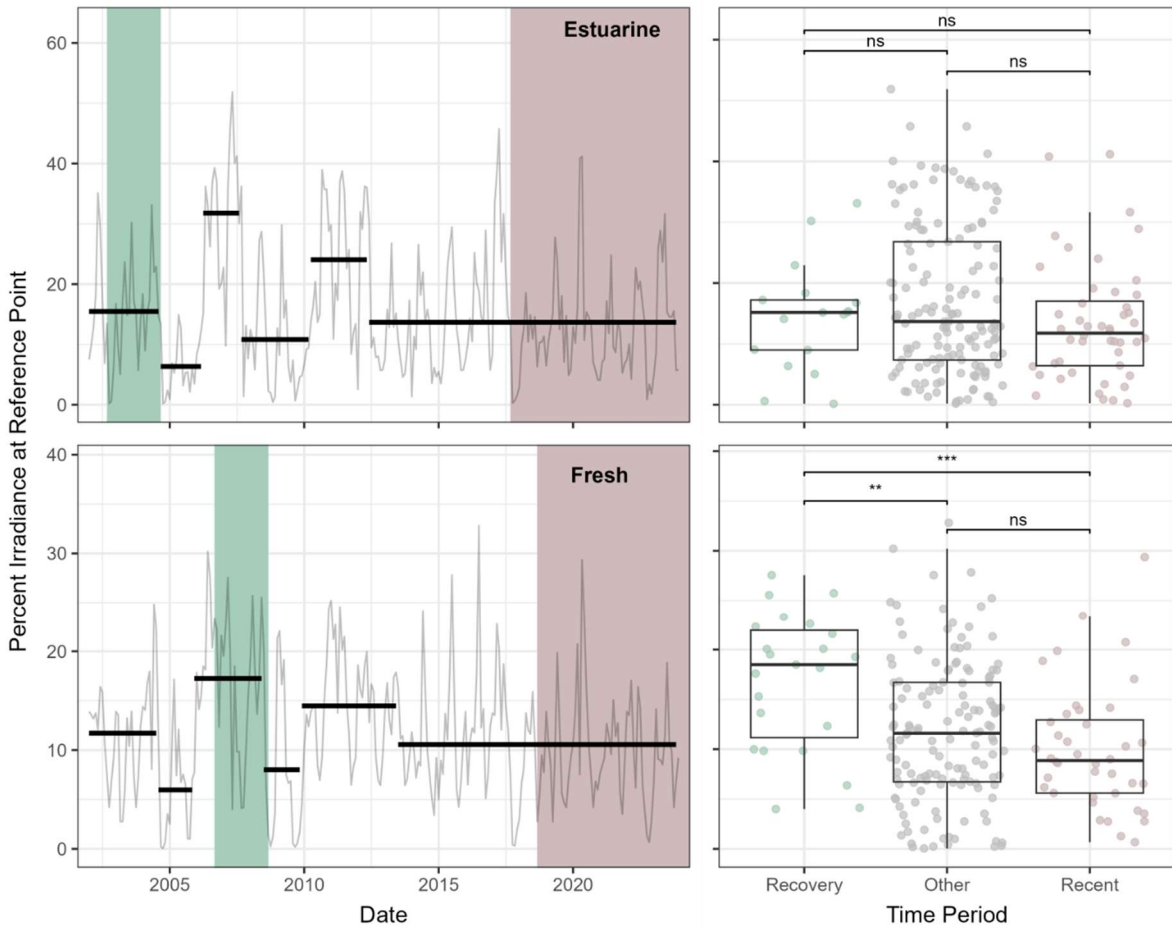


Figure 2.7 Changepoint analysis from 2002–2023 (left) and boxplots with results of Bonferroni-corrected Dunn’s tests (right) comparing percent surface irradiance at a fixed reference point among the recovery (green), background (grey), and recent (brown) periods in the estuarine and fresh sections of the study area. Statistical significance between monitoring periods is indicated with asterisks (* = $p < 0.05$, ** = $p < 0.01$, *** = $p < 0.001$, ns = $p > 0.05$).

Summary

Water elevations in the LSJR consistently increased during the study period and were higher during the recent period than during the recovery and background periods in both the estuarine and fresh sections. Color was the only variable of the K_d equation that varied consistently among periods in the freshwater Zones (5-6) and was likely the primary cause of the K_d changes during the study period. Additionally, lower water elevations enhanced light penetration to the benthic Zone during the recovery period. This was complemented by clearer water, evidenced by lower color and K_d values, leading to a marked increase in bottom irradiance. The average percent irradiance at the fixed reference point was 70% higher during recovery compared to the recent period. These increased light conditions likely facilitated the expansion and recovery of SAV beds, even under moderate nutrient and sediment load conditions.

In the estuarine Zones (1-3), light availability did not vary between the recovery and recent periods, despite the differences in water elevation. This suggests that light limitation may not be the primary driver of SAV dynamics in the estuarine Zones.

Salinity

Background

In the LSJR, salinity variation is driven by tides, freshwater inflow, and seasonal precipitation, resulting in diel pulses of seawater as well as prolonged periods of elevated or depressed salinity. Additionally, winds associated with tropical cyclones can create temporary reverse flows that increase salinity. During droughts or low-rainfall periods, salinity intrusions from the Atlantic Ocean can reach the entirety of the LSJR and into the Upper St. Johns River. Moreover, rising sea levels and anthropogenic influences such as dredging may exacerbate salinity intrusions into the LSJR.

The dominant SAV species in the LSJR, *V. americana*, faces physiological challenges due to salinity fluctuations that affect its cellular mechanisms and resilience. *V. americana* relies on several biochemical pathways to counter salinity stress, including osmotic adjustments via accumulation of metabolites, amino acids, and sugars, which help maintain ion balance and protect chloroplast functions (Rout and Shaw 2001). However, acclimation to increased salinity is limited: *V. americana* grows optimally in low-salinity environments (0–2) but encounters stress, such as reduced growth and survival, as salinity rises above this threshold (Stevenson and Confer 1978, Doering et al. 2001).

Salinity tolerance in *V. americana* is further influenced by the rate and duration of exposure. Rapid salinity increases pose greater risks, as acclimatization requires time and resources to produce protective biochemical responses. Net growth is almost completely halted at salinities of 9–12, with high mortality rates at prolonged exposures above 15 (Doering et al. 2001). Additionally, French and Moore 2003 and Dobberfuhr 2007 observed that *V. americana* plants grown in salinities of 5 required approximately 50% more light than those in fresh water due to reduced photosynthetic efficiency.

Higher salinities in LSJR may also elevate sulfate levels, leading to sediment sulfide production under anoxic conditions, which is toxic to SAV and interferes with nutrient uptake, photosynthesis, and cellular enzyme functions (Hasler-Sheetal and Holmer 2015, Fraser et al. 2023)

Because short-term and long-term changes in salinity both affect SAV, this section examines multiple salinity datasets with varying temporal resolutions in addition to salinity stress metrics.

Monthly Ambient Data

Results

The only groupwise difference among monitoring period means in the three estuarine Zones 1–3 was the mean salinity in Zone 1 during the recent period (2.7 ± 0.6) was lower than the background period means of 5.4 ± 0.4 ($p = 0.041$) (Figure 2.8). There were no differences in mean between the recovery and recent periods ($p_1 = 0.999$, $p_2 = 0.620$, $p_3 = 0.999$). However, maximum salinity during the recent period ranged from 63% to 300% greater than the maximum during the recovery period in each of Zones 1–3 (Table 2).

The mean salinity in Zone 4 during the recovery period was 1.2 ± 0.3 , greater than the recent period mean of 0.7 ± 0.1 ($p = 0.028$). Neither period was different than the background period mean ($p_{\text{Recovery}} = 0.890$, $p_{\text{Recent}} = 0.999$).

In the freshwater Zone 5, mean salinity was higher in the recovery period than both the background ($p < 0.001$) and the recent period ($p < 0.001$), which were not different from each other ($p = 0.999$). The means during all three periods were below 1, with maximums ranging from 1–3. Salinities were lower in Zone 6, but the same pattern in means was observed, with the recovery period mean greater than both the recent and background periods. (Figure 2.8).

Table 2.2: Maximum monthly salinity of ambient samples during each monitoring period in each Zone of the study area.

Zone	Background (Other) Period	Recovery Period	Recent Period
1	26.7	7.6	12.4
2	16.4	4.5	8.4
3	11.0	2.3	7.1
4	7.1	4.1	4.4
5	3.1	2.1	1.1
6	0.8	0.6	0.7

Assessment of Relationships Between SAV Recovery Periods and Environmental Conditions

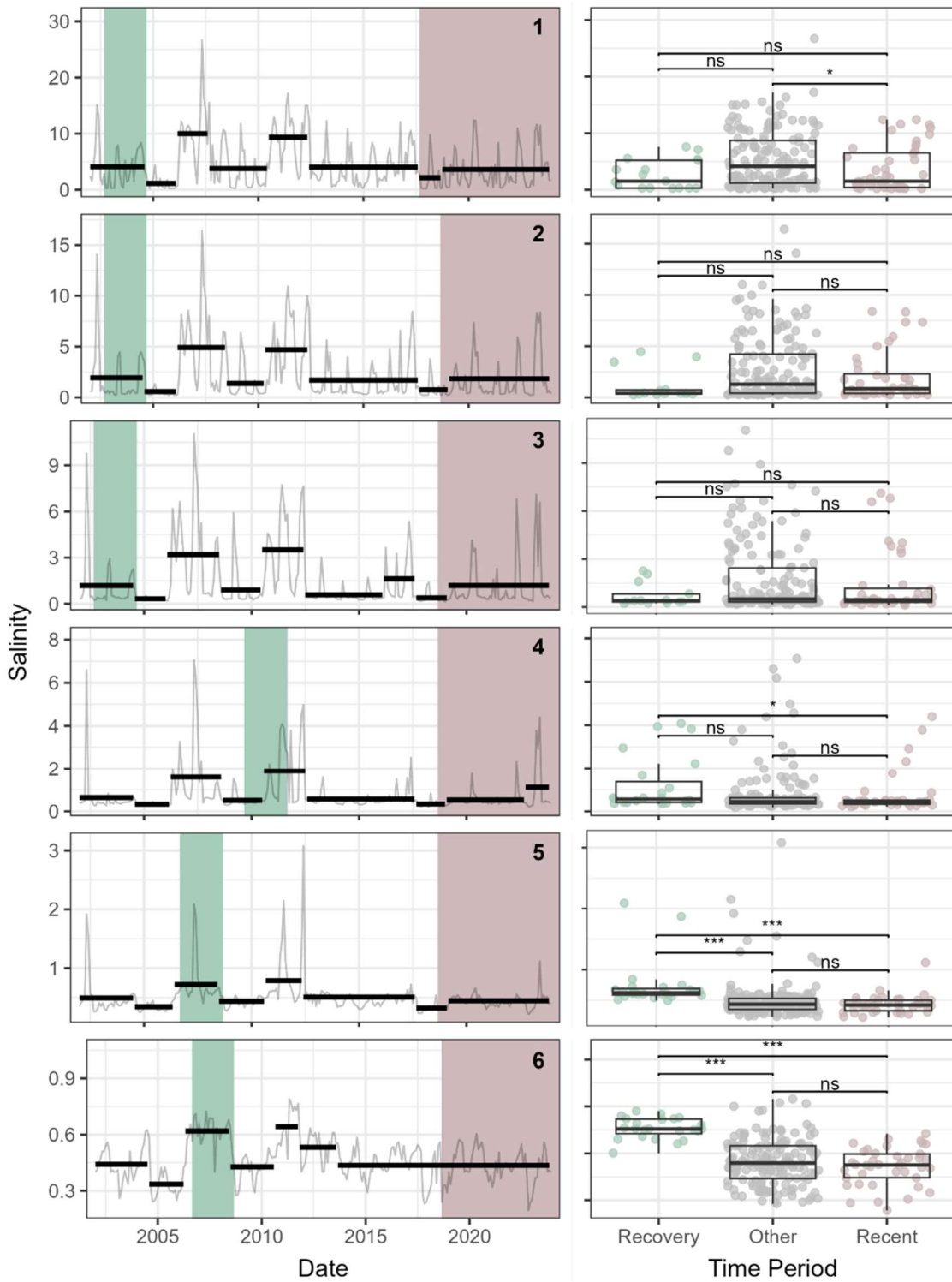


Figure 2.8 Changepoint analysis from 2002–2023 (left) and boxplots with results of Bonferroni-corrected Dunn’s tests (right) comparing monthly salinity among the recovery (green), background (grey), and recent (brown) periods in each Zone of the study area. Statistical significance between monitoring periods is indicated with asterisks (* = $p < 0.05$, ** = $p < 0.01$, *** = $p < 0.001$, ns = $p > 0.05$).

Salinity Suitability Index

Background

Chamberlain (Chamberlain 2012) used daily salinity values from 1995–2005 estimated by the LSJR hydrodynamic model of the LSJR to calculate a salinity suitability index (SSI) that quantified expected *V. americana* condition in response to temporal changes in salinity. The scale ranges from 0.0–1.0 with 0.0 indicating extreme stress and 1.0 indicating minimal stress. Table 2.3 from Chamberlain details the SSI and levels of stress based on duration and concentration of salinity exposure.

Table 2.3. Matrix of SSI values produced by combinations of salinity and exposure times and the level of stress associated with SSI values (from Chamberlain 2012).

Salinity	Time - Days of salinity exposure			
	1	7	30	90
25	0.05	0.01	0.00	0.00
15	0.44	0.42	0.33	0.09
10	0.70	0.68	0.59	0.35
5	0.96	0.94	0.85	0.61
3	1.00	1.00	0.95	0.71

Legend:

- * Stress level color code and naming designation
- * Salinity Suitability Index (SSI) range of values corresponding to stress level

G	No Effects - Good Condition (1.0 - 0.70)
S	Stressed (0.70 - 0.40)
ES	Extreme stress (0.40 - 0.10)
CS	Critical Stress (0.10 - 0.0)

Calculating the SSI required daily salinity data and the LSJR hydrodynamic model only output values from 1995–2005, largely outside of our 2002–2023 study period. The only dataset that spanned the entirety of our study period was monthly-bimonthly *in situ* ambient water quality data. To examine the viability of using the ambient data to calculate SSI we obtained daily salinity data from the LSJR hydrodynamic model from 1995–2005 at the locations of the ambient water quality sites. We then used linear interpolation to create a daily salinity dataset for each ambient site. Daily SSI was calculated for both the model salinity and *in situ* salinity datasets and the time series were compared (Figure 2.9).

Results

SSIs generated by the ambient dataset generally agreed with those of the modelled dataset in Zones 1, 2, and 3, but tended to under-detect instances of mild stress (SSI 0.75–1.0). The ambient dataset and was also slower to reach the maximum SSI (least stress) after detecting

stressful conditions. Agreement was strong enough to merit analysis of the interpolated SSI dataset for the calculated over the entirety the study period.

SSI was higher during the recovery period than the recent period in Zones 1, 2, and 3 ($p = 0.004$, $p < 0.001$, $p < 0.001$), indicating a more favorable salinity environment for *V. americana* during the recovery period. Zone 2 and 3 SSI values reached 1.0, the lowest possible salinity stress, for almost the entirety of the recovery period (Figures 2.10, 2.11). Zone 1 recovery period SSIs never fell into the extreme stress range but were within this range during two separate events in the recent period. Zone 2 SSI was at 1.0 (Ideal) for 77% of the recovery period compared to 22% of the recent period. Additionally, only 9% of the recovery period values were in the stressed category compared to 24% of the recent period. Zone 3 followed a similar pattern as Zone 2, though SSIs were generally higher for all periods and fell to stressful levels less frequently. Then 80% of Zone 3 recovery period SSIs were ideal, and none were within the stressed range, while 55% and 8% of recent period values were ideal and stressed, respectively. By contrast, the Zone 4 recovery period SSI was lower than the recent period ($p < 0.001$), though SSI values only dropped to stressful levels three times during the study period (Figures 2.10, 2.11).

Assessment of Relationships Between SAV Recovery Periods and Environmental Conditions

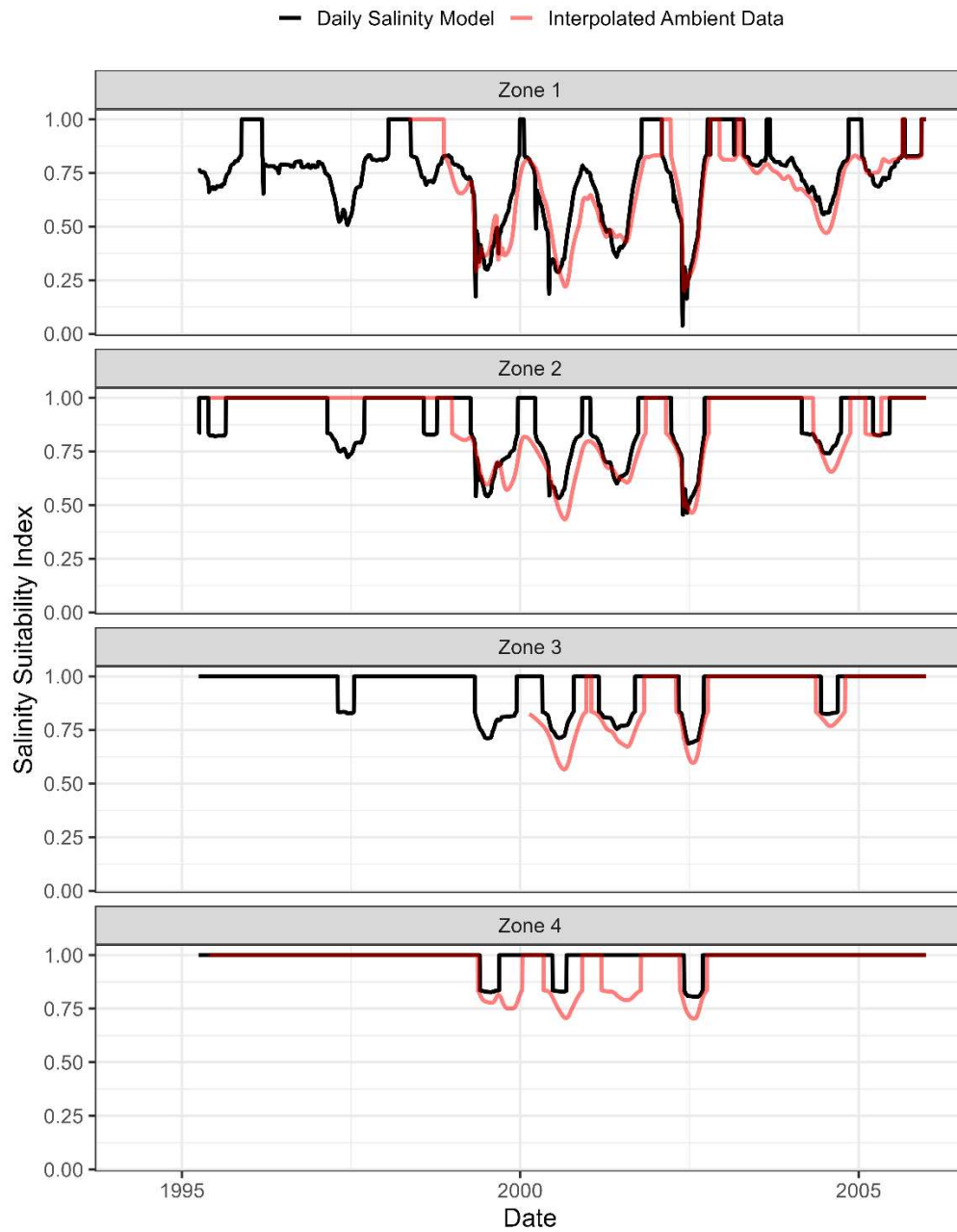


Figure 2.9 Line graphs of SSI calculated with salinity values from the daily salinity model (black) and interpolated ambient data (black) in the estuarine Zones of the study area.

Assessment of Relationships Between SAV Recovery Periods and Environmental Conditions

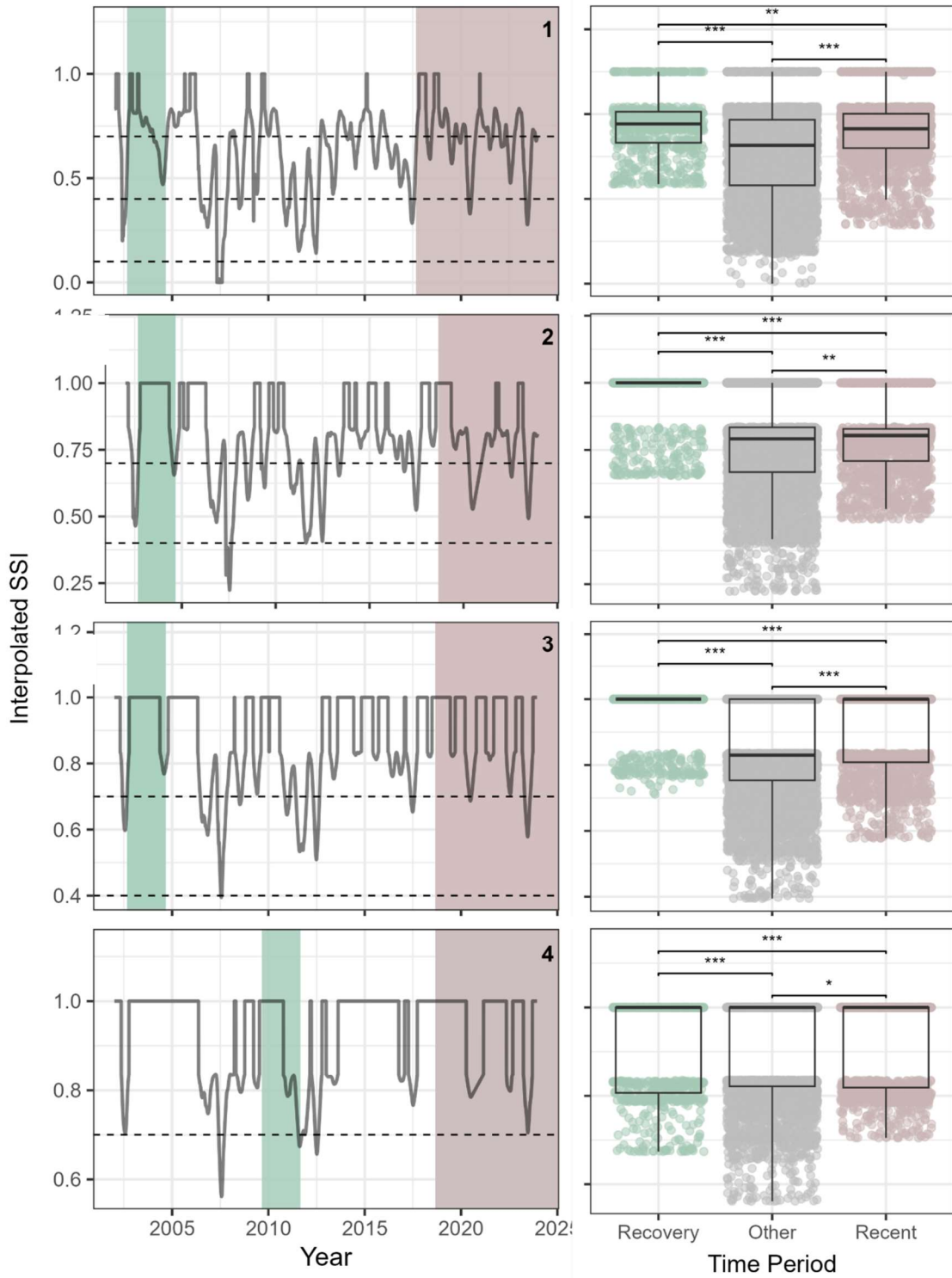


Figure 2.10 Time series from 2002–2023 (left) and boxplots with results of one-inflated beta models (right) comparing salinity suitability index among the recovery (green), background (grey), and recent (brown) periods in Zones 1–4 of the study area. Statistical significance between monitoring periods is indicated with asterisks (* = $p < 0.05$, ** = $p < 0.01$, *** = $p < 0.001$, ns = $p > 0.05$).

Assessment of Relationships Between SAV Recovery Periods and Environmental Conditions

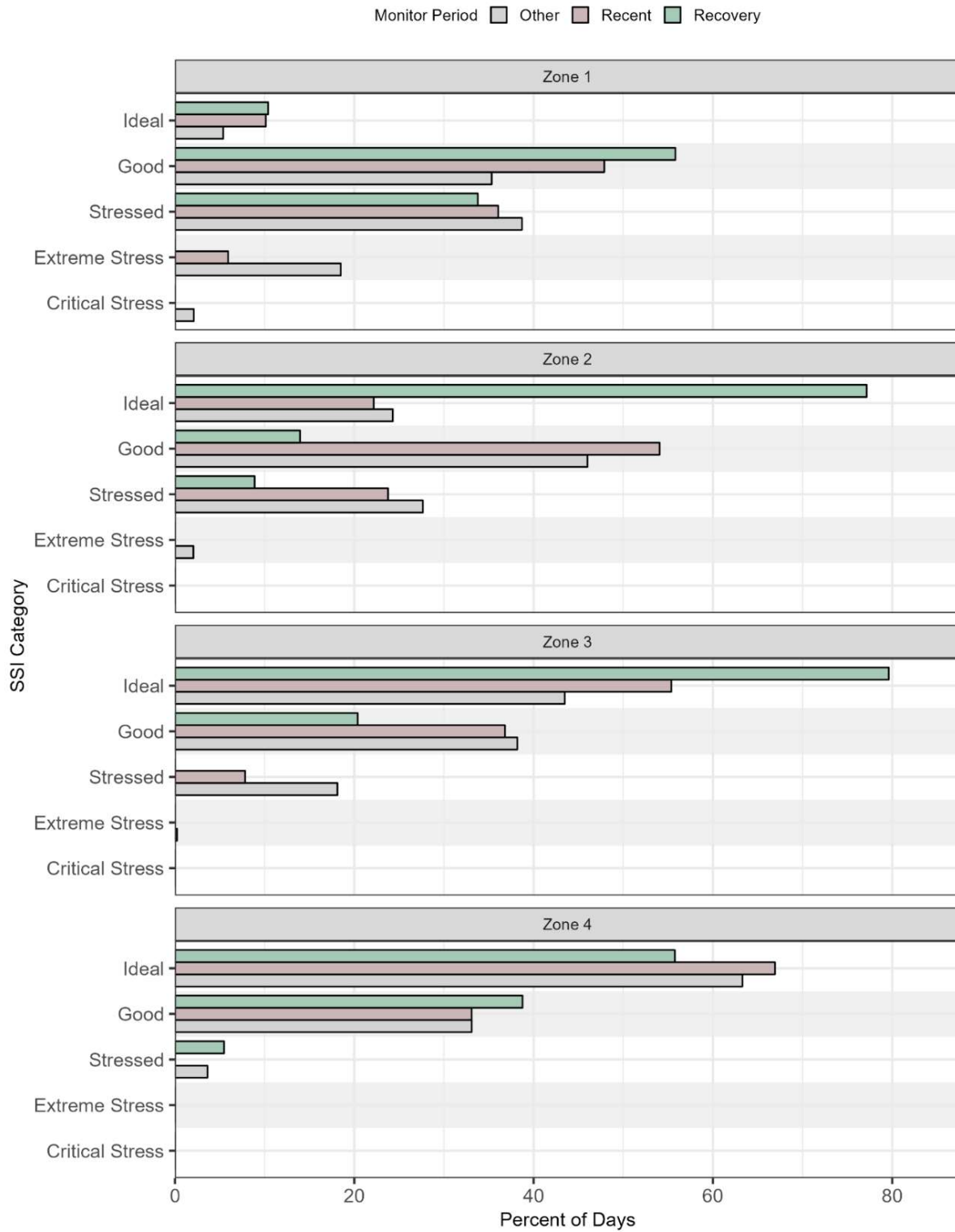


Figure 2.11 Bar graphs displaying the percent of days during the recovery (green), background (grey), and recent (brown) periods spent in each stress category of the SSI.

Summary

The comparison of salinity between the recovery and recent periods reveals distinct patterns across regions. In the estuarine Zones (1–3), mean salinity did not differ between the two periods, but maximum salinity during the recent period was higher, ranging from 63% to 300% above recovery period maxima, indicating salinity spikes that were absent in the recovery period. In these Zones, the SSI was significantly higher during the recovery period than the recent period, reflecting more favorable salinity conditions for *V. americana*, with SSI indicating ideal conditions (1.0) throughout much of the recovery period but consistently just above or below 0.7 (indicating potential stress) during the recent period.

In Zone 4, salinity was lower in the recent period than the recovery period, yet SSI remained above stress thresholds in both periods, signifying a stable salinity environment for *V. americana* throughout the study period despite the lower salinity in recent years.

In the freshwater Zones (5 and 6), mean salinity was higher in the recovery period than the recent period, though both periods maintained consistently low salinity levels typical of freshwater habitats. Collectively, these findings indicate salinity conditions were more favorable for *V. americana* in the estuarine Zones during the recovery period than during the recent period. This difference is potentially due to the increased salinity variability during the recent period, particularly in the form of maximum salinity spikes. The elevated salinity during the recovery period in the freshwater section may not have been causal for recovery, but instead may reflect the drought conditions that enabled greater light penetration while salinity remained outside of stressful levels.

These analyses are based on monthly and biweekly ambient data. This dataset may miss finer-scale variations, such as diel fluctuations or short-term salinity spikes, that could influence ecological conditions.

Nutrients

Background

Elevated nutrient concentrations promote the rapid growth of limnetic algae and formation of dense algal blooms that contribute to the attenuation of light available to the seagrasses below, reducing their ability to photosynthesize (Dennison et al. 1993, Orth et al. 2006).

High concentrations of nutrients can also foster the growth of epiphytic algae on SAV that can further limit light penetration to the SAV's leaves (Michael Kemp et al. 2004, Moore 2012). Also, the additional biomass of epiphytic algae may increase the risk of physical disturbance to seagrass beds by wave action, making them more susceptible to uprooting or damage from strong currents or waves (Dunn et al. 2008). Dense, floating, detached epiphytic algal mats block sunlight and their decomposition may contribute to anoxic conditions. Such mats were suspected to cause SAV loss in the LSJR during the spring of 1997 (Sagan 2003, Magley and Joyner 2008). The association between these species and SAV beds in the littoral Zones limits their detectability by ambient monitoring of center-channel water quality, but ambient nutrient concentrations reflect the resources available to them for growth.

Phosphorus

Background

Variation in phosphorus concentrations primarily limit algal blooms in freshwater Zones of the river, where it acts as the primary limiting nutrient. Excessive phosphorus inputs from sources such as agricultural runoff, urban stormwater, and wastewater discharges can fuel harmful algal blooms.

This section examines the concentration of total phosphorus (TP) in the water column. TP includes all forms of phosphorus present in the water column, encompassing both particulate and dissolved forms. TP represents the combined amount of organic phosphorus (associated with living organisms and decomposed organic matter) and inorganic phosphorus, which includes dissolved reactive phosphorus (orthophosphate), typically the most bioavailable form for algal uptake.

Results

Mean total phosphorus did not vary between the successful recovery period and the recent period in the three estuarine Zones of the mainstem ($p_1 = 0.931$, $p_2 = 1.000$, $p_3 = 1.000$). The only groupwise difference across all three sections was the recent period had lower mean TP than the background period in Zone 1 ($0.109 \pm .003$ mg/L vs 0.121 ± 0.003 mg/L, $p = 0.046$).

In the transitional Zone 4, there was no difference among the three groups ($p = 1.000$).

Mean total phosphorus was 0.080 ± 0.008 mg/L and 0.050 ± 0.002 mg/L during the recovery period in the freshwater Zones 5 and 6, respectively. These means are approximately 20% lower than during both the background ($p_5 = 0.007$, $p_6 < 0.001$) and recent periods ($p_5 = 0.001$, $p_6 < 0.001$) which were not different from each other ($p_5 = 0.452$, $p_6 = 0.133$, Figure 2.12).

Assessment of Relationships Between SAV Recovery Periods and Environmental Conditions

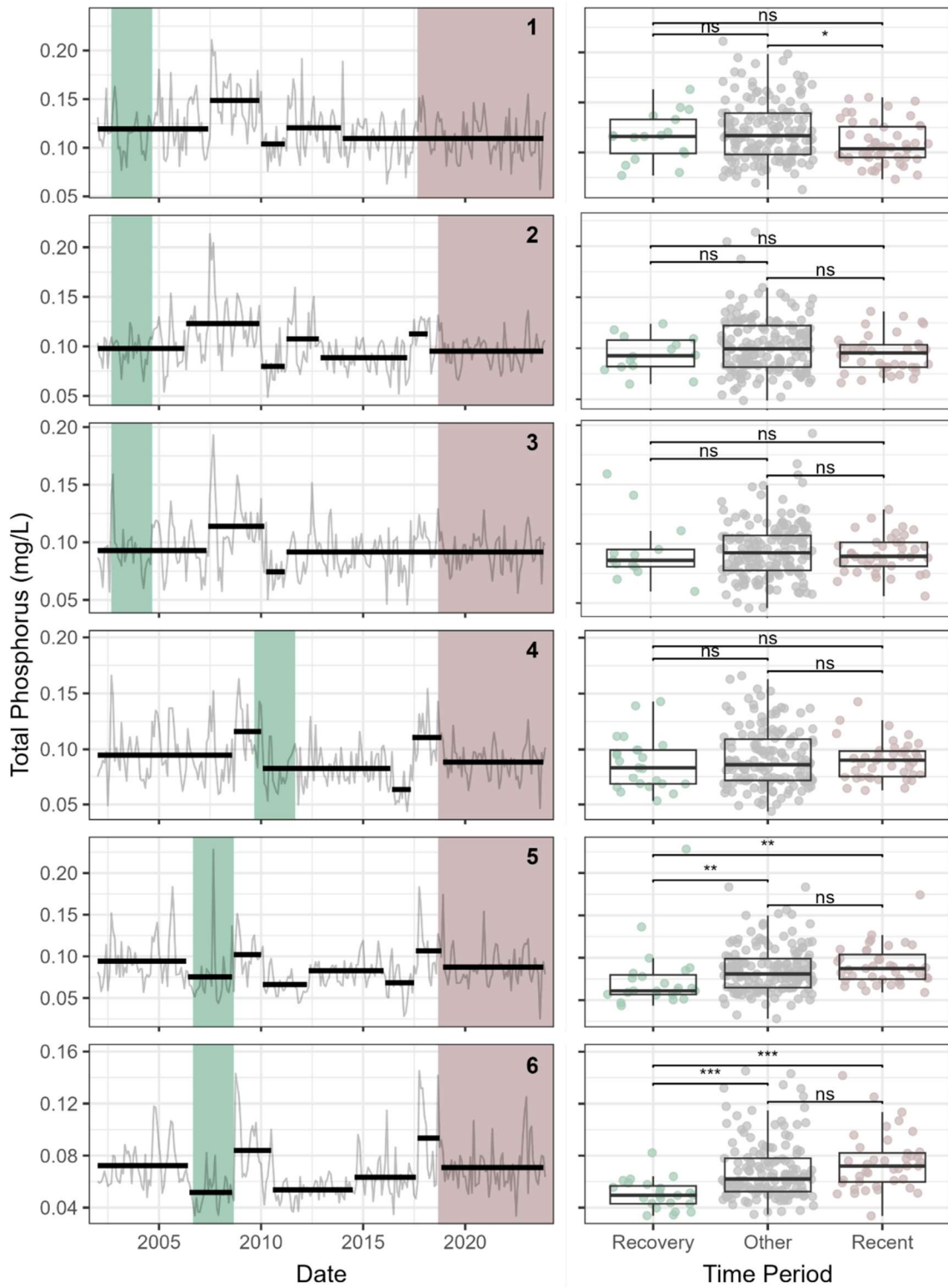


Figure 2.12 Changepoint analysis from 2002–2023 (left) and boxplots with results of Bonferroni-corrected Dunn’s tests (right) comparing total phosphorus among the recovery (green), background (grey), and recent (brown) periods in each Zone of the study area. Statistical significance between monitoring periods is indicated with asterisks (* = $p < 0.05$, ** = $p < 0.01$, *** = $p < 0.001$, ns = $p > 0.05$).

Nitrogen

Background

Like phosphorus, elevated amounts of nitrogen in the water column can promote growth of limnetic and epiphytic algae that attenuate light and increase vulnerability to physical disturbance. Nitrogen becomes increasingly more limiting to algal growth as salinity increases and tends to surpass phosphorus as the limiting nutrient in brackish waters (Neundorfer and Kemp 1993).

This section examines concentrations of total nitrogen (TN). TN similarly includes all forms of nitrogen present in the water, combining both organic and inorganic nitrogen species. TN accounts for dissolved inorganic nitrogen forms, such as nitrate, nitrite, and ammonium, as well as dissolved and particulate organic nitrogen.

Results

Despite some fluctuations in the changepoint analysis over the study period, mean total nitrogen did not vary among any of the monitoring periods in any Zone of the study area (Figure 2.13).

Assessment of Relationships Between SAV Recovery Periods and Environmental Conditions

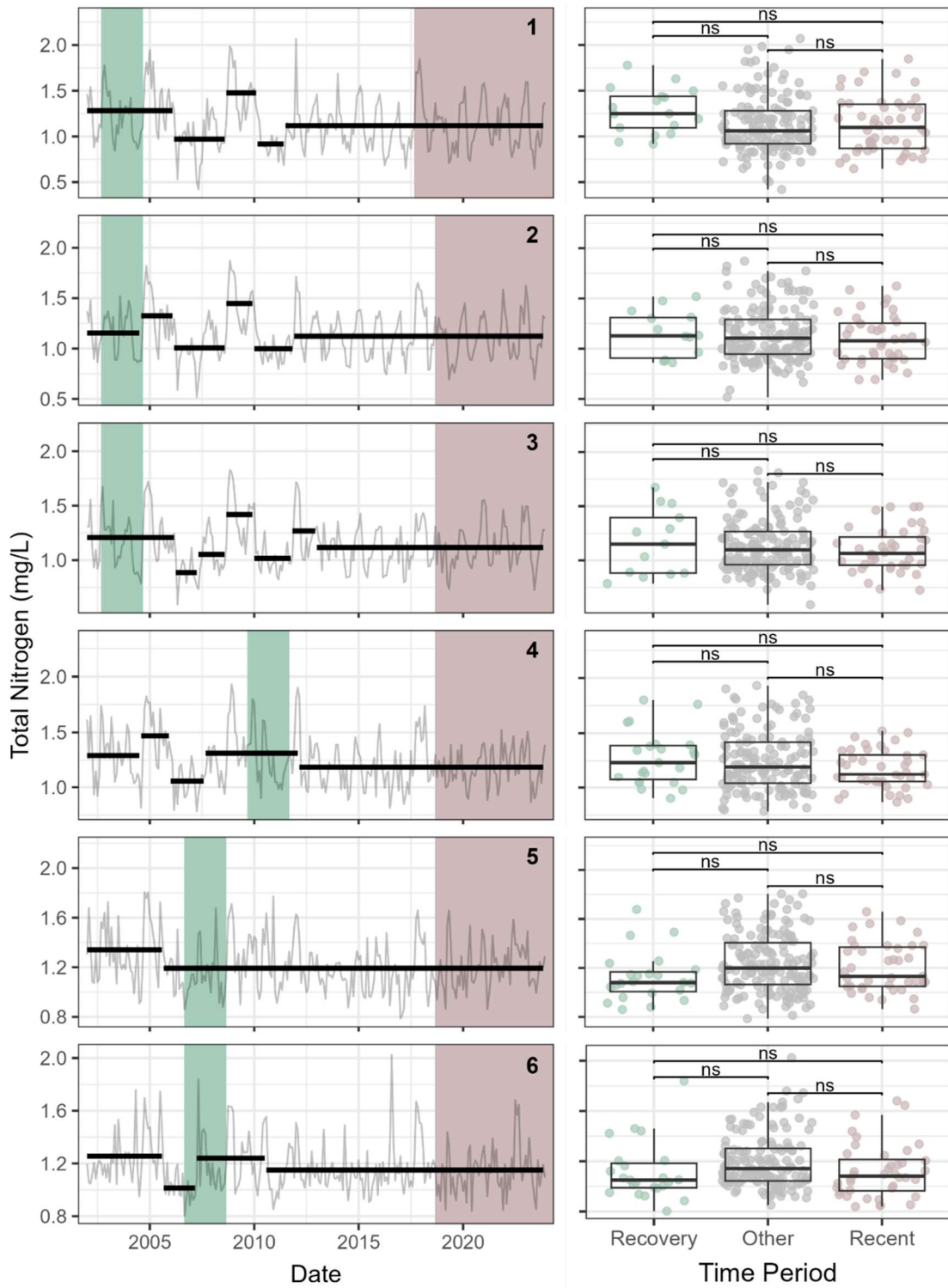


Figure 2.13 Changepoint analysis from 2002–2023 (left) and boxplots with results of Bonferroni-corrected Dunn’s tests (right) comparing total nitrogen among the recovery (green), background (grey), and recent (brown) periods in each Zone of the study area. Statistical significance between monitoring periods is indicated with asterisks (* = $p < 0.05$, ** = $p < 0.01$, *** = $p < 0.001$, ns = $p > 0.05$).

Summary

Both total phosphorus and total nitrogen varied over the study period, but there were no among group differences in TN in any Zones and differences in TP only occurred in the freshwater Zones. Most notably, TP was lower during the recovery period than during both the background and recent periods in the freshwater Zones (5–6). The potential effect this had on SAV is difficult to infer as the difference in TP between the recent and recovery periods did not coincide with a difference in chlorophyll *a* concentration between the groups (Figures 2.3, 2.12). This is further confounded by the greater light availability during the recovery period that may have contributed to SAV canopy height increases and bed width expansion (Figure 2.7). It is possible that the higher ambient TP concentrations in the recent period contributed to a greater epiphyte load on SAV or contributed to algal blooms localized to the littoral areas inhabited by SAV, but these data are not collected by the current ambient center-channel monitoring.

Discussion

It is important to contextualize any discussion of external factors potentially inhibiting post-Irma SAV recovery by noting that the initial die-off preceding the recent period was more severe than any observed previously in the study period. Zones 2–5 began the recent period with mean bed widths that were approximately half as long as those at the beginning of the recovery periods (Figure 1.2).

Our analyses indicate that SAV in the estuarine Zones of the LSJR may have been exposed to more stressful salinity intrusions in the recent period than during the successful recovery that occurred from 2002–2004. During the recovery phase, Zones 1, 2, and 3 had more stable salinity conditions, with maximum salinity values remaining within tolerable limits for *V. americana*. However, while mean monthly salinity during the recent period was not different than during the recovery period, salinity spikes were more severe, with maxima ranging from 63% to 300% higher than those observed during recovery (Figure 2.8, Table 2.2).

Additionally, interpolated recovery period SSI values were among the most favorable of the entire study period, while recent period values remained consistently at or near stressful levels (Figure 2.10). Elevated water elevations in the region did not result in lower light availability in the recent period (Figures 2.5, 2.7) but present a potential long-term threat if they continue to rise. Higher water elevations may also increase grazing pressure by increasing the ability of large herbivores like manatees to access SAV beds that may have been too shallow in previous years.

Light availability was the largest differentiating factor among periods in freshwater Zones (5 and 6). During the recovery period lower water elevations and water color enhanced bottom irradiance compared to the recent and background periods (Figures 2.2, 2.5, 2.7). Although the average bottom irradiance at a fixed reference point following the post-Irma die-off was equal to the background mean, both were 70% lower than during the successful recovery. This indicates that unusually favorable light availability conditions may be required for recovery, especially in the recent period, when SAV biomass is at a study-period low and few, if any, leaves reach into the upper water column. Recovery to the study period maxima may be slow in coming as decadal increases in water elevation reduce the future likelihood of high-light conditions and increasingly hardened shorelines block retreat pathways for SAV to colonize shallower areas.

Chlorophyll *a* and TSS concentrations did not differ consistently between recovery and recent periods in any Zone, indicating limited influence on observed SAV trends (Figures 2.3, 2.4). Spatial and temporal variability in chlorophyll *a* was high, but patterns were not aligned with SAV recovery or decline. Similarly, fluctuations of TN concentrations over the study period did not correspond with changes in SAV abundance (Figure 2.13). TP concentrations were lower during recovery period than in the post-Irma period within the freshwater Zones (Figure 2.12); however, this did not coincide with reductions in chlorophyll *a*, suggesting limited phytoplankton response. While reduced TP during recovery may have lowered epiphytic or benthic algal loads, these variables were not measured in the SJRWMD

ambient water quality or SAV datasets and cannot be quantified. Our results indicate that nutrient-driven algal proliferation was not a primary driver of large-scale SAV dynamics in the LSJR during the study period.

Overall, SAV recovery in both the estuarine and fresh sections of the river coincided with highly favorable conditions that have not been met during the recent period, which followed the most severe die-off of the analysis window. Management options to mitigate salinity in the estuarine Zones and water elevation and color in the fresh Zones are limited as all three are linked to long-term climatic changes in sea level and rainfall patterns. Although chlorophyll *a* did not correlate with recovery, limiting nutrient loads and algal blooms should remain a priority as dense limnetic and epiphytic algae can only exacerbate light limitation and weaken SAV physiological tolerance to varying salinity.

SECTION 3 ASSESSMENT OF RELATIONSHIPS BETWEEN SAV RECOVERY PERIODS AND ABUNDANCES OF SELECTED FISH AND MACROINVERTEBRATES

Methods

Survey Design

The focus of this section was to investigate the abundances of selected fish and macroinvertebrate species that are present and may be contributing to the herbivory of recovering SAV populations in the LSJR. It uses data collected in the LSJR from September 2005 to August 2022 by staff from the Fisheries-Independent Monitoring (FIM) program of the Florida Fish and Wildlife Conservation Commission's Fish and Wildlife Research Institute (FWRI). Although not specifically designed to assess SAV and its recovery, the survey and collected data are amendable to analyses that assess the composition of the nekton community in the areas where SAV is present in the LSJR. In addition, the survey data allow for the investigation of relationships between the distribution and abundance of individual species and variations in season, habitat, salinity, and water quality in the area in question. The FIM program uses a stratified-random sampling design and a multi-gear approach to collect data on fish and select invertebrates from a wide range of habitats and life history stages. This sampling design provides comprehensive data on size-specific, spatial, and temporal patterns of abundance for the nekton community and for individual species. Specimens collected during this sampling are also used for various other assessments, such as fish health, mercury concentrations, diet, age/growth, and reproduction. All samples utilized for this study were from the 21.3 m center-bag seines which, generally speaking, document habitat use by shallow-water shoreline-associated organisms. The dominant catch for the 21.3 m seine is juvenile fishes, although smaller sub-adults are also commonly caught. The seines also regularly collect a few of the larger macroinvertebrate species from tidal rivers, notably blue crabs (*Callinectes sapidus*), and white shrimp (*Litopenaeus setiferus*).

Monthly sampling in portions of the LSJR began in May 2001 and is currently ongoing. However, for the purpose of this study data from September 2005 through August 2022 will be used as this is when consistent long-term sampling has been conducted in the area of interest. The study area was post stratified into seven collection Zones (Zones 1–7; Figure 3.1) to match current SJRWMD sampling water bodies (WBIDS). In addition, samples were post-stratified into a “growing year” to match the SJRWMD SAV sampling seasons. For this purpose, a “growing year” was defined as having a beginning month of September and an ending month of August.

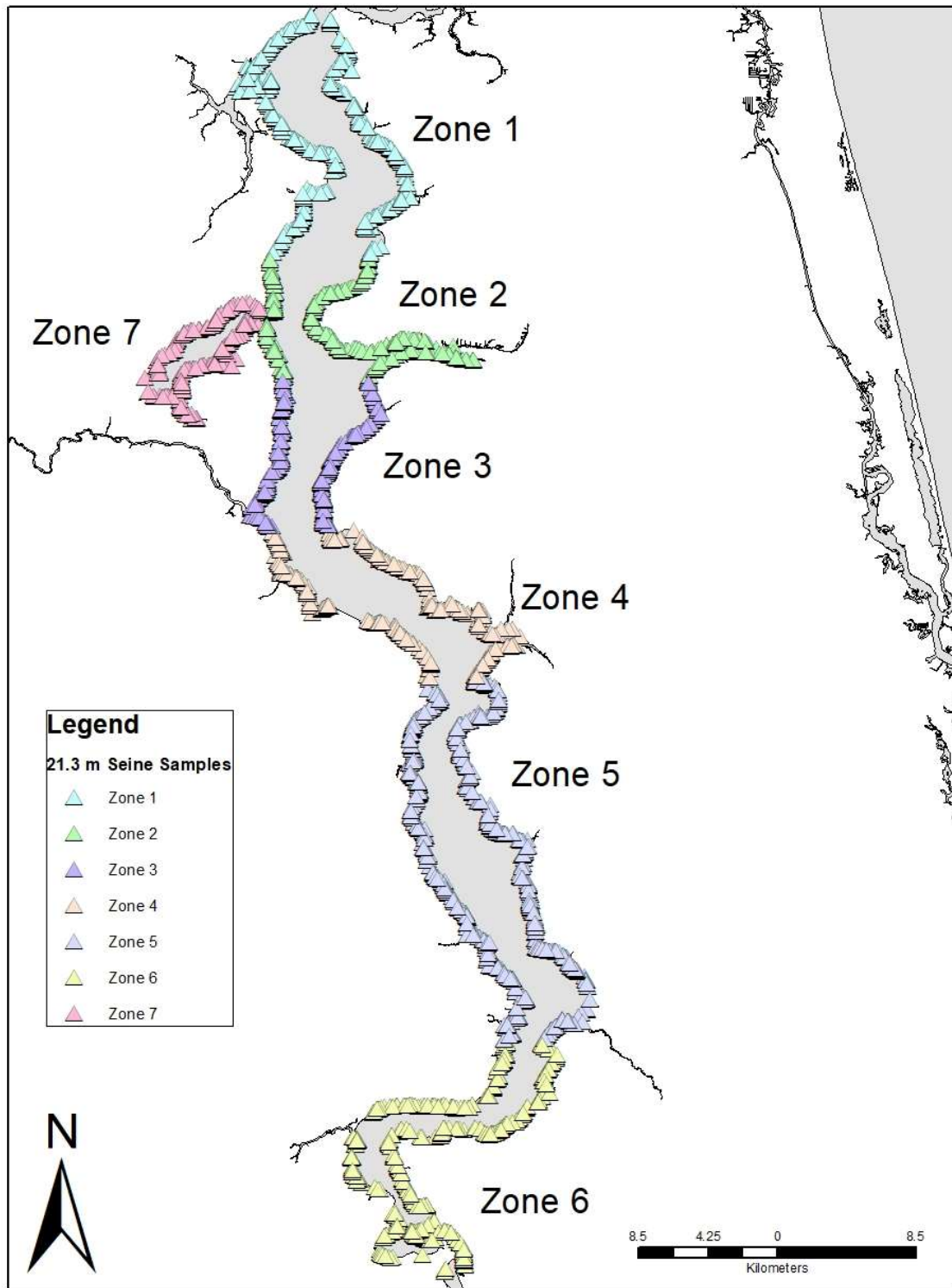


Figure 3.1 Fisheries-Independent Monitoring program 21.3 m seine sampling sites in the lower St. Johns River, September 2005 through August 2022 by Zone. Sampling Universe was post stratified into seven collection Zones (Zones 1–7) to match SJRWMD sampling water bodies.

Seine Specifications and Deployment

The gear used to collect smaller nekton associated with the shallow, nearshore habitats was a 21.3 m center-bag seine with 3.2 mm mesh and lead weights spaced every 150 mm. The net is exactly 21.3 m (70') long and 1.8 m (6') high with a 1.8 m x 1.8 m x 1.8 m bag placed in the center. To deploy the seine along a nearshore habitat (i.e., shorelines with water depth ≤ 1.8 m), the boat dropped off a member of the seine crew near the shoreline with one end of the seine, and the boat deployed the net in a semicircle until the boat reached a second drop-off point near the shoreline. The net forms a vertical "wall" in the water, with the top supported at the surface by floats and the bottom held on the substrate by lead weights. The "bag," positioned at the center of the net, is an enlarged area of mesh that serves to enclose or box the fish and prevent escapement. The lead line was retrieved simultaneously from both ends, with effort made to keep the lead line in contact with the bottom. This process forced the catch into the bag portion of the seine. Area sampled by each boat-deployed seine collection was approximately 68 m².

Salinity, temperature, pH, and dissolved oxygen were measured at the surface and at 1 m intervals to the bottom in association with each gear deployment. A variety of qualitative habitat assessments were also made, such as characteristics of the shoreline (e.g., vegetation type, inundation), substrate (e.g., sediment type, presence of SAV), and bycatch (i.e., total volume, type, and composition). Full details of the FIM habitat assessment protocol are available in the Fisheries-Independent Monitoring Program Procedure manual (contact J.J. Solomon; Justin.Solomon@MyFWC.com).

Seine Sample Processing

Fish and selected invertebrates collected in seine samples were removed from the net and processed onboard. Animals were identified to the lowest practical taxonomic category, generally species. Representative samples (three individuals of each species from the 21.3 m seines on each sampling trip) were brought back to the FWC/FWRI laboratory to confirm field identification. Species for which field identification was uncertain were also brought back to the laboratory for positive identification. A maximum of 20 measurements (mm) were made per taxon, unless distinct cohorts were identifiable, in which case a maximum of 20 measurements were taken from each cohort; for certain economically valuable fish species, forty individuals were measured. Standard length (SL) was used for fish (total length [TL] for seahorses and disk width [DW] for rays), post-orbital head length (POHL) for shrimp, and carapace width (CW) for crabs. Animals that were not measured were identified and counted. When large numbers of individuals ($> 1,000$) were captured, the total number was estimated by fractional expansion of sub-sampled portions of the total catch split with a modified Motoda box splitter (Winner and McMichael 1997). Animals not chosen for further laboratory examination were returned to the river.

Analysis

Species Overviews - Habitat Characteristics and Relative Abundance

Prior to the final data analysis contained in this report a cursory data analysis and literature search was conducted in which thirteen species were identified for further analysis. The criteria for being chosen for further analysis was that the species was abundant in the study

area (>500 individuals collected) and was shown in the literature to either directly ingest SAV, indirectly ingest SAV during grazing, or feed on bottom sediments which may affect SAV recovery. Gear-specific overviews of relative abundance and monthly length-frequency were carried out for the species that were identified. Prior to analysis, catches were standardized to area sampled (animals · 100 m⁻²). Geometric mean abundance ± 95% confidence limits (Sokal and Rohlf 1981) were calculated by year, month, Zone (SJRWMD defined Zones), salinity, dominant shore type, bottom type, and the presence of submerged aquatic vegetation for 21.3 m seines.

Salinity classification used in this analysis was a modification of the Venice system (Anonymous 1958), with categories as follows: limnetic (< 0.5), oligohaline (0.5–4.99), low mesohaline (5–11.99), high mesohaline (12–17.99), polyhaline (18–29.99), and euhaline (≥ 30). Shore types were classified as estuarine marsh (primarily black needlerush, *Juncus roemarianus*; and cordgrass, *Spartina spp.*), freshwater marsh (cattail, *Typha latifolia*; bulrush, *Scirpus spp.*; common reed, *Phragmites spp.*), hardened shoreline (seawall, rip-rap, rocks, and oysters), terrestrial vegetation (primarily cypress trees, *Taxodium spp.*; and terrestrial grasses or other terrestrial vegetation), or miscellaneous. In the case of several shore types within one sampling area, the dominant shore type was assessed by scoring 10 points if the shore type was inundated and adding to this the proportion of the shoreline (expressed as a score out of 10) covered by the shore type. If ties arose, the shore type was selected from an order of priority based on the likelihood that the shore type was in the water and forming structural habitat for nekton. Bottom type was classified as mud, mud-sand, sand, some oyster (at least present), some rock (at least present), or other. Vegetation refers to the presence of SAV and was classified as some (at least present) or none.

Spatial and temporal trends in relative abundance with SAV recovery periods

To determine differences in potential stressors between times of successful SAV recovery and the recent scenario, yearly abundances for estuarine, transitional, and freshwater regions were grouped into three monitoring periods based on the temporal dynamics of SAV bed width, canopy height, and percent occurrence. Periods begin the month after a complete monitoring season (September) and end in the final month of a following season (August). The details and rationale of these selections can be found in Section 1. The three periods are generally defined below:

- Recovery period – Before and during annual summer SAV monitoring when canopy height, bed width, and/or percent occurrence increased.
- Recent period – Samples after 2016–2018 die-off.
- Background (other) period – All other samples during the 2001–2023 study period.

Data were often non-normally distributed, and monitoring period sample sizes were not equal so Kruskal-Wallis and Bonferroni-corrected pairwise Dunn's tests were used to detect among-group differences within each region (Estuarine, Transitional, and Fresh). Alpha was set at 0.05. The SAV recovery period for the estuarine section occurred before the FWC sampling period (2005–2022), so recent and background periods were compared by a Mann-Whitney U test. Box plots on the right side of each figure present these comparisons across the predefined periods (Recovery, Other, and Recent). Each plot displays the raw data within each period as points and median and interquartile range as the boxes. Statistical significance

between periods is indicated with asterisks (* = $p < 0.05$, ** = $p < 0.01$, *** = $p < 0.001$, ns = $p > 0.05$).

Results

Species Profiles

In the following sections, we have profiled selected species that both commonly occur alongside SAV as well as potentially interact with SAV during feeding by either direct or indirect digestion. Species are detailed in terms of seasonal abundance, sizes collected, spatial distribution, distribution in relation to salinity, and shoreline and bottom habitat preference.

White Shrimp, *Litopenaeus setiferus*

Habitat characteristics and relative abundance

White shrimp, range from New York to Saint Lucie Inlet, Florida on the Atlantic coast, and from the Ochlocknee River, Florida to Campeche, Mexico on the Gulf coast (Carpenter 2002a). This species is of great economic importance to both the United States and Mexico. They spawn offshore and enter estuaries as postlarvae (Williams 1984). The different life stages of white shrimp all exhibit a broad range of salinity tolerance, although juvenile white shrimp have been reported to live in lower salinity waters than other commercially important penaeid shrimp (Farfante 1969). Juvenile and adult shrimp are benthic omnivores that feed primarily on detritus, plants, microorganisms, macroinvertebrates, and small fish. Cannibalism is also common among adult white shrimp. White shrimp have also been shown in other estuaries to feed primarily on the grass *V. americana* and detritus (Davis 2009).

The white shrimp was most abundant in the study area between the months of June and November (Figure 3.2). Within the nearshore habitat sampled with 21.3 m seines, white shrimp were most abundant in salinities ranging from 5.0–29.99 and were most abundant in Zones 1, 2, and 7. White shrimp were commonly collected on both vegetated and unvegetated bottom habitats (Figure 3.2).

Litopenaeus setiferus (White Shrimp) in 21.3-m seines

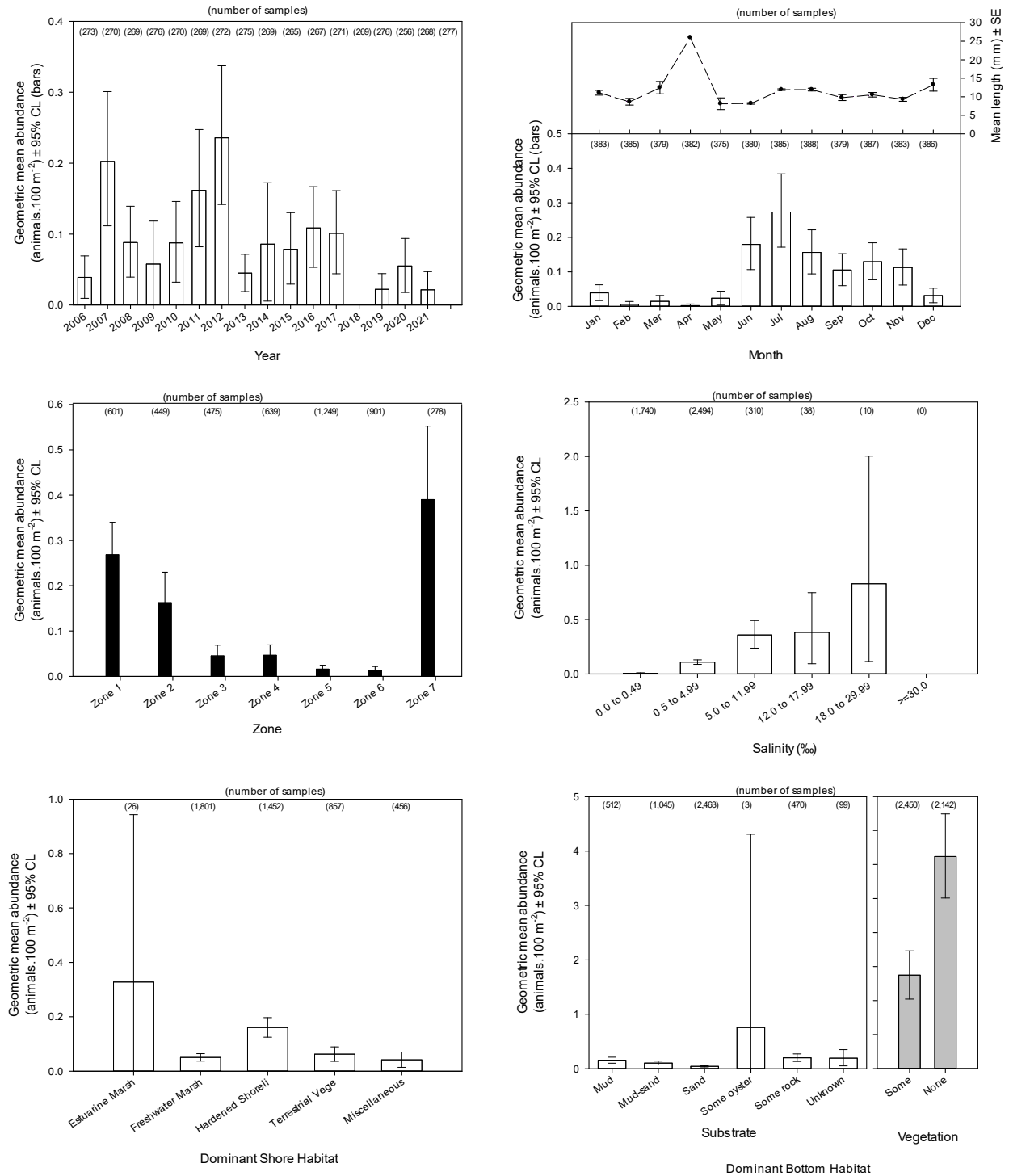


Figure 3.2 Relative abundance of white shrimp collected with 21.3 m seines (water depths ≤ 1.8 m) in the lower St. Johns River. Box: average relative abundance; error bars: 95% CI.

Spatial and temporal trends in relative abundance with SAV recovery periods

Despite some fluctuations, the average yearly abundance within each region did not vary among any of the monitoring periods in any Zone of the study area for white shrimp (Figure 3.3) (Table 3.1).

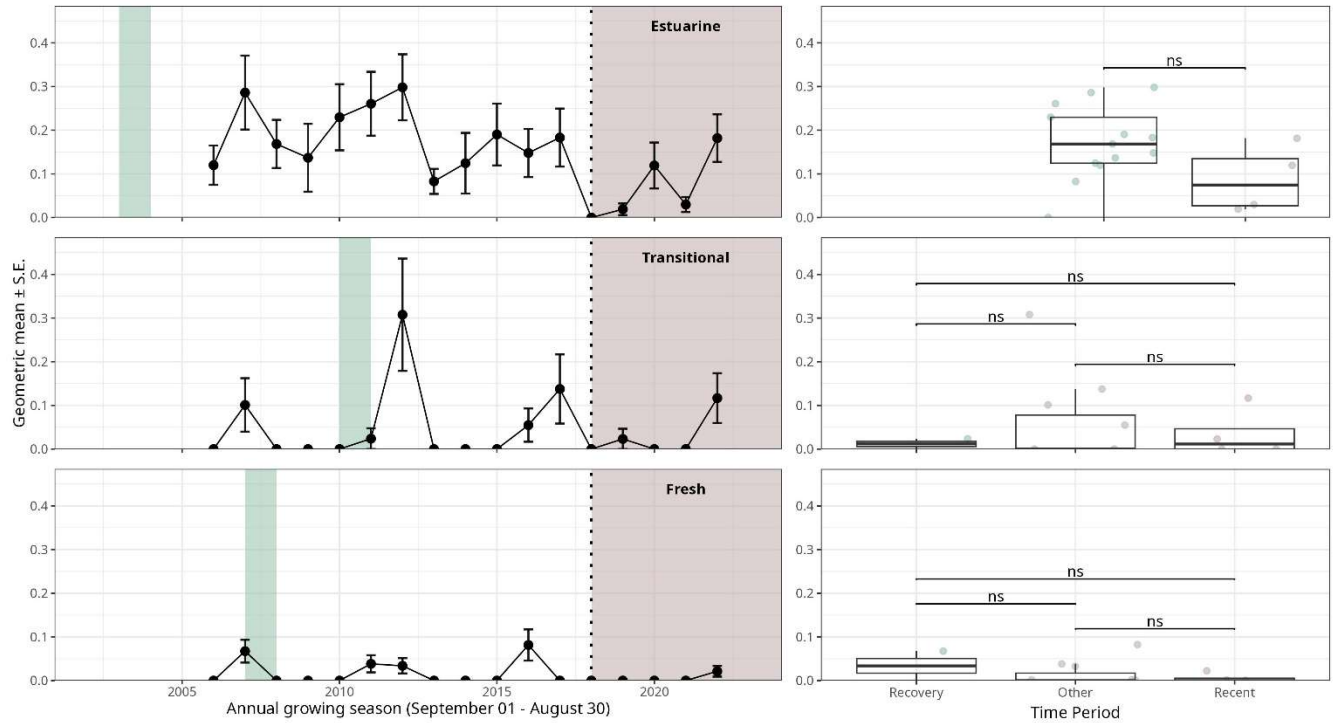


Figure 3.3 Relative abundance with standard error of white shrimp collected with 21.3 m seines (water depths ≤ 1.8 m) within the estuarine, transitional, and freshwater regions of the lower St. Johns River throughout long-term temporal periods of SAV abundance (recovery, recent, and other). The background colors represent the selected periods for groupwise comparisons (Recovery Period = green, Recent Period = brown). Statistical significance between temporal periods is indicated with asterisks (* = $p < 0.05$, ** = $p < 0.01$, *** = $p < 0.001$, ns = $p > 0.05$).

Blue Crab, *Callinectes sapidus*

Habitat characteristics and relative abundance

Blue crabs occur in the western Atlantic from Canada to Argentina, including Bermuda and the Antilles, and have been successfully introduced in Europe and Japan (Carpenter 2002a). This species supports large commercial fisheries and is an important predator and prey species in inshore waters (Steele and Bert 1994). Blue crabs are transients in estuaries: spawning and larval development occurs in marine waters, but juveniles and adults spend most of their time in estuaries (Steele and Bert 1994). Both larval Blue crabs recruiting to the estuary and females leaving the estuary to spawn use selective tidal stream transport (Olm 1994, Tankersley et al. 1998), and odors emanating from estuarine and freshwater watersheds promote settlement by triggering metamorphosis in larvae (Wolcott and Vries 1994, Forward et al. 1997). Blue crabs tolerate salinities from freshwater to at least 50, but optimal salinities vary among life-history stages: 12–36 for larvae, 2–21 for juveniles, less than 10 for adult males, and 23–33 for egg-bearing females (Pattillo et al. 1997). Blue crabs eat almost anything, including clams, oysters, mussels, smaller crustaceans, freshly dead fish, vegetation, plant and animal detritus—and smaller and soft-shelled Blue crabs.

Blue crabs were commonly collected throughout all months and all Zones of the study area (Figure 3.4). They were also found throughout a wide range of salinities but were most abundantly captured in salinities between 5.0–11.99. Blue crabs were commonly collected on both vegetated and unvegetated bottom habitats (Figure 3.4).

Callinectes sapidus (Blue Crab) in 21.3-m seines

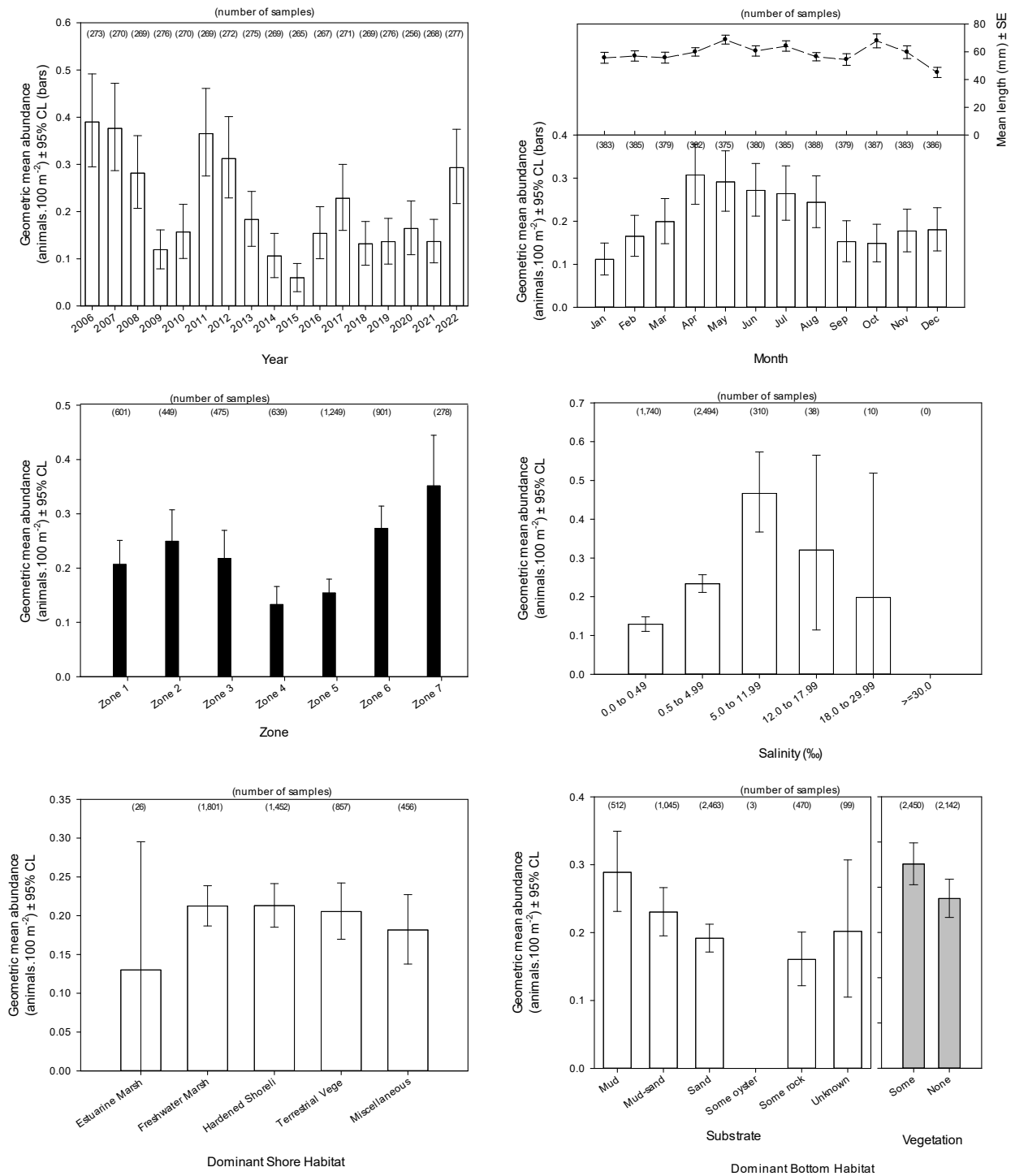


Figure 3.4 Relative abundance of blue crab collected with 21.3 m seines (water depths ≤ 1.8 m) in the lower St. Johns River. Box: average relative abundance; error bars: 95% CI.

Spatial and temporal trends in relative abundance with SAV recovery periods

Despite some fluctuations, the average yearly abundance within each region did not vary among any of the monitoring periods in any Zone of the study area for blue crab (Figure 3. 5) (Table 3.1).

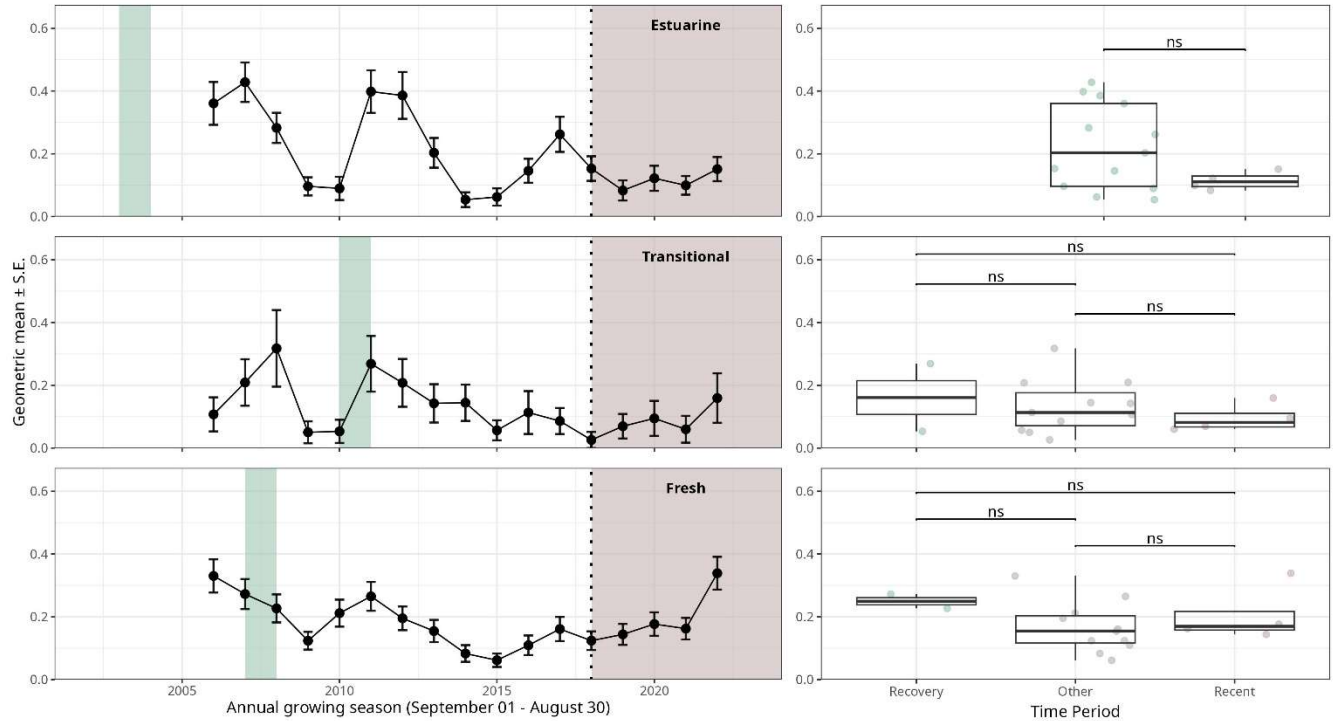


Figure 3.5 Relative abundance with standard error of blue crab collected with 21.3 m seines (water depths ≤ 1.8 m) within the estuarine, transitional, and freshwater regions of the lower St. Johns River throughout long-term temporal periods of SAV abundance (recovery, recent, and other). The background colors represent the selected periods for groupwise comparisons (Recovery Period = green, Recent Period = brown). Statistical significance between temporal periods is indicated with asterisks (* = $p < 0.05$, ** = $p < 0.01$, *** = $p < 0.001$, ns = $p > 0.05$).

Gizzard Shad, *Dorosoma cepedianum*

Habitat characteristics and relative abundance

The gizzard shad, also known as the mud shad, is a member of the herring family of fish and is native to large swaths of fresh and brackish waters in the United States of America (Wuellner et al. 2008). Gizzard shad are primarily found in large rivers, reservoirs, lakes, swamps, and other freshwater environments with turbidity ranging from clear to silty. They prefer quieter open waters although they can be commonly found in the strong current of the upper Mississippi River (Miller 1960). Adults can also be found in brackish and saline waters of estuaries and bays (Whitehead 1985). Gizzard shad are planktivores, straining minute organic particles with their gill rakers into their pharyngeal organ which is thought to concentrate and process food for swallowing. They also feed heavily on detritus found on bottom sediments; individuals consume an average of 13% of their wet weight biomass in dry sediment each day. Their diet remains largely similar at different sizes and has been found to contain algae, phytoplankton, zooplankton, and plant debris (Miller 1960, Mundahl 1991).

The Gizzard shad was most abundant between the months of June – November and was commonly collected throughout all Zones of the study area (Figure 3.6). They were also found throughout a wide range of salinities but were most abundantly captured in salinities between 5.0–11.99. Gizzard shad were commonly collected on both vegetated and unvegetated bottom habitats (Figure 3. 6).

Dorosoma cepedianum (Gizzard Shad) in 21.3-m seines

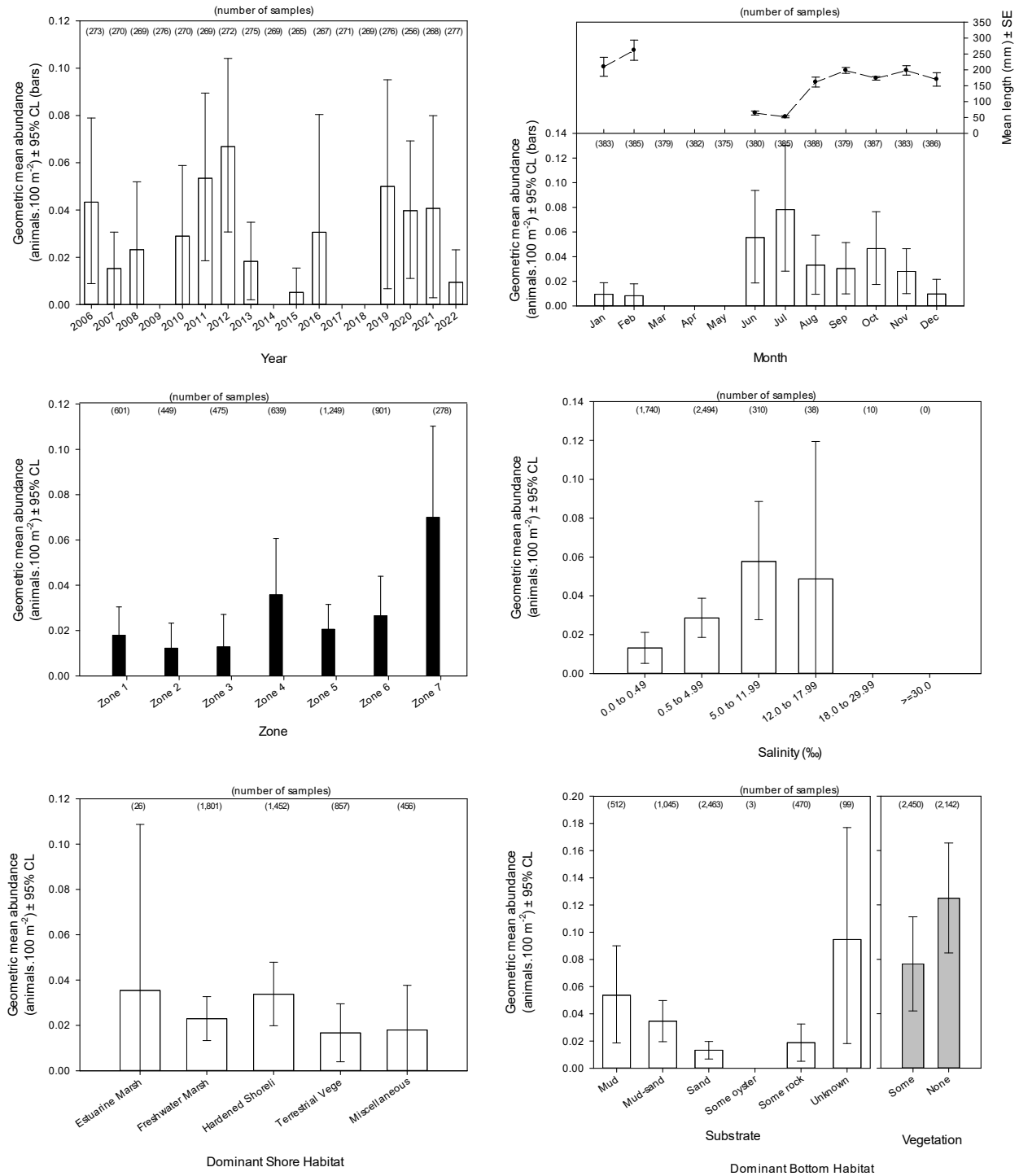


Figure 3.6 Relative abundance of gizzard shad collected with 21.3 m seines (water depths ≤ 1.8 m) in the lower St. Johns River. Box: average relative abundance; error bars: 95% CI.

Spatial and temporal trends in relative abundance with SAV recovery periods

Despite some fluctuations, the average yearly abundance within each region did not vary among any of the monitoring periods in any Zone of the study area for gizzard shad (Figure 3.7) (Table 3.1).

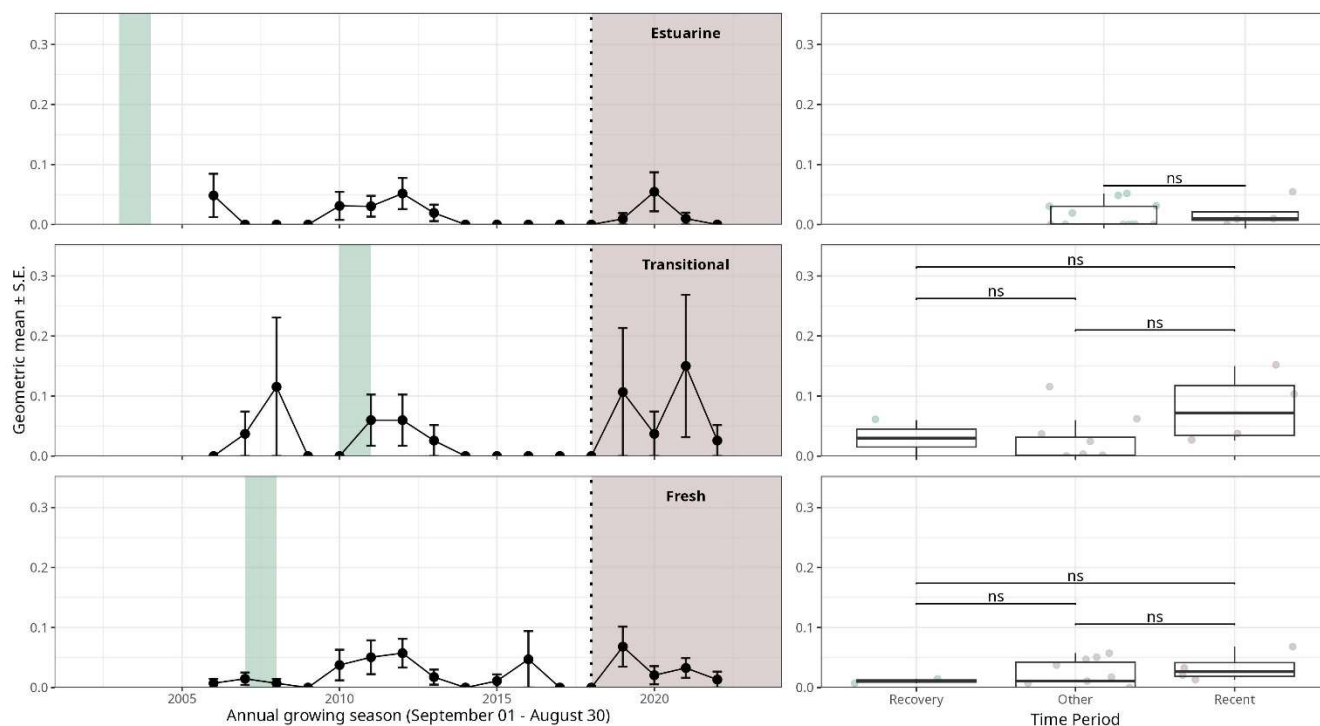


Figure 3.7 Relative abundance with standard error of gizzard shad collected with 21.3 m seines (water depths ≤ 1.8 m) within the estuarine, transitional, and freshwater regions of the lower St. Johns River throughout long-term temporal periods of SAV abundance (recovery, recent, and other). The background colors represent the selected periods for groupwise comparisons (Recovery Period = green, Recent Period = brown). Statistical significance between temporal periods is indicated with asterisks (* = $p < 0.05$, ** = $p < 0.01$, *** = $p < 0.001$, ns = $p > 0.05$).

Threadfin Shad, *Dorosoma petenense*

Habitat characteristics and relative abundance

The threadfin shad, *Dorosoma petenense*, is a small pelagic freshwater forage fish common in the Southeastern United States. They are found in lakes, backwaters, and ponds of medium to large rivers usually in open waters over sand, mud, and detrital bottoms, occasionally entering brackish waters (Page and Burr 2011). Threadfin shad is a very important food source for many game fish such as the largemouth bass. They are primarily filter-feeders, but not entirely herbivorous since recorded food items include copepods, cladocerans, fish fry, and organic material of sand and detritus bottoms similar to that of the gizzard shad (Carpenter 2002b).

The Threadfin shad was most abundant between the months of June – November with a peak of abundance in August (Figure 3.8). They were most abundant in Zones 5 and 6, typically in salinities less than 12.0. Threadfin shad were commonly collected on both vegetated and unvegetated bottom habitats (Figure 3.8).

Dorosoma petenese (Threadfin Shad) in 21.3-m seines

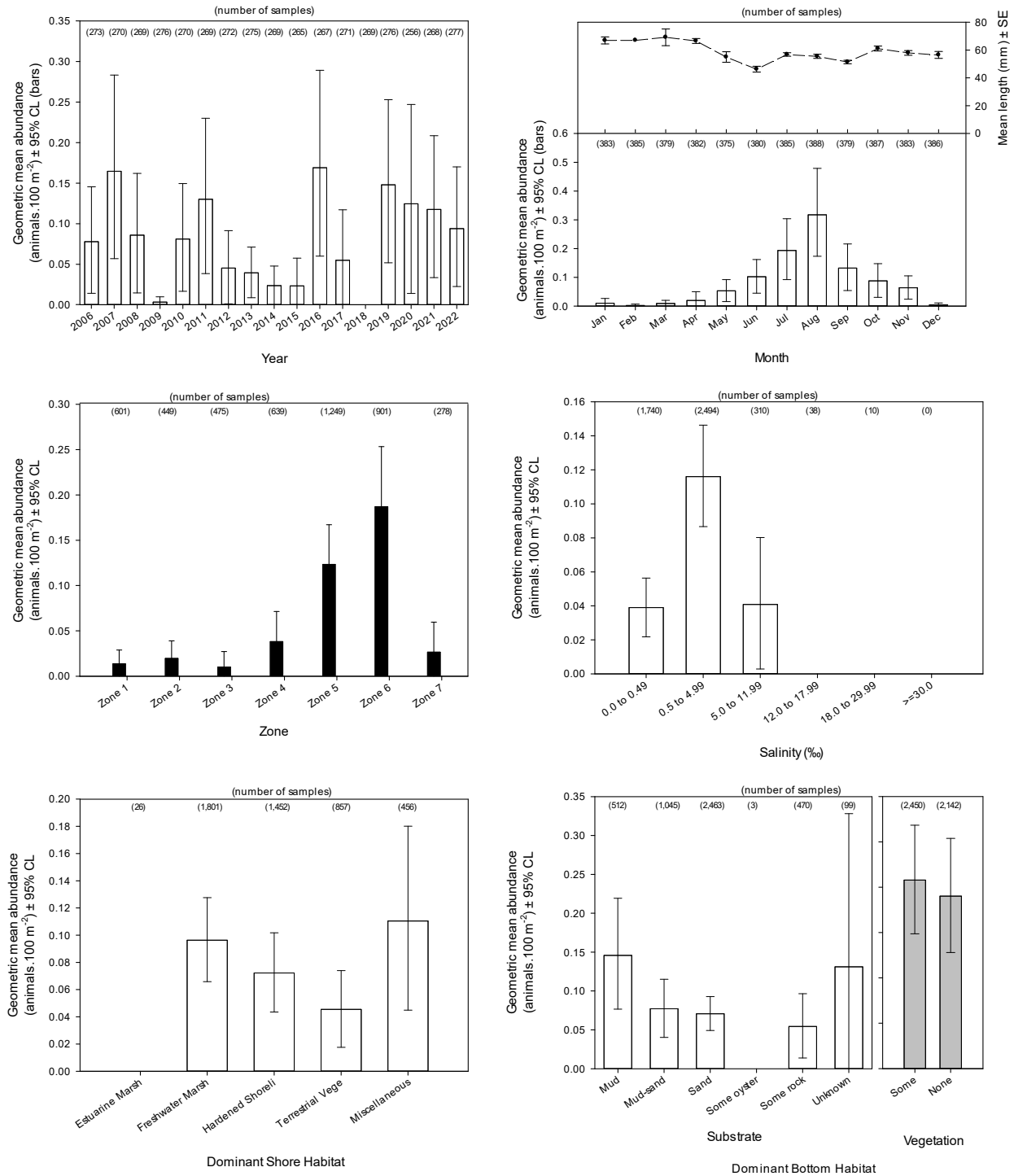


Figure 3.8 Relative abundance of threadfin shad collected with 21.3 m seines (water depths ≤ 1.8 m) in the lower St. Johns River. Box: average relative abundance; error bars: 95% CL.

Spatial and temporal trends in relative abundance with SAV recovery periods

Despite some fluctuations, the average yearly abundance within each region did not vary among any of the monitoring periods in any Zone of the study area for threadfin shad (Figure 3.9) (Table 3.1).

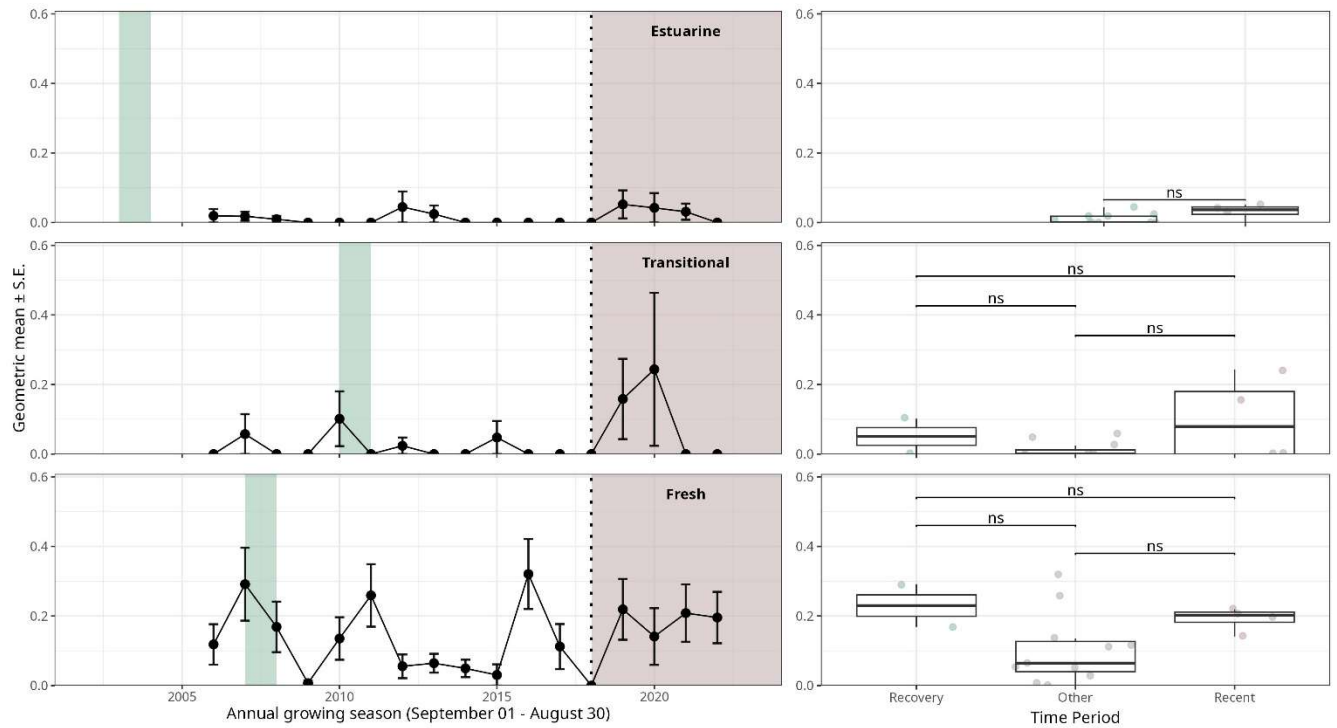


Figure 3.9 Relative abundance with standard error of threadfin shad collected with 21.3 m seines (water depths ≤ 1.8 m) within the estuarine, transitional, and freshwater regions of the lower St. Johns River throughout long-term temporal periods of SAV abundance (recovery, recent, and other). The background colors represent the selected periods for groupwise comparisons (Recovery Period = green, Recent Period = brown). Statistical significance between temporal periods is indicated with asterisks (* = $p < 0.05$, ** = $p < 0.01$, *** = $p < 0.001$, ns = $p > 0.05$).

Golden Shiner, *Notemigonus crysoleucas*

Habitat characteristics and relative abundance

Golden shiners are small to mid-sized freshwater fish from the carp and minnow family. Golden shiners are widely used as bait and as an ornamental. They inhabit lakes and sluggish pools of medium and large rivers (Page and Burr 2011). They can tolerate low oxygen levels, high turbidity, and high temperature; omnivorous but principally feed on plankton, insects, and mollusks (Murdy et al. 1997).

Golden shiners were commonly collected throughout all months with a peak of abundance in July (Figure 3.10). They were most abundant in Zones 5 and 6, typically in salinities less than 5.0. Golden shiners were most abundantly collected on vegetated bottom habitats (Figure 3.10).

Notemigonus crysoleucas (Golden Shiner) in 21.3-m seines

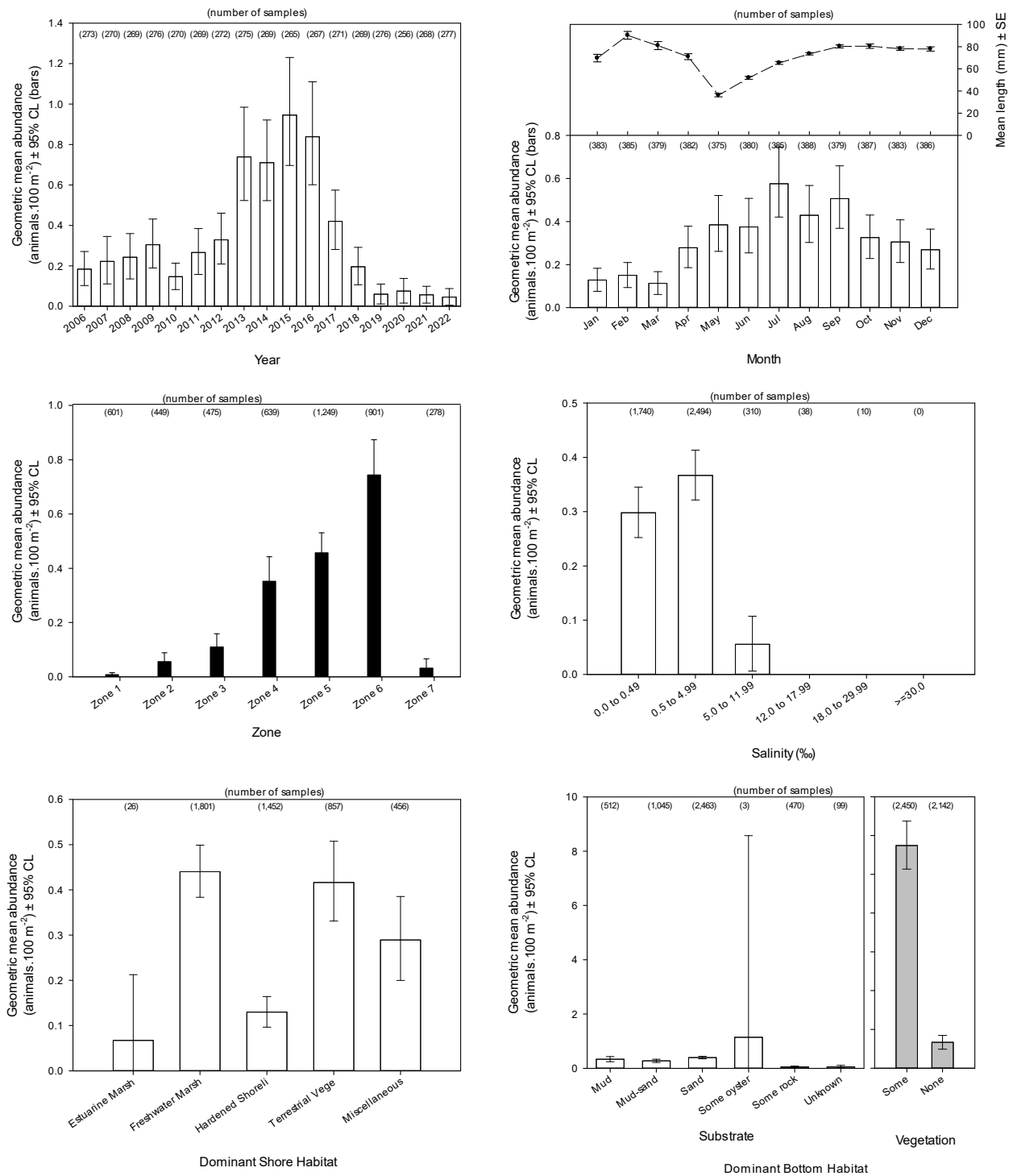


Figure 3.10 Relative abundance of golden shiner collected with 21.3 m seines (water depths ≤ 1.8 m) in the lower St. Johns River. Box: average relative abundance; error bars: 95% CI.

Spatial and temporal trends in relative abundance with SAV recovery periods

The yearly abundance of the golden shiner for any sections of the mainstem did not vary between the successful SAV recovery period and the background period ($p_T = 0.23$, $p_F = 1.00$) nor the successful SAV recovery period and the recent period ($p_T = 1.00$, $p_F = 0.51$). Additionally, the yearly abundance in the estuarine section did not vary between the background period and the recent period ($p_E = 0.40$). The only groupwise differences of yearly abundance of the golden shiner occurred in the transitional and fresh regions between the background period and the recent periods ($p_T = 0.01$, $p_F = 0.01$). (Figure 3.11) (Table 3.1).

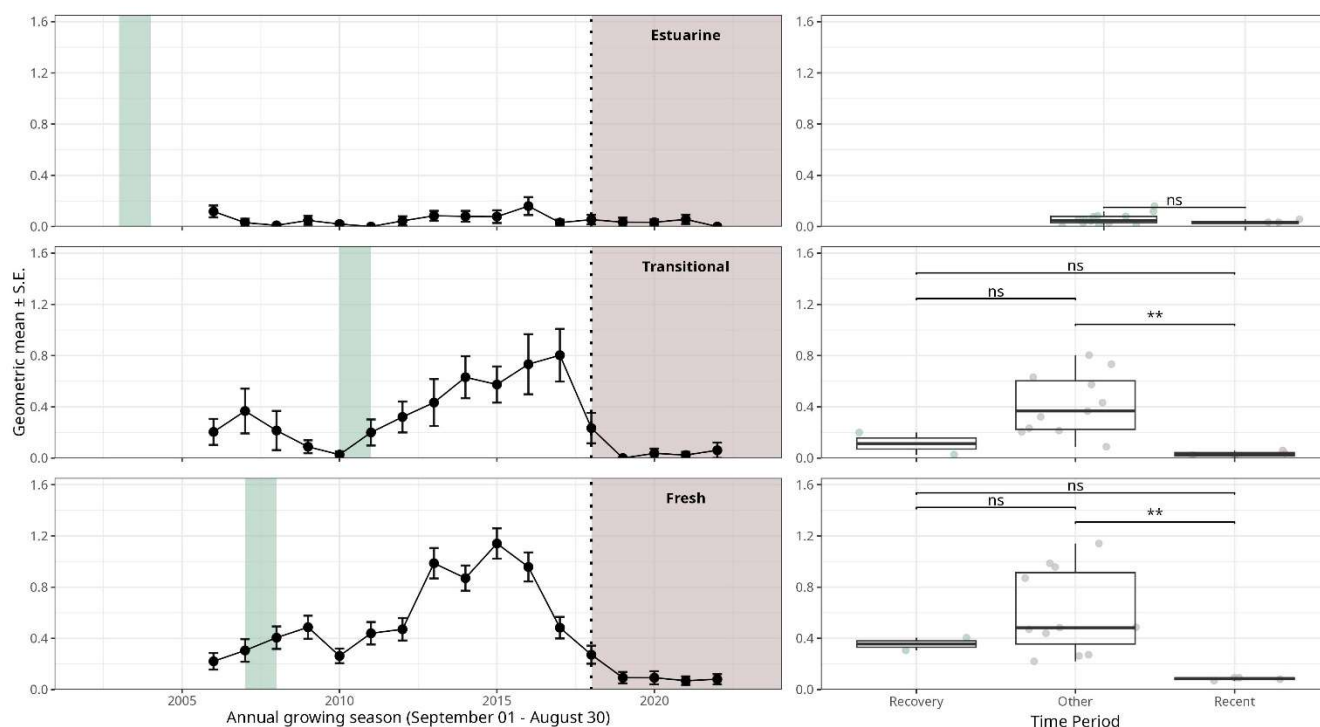


Figure 3.11 Relative abundance with standard error of golden shiner collected with 21.3 m seines (water depths ≤ 1.8 m) within the estuarine, transitional, and freshwater regions of the lower St. Johns River throughout long-term temporal periods of SAV abundance (recovery, recent, and other). The background colors represent the selected periods for groupwise comparisons (Recovery Period = green, Recent Period = brown). Statistical significance between temporal periods is indicated with asterisks (* = $p < 0.05$, ** = $p < 0.01$, *** = $p < 0.001$, ns = $p > 0.05$).

Rainwater Killifish, *Lucania parva*

Habitat characteristics and relative abundance

The rainwater killifish is a small, mostly estuarine fish, but also occurs in freshwater and marine waters (Hildebrand and Schroeder 1928, Page and Burr 2011). They primarily inhabit shallow water along the coast but are also found well inland. They are usually found over sand or mud bottoms in vegetated areas, and feed on larval crustaceans (mainly cyclopoid and harpacticoid copepods), mosquito larvae, small worms, and mollusks (Hassan-Williams et al. 2007).

Rainwater killifish were commonly collected throughout all months but had peak abundances in the months of April – June (Figure 3.12). They were collected in high abundances in Zones 3–6, typically in salinities between 0.5 and 4.99. Rainwater killifish were most abundant on vegetated bottom habitats (Figure 3.12).

Lucania parva (Rainwater Killifish) in 21.3-m seines

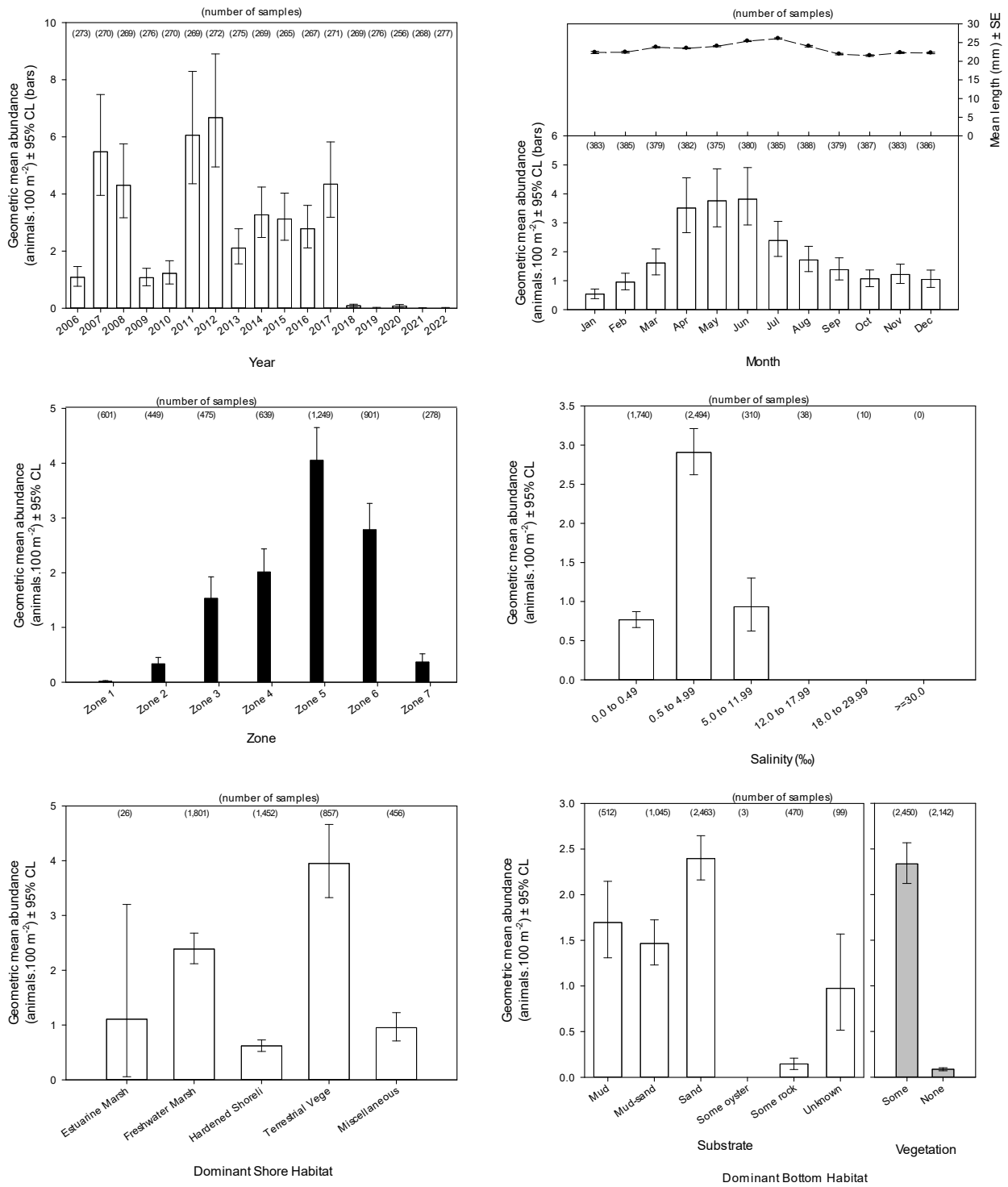


Figure 3.12 Relative abundance of rainwater killifish collected with 21.3 m seines (water depths ≤ 1.8 m) in the lower St. Johns River. Box: average relative abundance; error bars: 95% CI.

Spatial and temporal trends in relative abundance with SAV recovery periods

The yearly abundance of the rainwater killifish for any sections of the mainstem did not vary between the successful SAV recovery period and the background period ($p_T = 1.00$, $p_F = 0.86$). Additionally, the yearly abundance in the transitional sections did not vary between the successful SAV recovery period and the recent periods ($p_T = 0.33$). The groupwise differences of yearly abundance of the rainwater killifish occurred in all mainstem regions between the background period and the recent period ($p_E = 0.01$, $p_T = 0.01$, $p_F = 0.02$) and in the fresh region between the successful SAV recovery period and the recent periods ($p_T = 0.02$). (Figure 3.13) (Table 3.1).

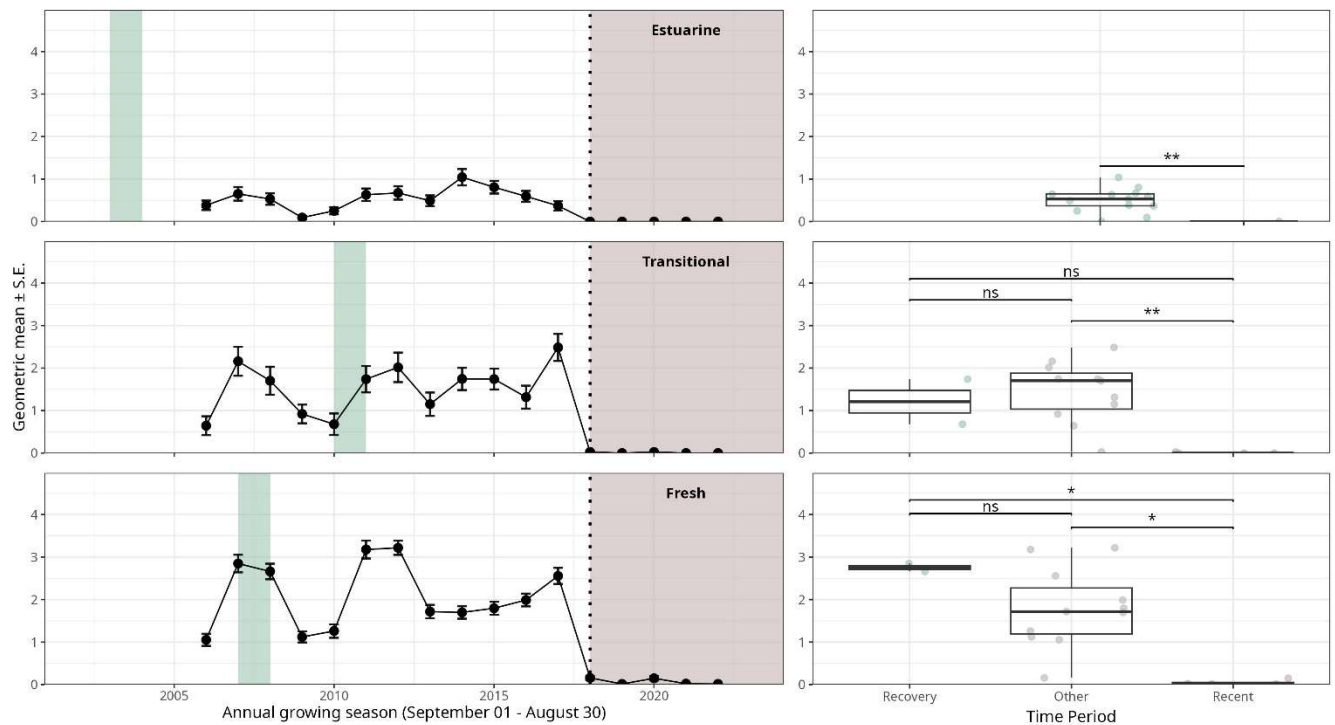


Figure 3.13 Relative abundance with standard error of rainwater killifish collected with 21.3 m seines (water depths ≤ 1.8 m) within the estuarine, transitional, and freshwater regions of the lower St. Johns River throughout long-term temporal periods of SAV abundance (recovery, recent, and other). The background colors represent the selected periods for groupwise comparisons (Recovery Period = green, Recent Period = brown). Statistical significance between temporal periods is indicated with asterisks (* = $p < 0.05$, ** = $p < 0.01$, *** = $p < 0.001$, ns = $p > 0.05$).

Eastern Mosquitofish, *Gambusia holbrooki*

Habitat characteristics and relative abundance

The Eastern Mosquito, *Gambusia holbrooki*, fish is the most common freshwater fish in Florida. They are typically found on the surface and edges of ponds, lakes, backwaters, canals, and sluggish streams (Boschung and Mayden 2004, Page and Burr 2011). They are also sometimes found in brackish waters (Robins et al. 2018). Mosquitofish are commonly used in Florida to reduce mosquito populations (Connelly et al. 2014). Mosquitofish can tolerate variation in water temperature, salinity, and dissolved oxygen, making them adept at surviving in stagnant pools, large puddles, and swamps. They are often associated with vegetated areas in these water bodies where they feed on small insects, crustaceans, and plant material (Page and Burr 2011).

Mosquitofish were commonly collected throughout all months but typically had lower abundances in the months of June and July (Figure 3.14). They were most abundantly collected in Zone 5, typically in salinities less than 4.99. Mosquitofish were most abundantly collected on vegetated bottom habitats (Figure 3.14).

Gambusia holbrooki (Mosquitofish) in 21.3-m seines

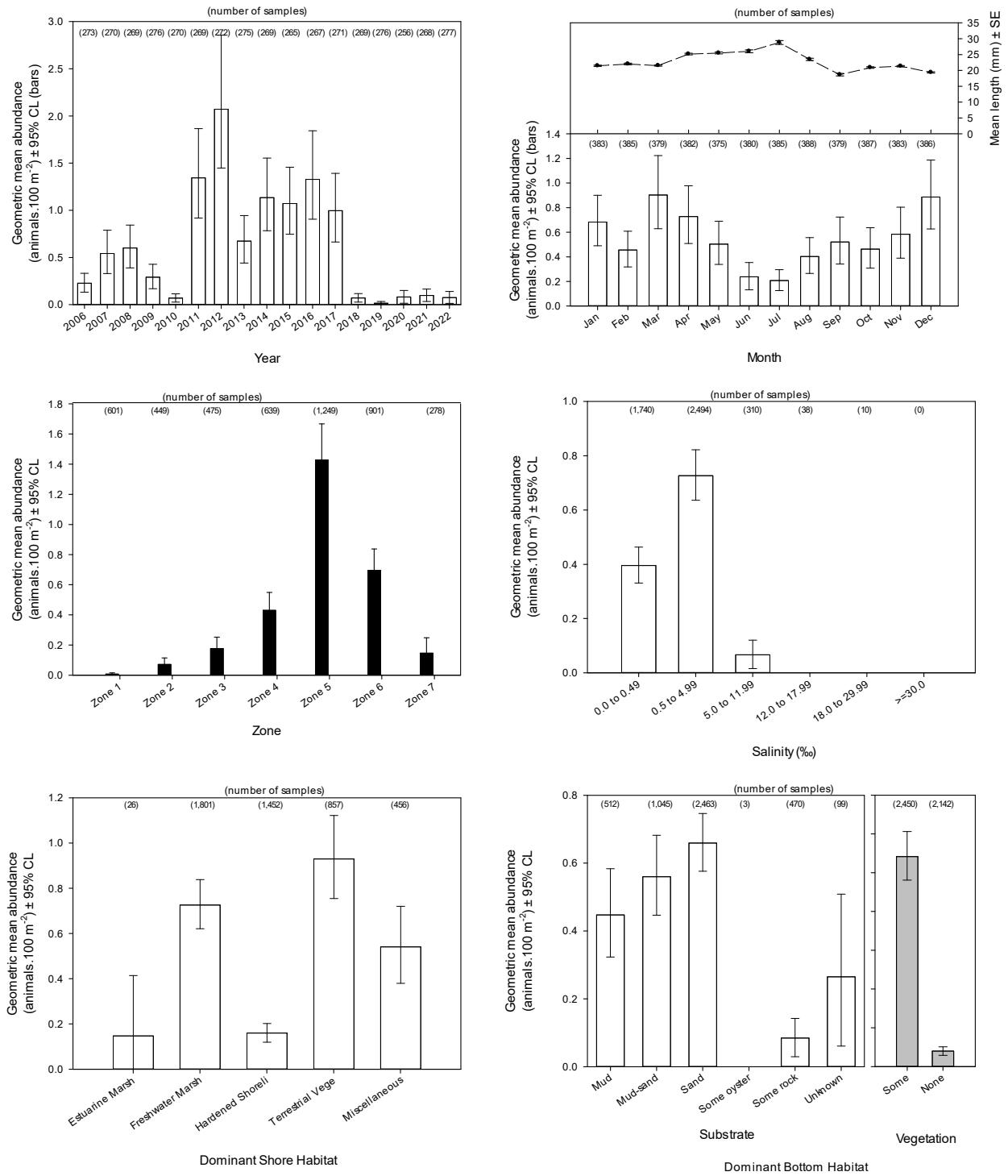


Figure 3.14 Relative abundance of Mosquitofish collected with 21.3 m seines (water depths ≤ 1.8 m) in the lower St. Johns River. Box: average relative abundance; error bars: 95% CI.

Spatial and temporal trends in relative abundance with SAV recovery periods

The yearly abundance of the eastern mosquitofish for any sections of the mainstem did not vary between the successful SAV recovery period and the background period ($p_T = 0.49$, $p_F = 1.00$) nor the successful SAV recovery period and the recent period ($p_T = 1.00$, $p_F = 0.63$). Additionally, the yearly abundance in the estuarine and fresh sections did not vary between the background period and the recent period ($p_E = 0.11$, $p_F = 0.07$). The only groupwise differences of yearly abundance of the eastern mosquitofish occurred in the transitional region between the background period and the recent periods ($p_T = 0.01$) (Figure 3.15) (Table 3.1).

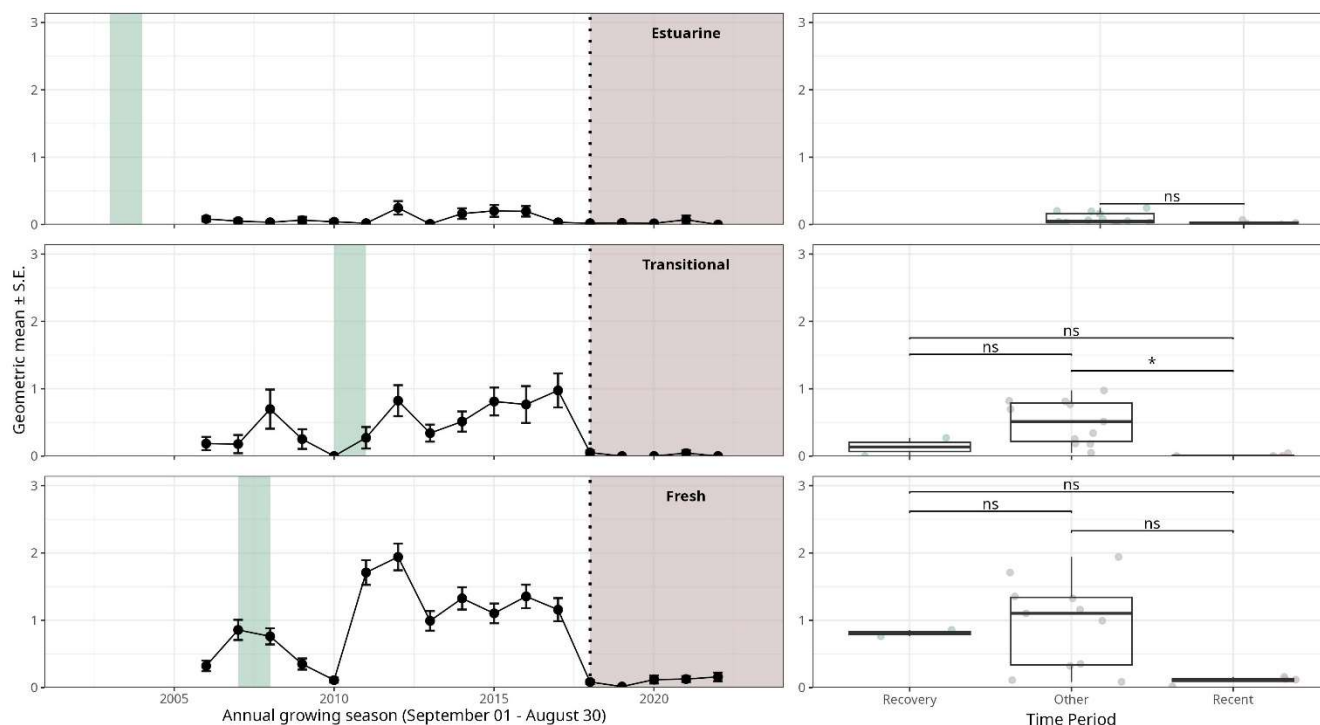


Figure 3.15 Relative abundance with standard error of eastern mosquitofish collected with 21.3 m seines (water depths ≤ 1.8 m) within the estuarine, transitional, and freshwater regions of the lower St. Johns River throughout long-term temporal periods of SAV abundance (recovery, recent, and other). The background colors represent the selected periods for groupwise comparisons (Recovery Period = green, Recent Period = brown). Statistical significance between temporal periods is indicated with asterisks (* = $p < 0.05$, ** = $p < 0.01$, *** = $p < 0.001$, ns = $p > 0.05$).

Bluefin Killifish, *Lucania goodei*

Habitat characteristics and relative abundance

The bluefin killifish is a small freshwater fish, which occasionally enters brackish and even marine waters. They inhabit vegetated sloughs, ditches, ponds, lakes, spring effluents, and pools and backwaters of creeks and rivers (Page and Burr 2011, Robins 2018). Bluefin killifish prefer thickly vegetated habitats, where they usually swim well below the surface. Their food consists of invertebrates, algae, and bits of aquatic plants, such as *Vallisneria sp.* (Rohde et al. 1994, Froese and Pauly 2018).

Bluefin killifish were commonly collected throughout all months but typically had lower abundances in January (Figure 3.16). They were most abundantly collected in Zone 5, typically in salinities less than 4.99. Bluefin killifish were most abundantly collected on vegetated bottom habitats (Figure 3.16).

Lucania goodei (Bluefin Killifish) in 21.3-m seines

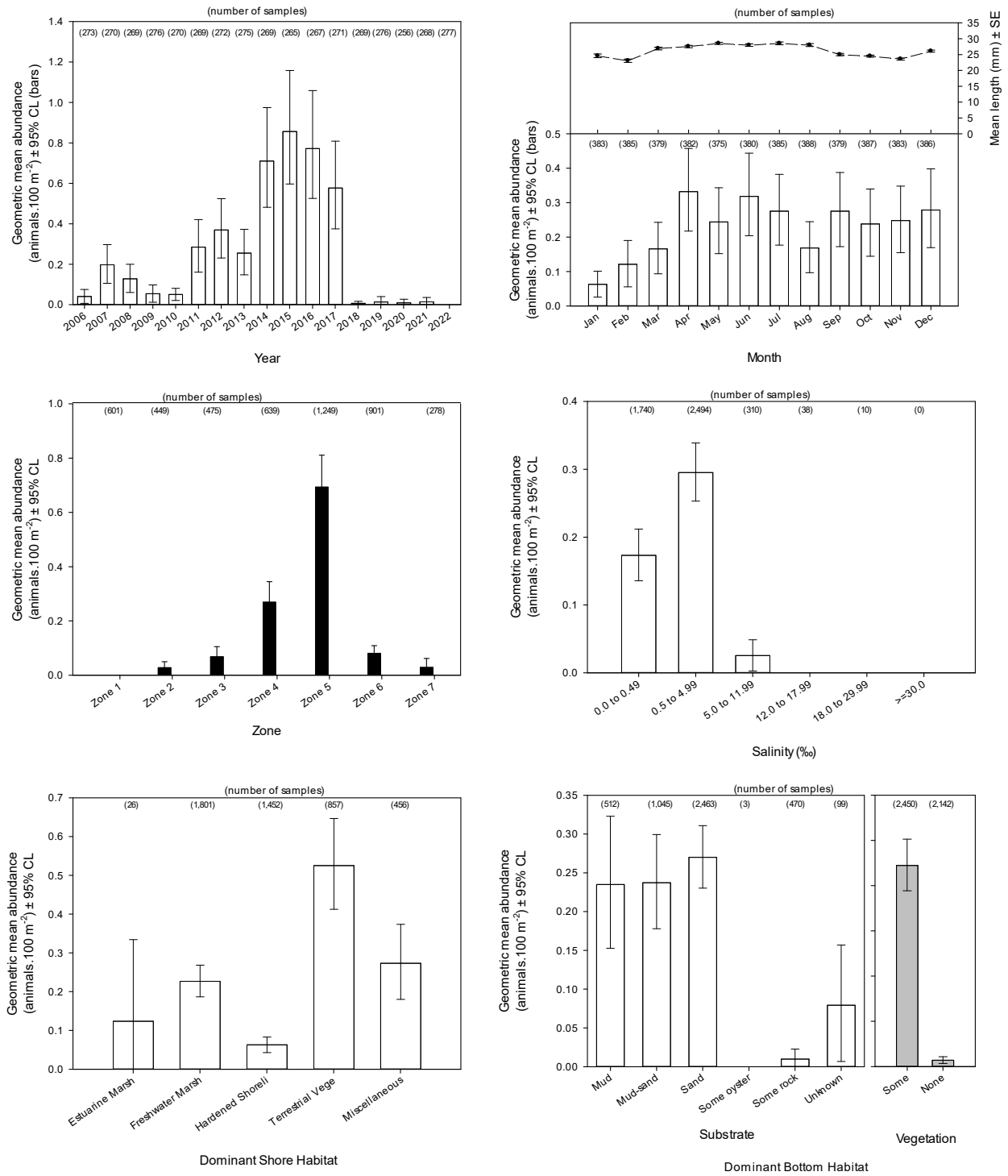


Figure 3.16 Relative abundance of bluefin killifish collected with 21.3 m seines (water depths ≤ 1.8 m) in the lower St. Johns River. Box: average relative abundance; error bars: 95% CI.

Spatial and temporal trends in relative abundance with SAV recovery periods

The yearly abundance of the bluefin killifish for any sections of the mainstem did not vary between the successful SAV recovery period and the background period ($p_T = 0.46$, $p_F = 1.00$) nor the successful SAV recovery period and the recent period ($p_T = 1.00$, $p_F = 0.32$). Additionally, the yearly abundance in the estuarine section did not vary between the background period and the recent period ($p_E = 0.18$). The only groupwise differences of yearly abundance of the bluefin killifish occurred in the transitional and fresh regions between the background period and the recent periods ($p_T = 0.03$, $p_F = 0.01$). (Figure 3.17) (Table 3.1).

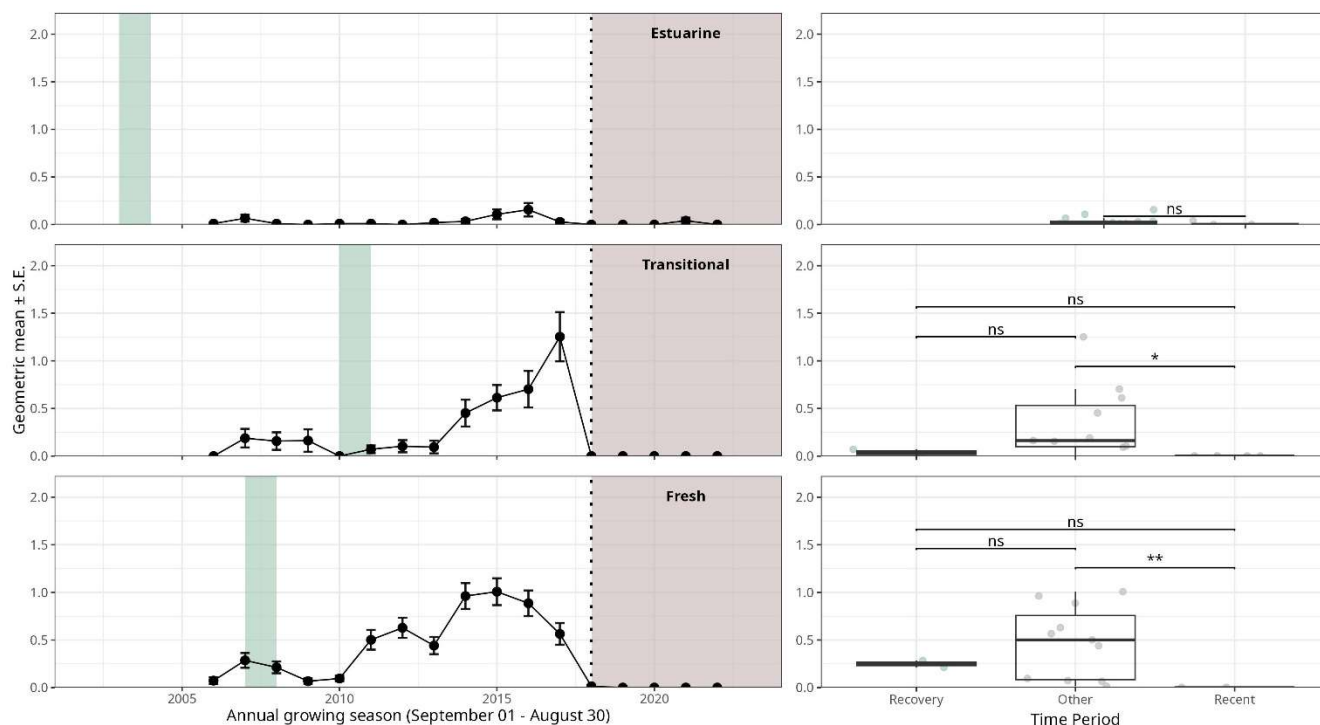


Figure 3.17 Relative abundance with standard error of bluefin killifish collected with 21.3 m seines (water depths ≤ 1.8 m) within the estuarine, transitional, and freshwater regions of the lower St. Johns River throughout long-term temporal periods of SAV abundance (recovery, recent, and other). The background colors represent the selected periods for groupwise comparisons (Recovery Period = green, Recent Period = brown). Statistical significance between temporal periods is indicated with asterisks (* = $p < 0.05$, ** = $p < 0.01$, *** = $p < 0.001$, ns = $p > 0.05$).

Seminole Killifish, *Fundulus seminolis*

Habitat characteristics and relative abundance

The seminole killifish is one of the largest species of *Fundulus* in North America and is endemic to Florida. They inhabit lakes and quiet pools of streams. Small individuals are most often found near vegetation, and adults are more often found in open water (Page and Burr 2011, Robins 2018). Their diet consists of insect larvae, plant seeds, fish eggs, and small crustaceans (Durant et al. 1979).

The seminole killifish was commonly collected throughout all months but typically had peak abundances in the months of June–August (Figure 3.18). They were most abundantly collected in Zone 6, typically in salinities less than 4.99. Seminole killifish were most abundantly collected on vegetated bottom habitats but were also collected on unvegetated bottom habitats (Figure 3.18).

Fundulus seminolis (Seminoe Killifish) in 21.3-m seines

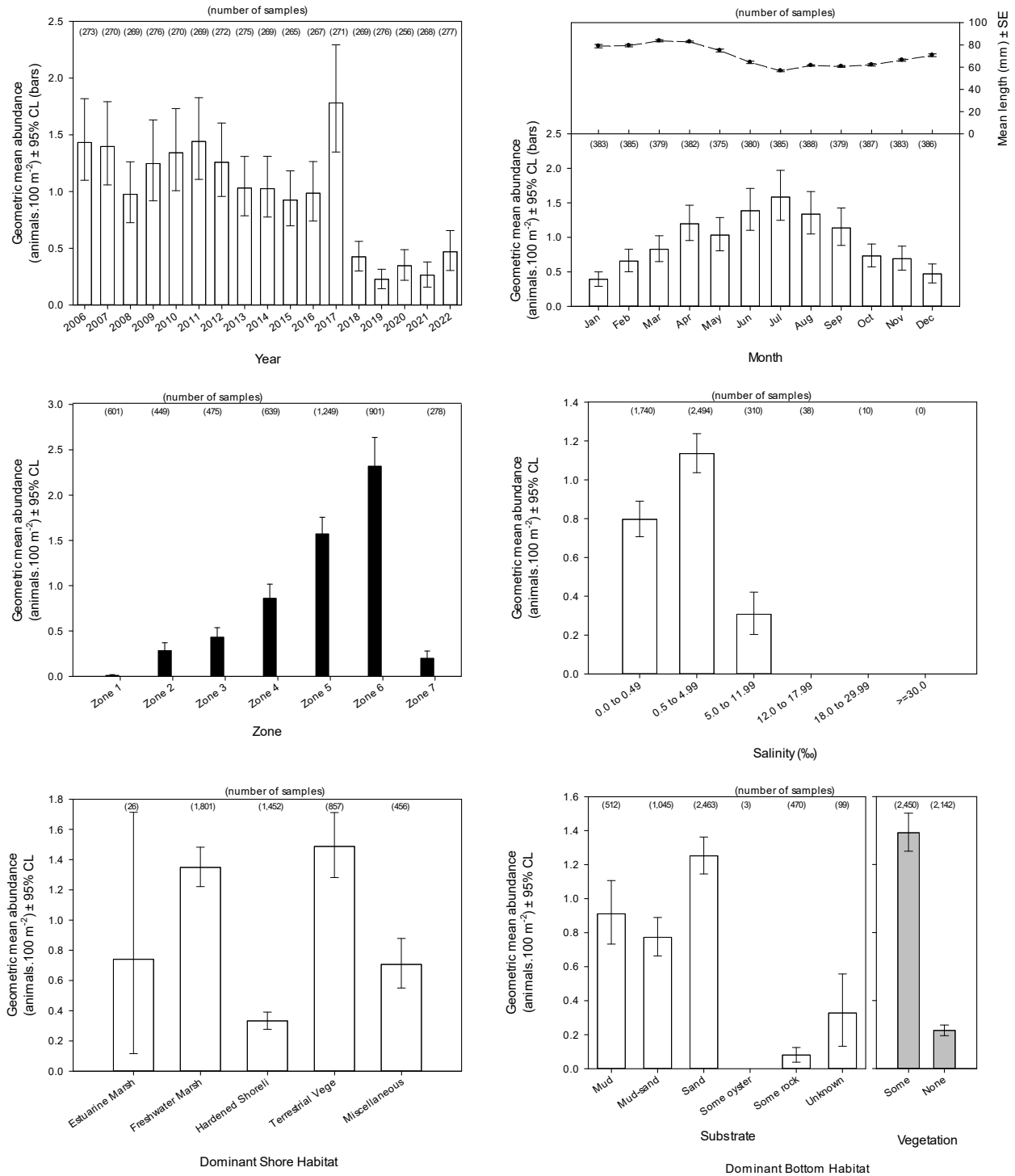


Figure 3.18 Relative abundance of seminoe killifish collected with 21.3 m seines (water depths ≤ 1.8 m) in the lower St. Johns River. Box: average relative abundance; error bars: 95% CL.

Spatial and temporal trends in relative abundance with SAV recovery periods

The yearly abundance of the seminole killifish for any sections of the mainstem did not vary between the successful SAV recovery period and the background period ($p_T = 1.00$, $p_F = 1.00$). Additionally, the yearly abundance in the transitional sections did not vary between the successful SAV recovery period and the recent periods ($p_T = 0.09$). The groupwise differences of yearly abundance of the seminole killifish occurred in all mainstem regions between the background period and the recent period ($p_E < 0.01$, $p_T = 0.01$, $p_F = 0.04$) and in the fresh region between the successful SAV recovery period and the recent periods ($p_T = 0.04$). (Figure 3.19) (Table 3.1).

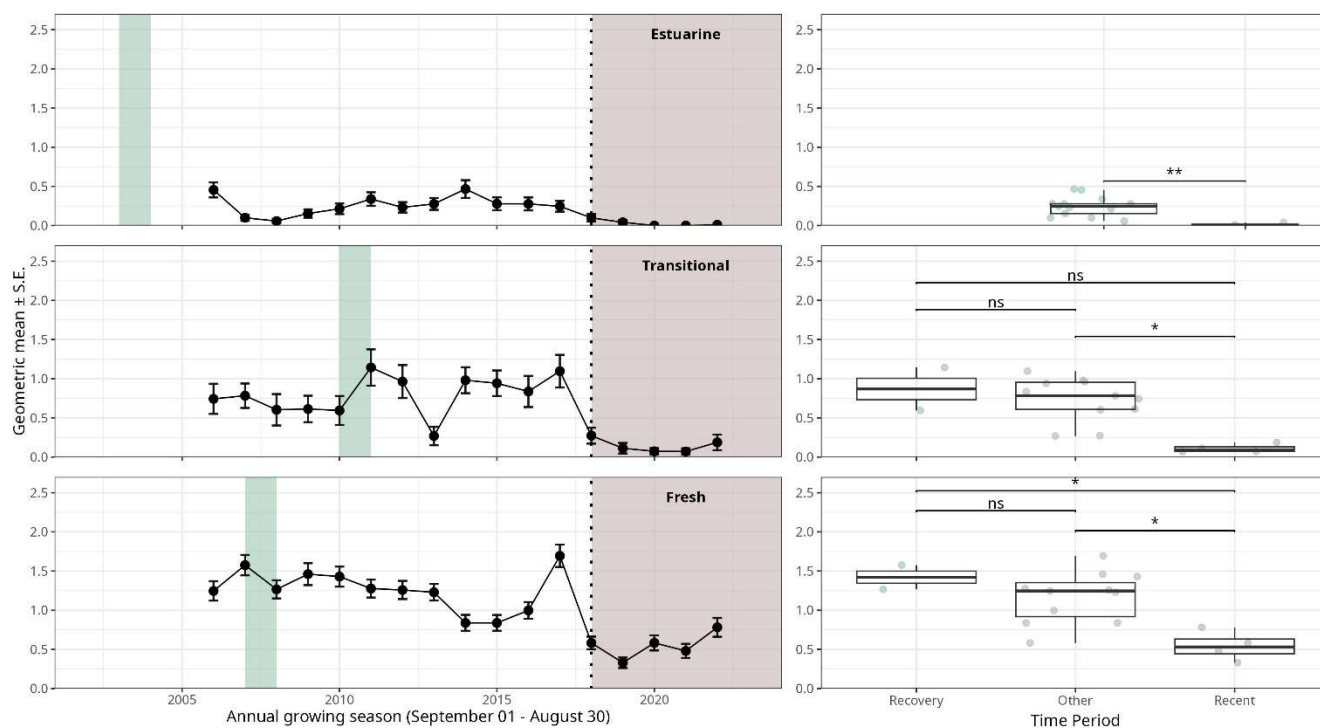


Figure 3.19 Relative abundance with standard error of seminole killifish collected with 21.3 m seines (water depths ≤ 1.8 m) within the estuarine, transitional, and freshwater regions of the lower St. Johns River throughout long-term temporal periods of SAV abundance (recovery, recent, and other). The background colors represent the selected periods for groupwise comparisons (Recovery Period = green, Recent Period = brown). Statistical significance between temporal periods is indicated with asterisks (* = $p < 0.05$, ** = $p < 0.01$, *** = $p < 0.001$, ns = $p > 0.05$).

Least Killifish, *Heterandria formosa*

Habitat characteristics and relative abundance

The least killifish is one of the smallest freshwater fish species in North America, with females maturing at 15 mm SL (Bennett and Conway 2010). The least killifish inhabits vegetated areas of lakes, ponds, sloughs, ditches, swamps, and backwaters of pools and streams. They are sometimes found in brackish water (Robins et al. 2018). Least killifish primarily eats aquatic invertebrates such as worms, crustaceans, and plant (Mills and Vevers 1989, Boschung and Mayden 2004).

Least killifish were commonly collected throughout all months but typically had lower abundances in July (Figure 3.20). They were most abundantly collected in Zone 5, typically in salinities less than 4.99. Least killifish were most abundantly collected on vegetated bottom habitats (Figure 3.20).

Heterandria formosa (Least Killifish) in 21.3-m seines

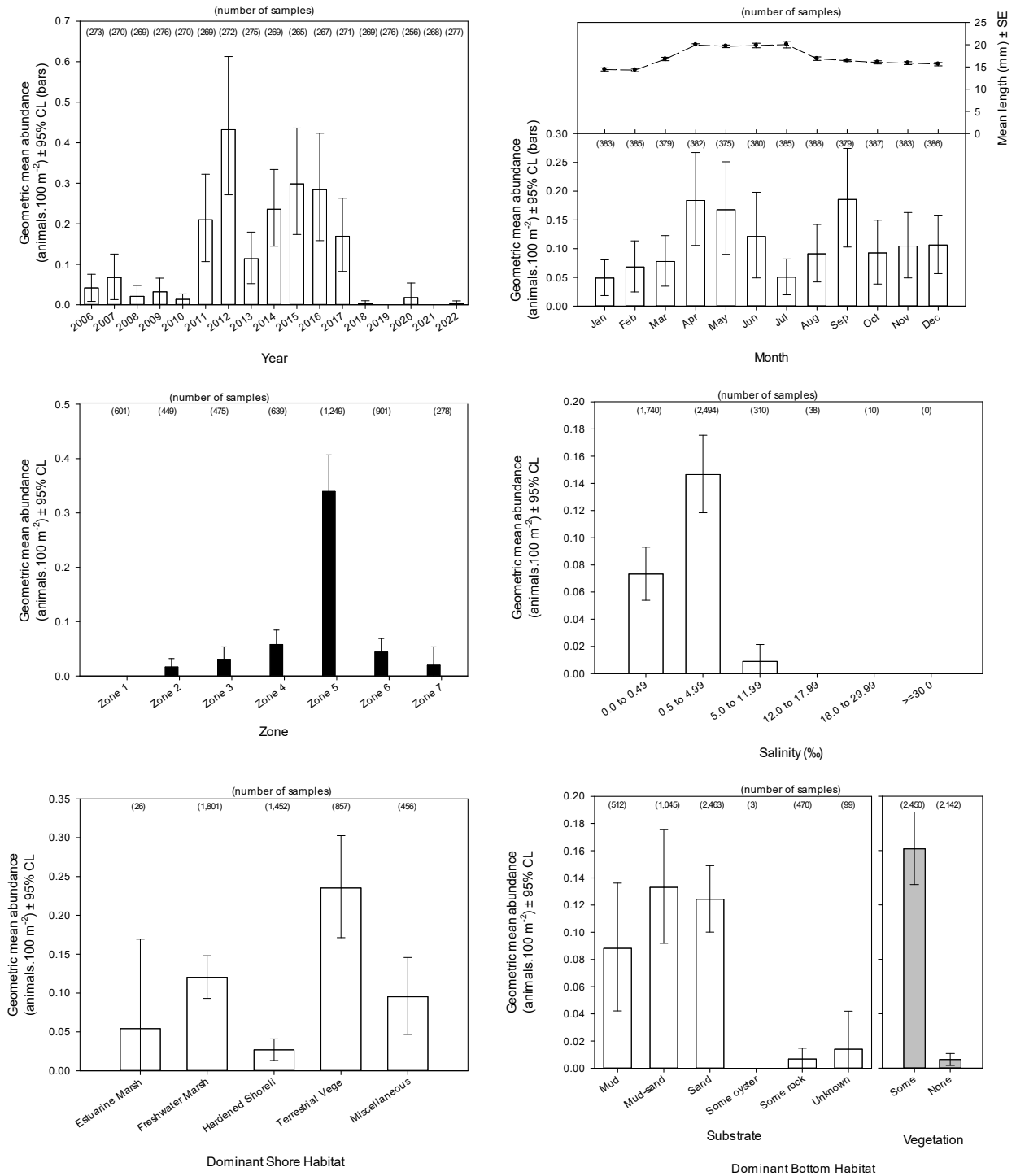


Figure 3.20 Relative abundance of least killifish collected with 21.3 m seines (water depths ≤ 1.8 m) in the lower St. Johns River. Box: average relative abundance; error bars: 95% CI.

Spatial and temporal trends in relative abundance with SAV recovery periods

The yearly abundance of the least killifish for any sections of the mainstem did not vary between the successful SAV recovery period and the background period ($p_T = 1.00$, $p_F = 1.00$) nor the successful SAV recovery period and the recent period ($p_T = 1.00$, $p_F = 0.46$). Additionally, the yearly abundance in the estuarine and transition sections did not vary between the background period and the recent period ($p_E = 0.11$, $p_T = 0.11$). The only groupwise differences of yearly abundance of the least killifish occurred in the fresh region between the background period and the recent periods ($p_F = 0.01$). (Figure 3.21) (Table 3.1).

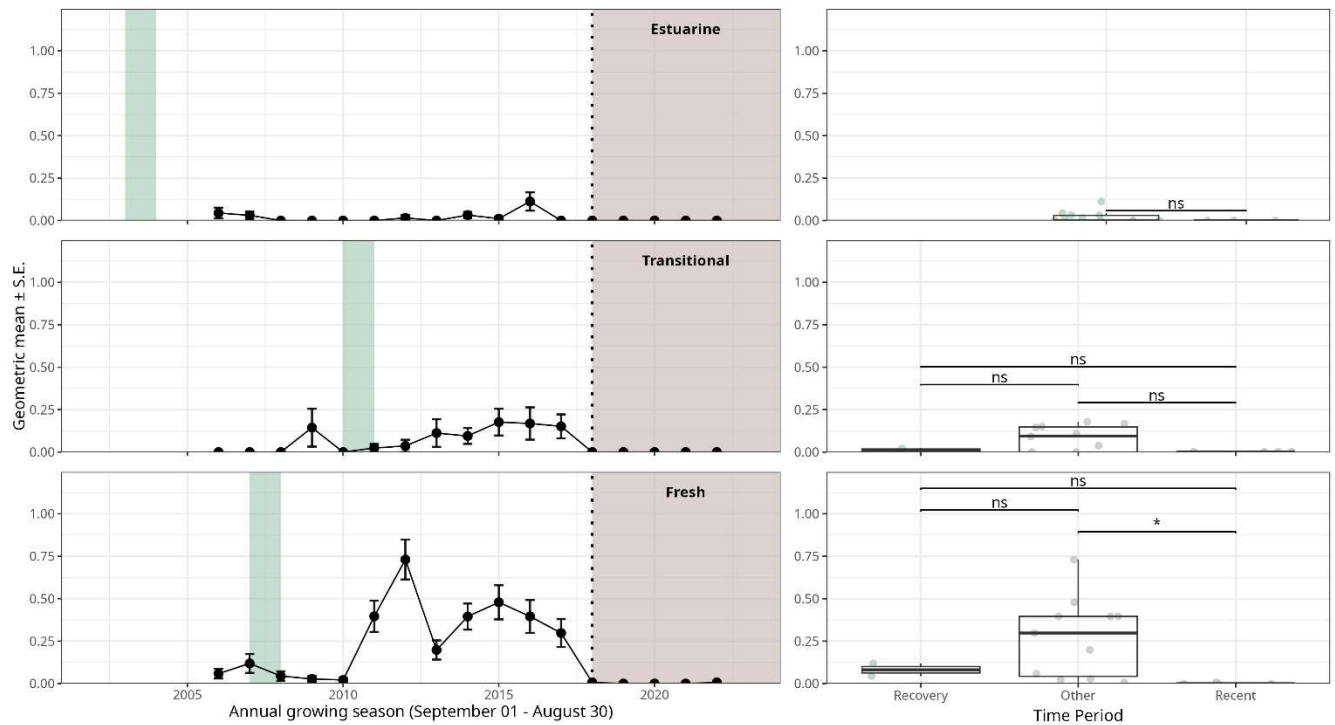


Figure 3.21 Relative abundance with standard error of least killifish collected with 21.3 m seines (water depths ≤ 1.8 m) within the estuarine, transitional, and freshwater regions of the lower St. Johns River throughout long-term temporal periods of SAV abundance (recovery, recent, and other). The background colors represent the selected periods for groupwise comparisons (Recovery Period = green, Recent Period = brown). Statistical significance between temporal periods is indicated with asterisks (* = $p < 0.05$, ** = $p < 0.01$, *** = $p < 0.001$, ns = $p > 0.05$).

Sailfin Molly, *Poecilia latipinna*

Habitat characteristics and relative abundance

Sailfin Mollies are small live-bearing fish that inhabits fresh, brackish, and marine waters. Sailfin Mollies inhabit lakes, ponds, sloughs, pools and backwaters of creeks and small rivers (Robins 2018). They are omnivores, feeding on algae, vegetation, benthic invertebrates, mosquito larvae, and detritus (Rohde et al. 1994).

Sailfin Mollies were commonly collected throughout all months but typically had lower abundances in February (Figure 3.22). They were most abundantly collected in Zones 5 and 6 and were most common in salinities between 0.5 and 4.99. Sailfin Mollies were most abundantly collected on vegetated bottom habitats (Figure 3.22).

Poecilia latipinna (Sailfin Molly) in 21.3-m seines

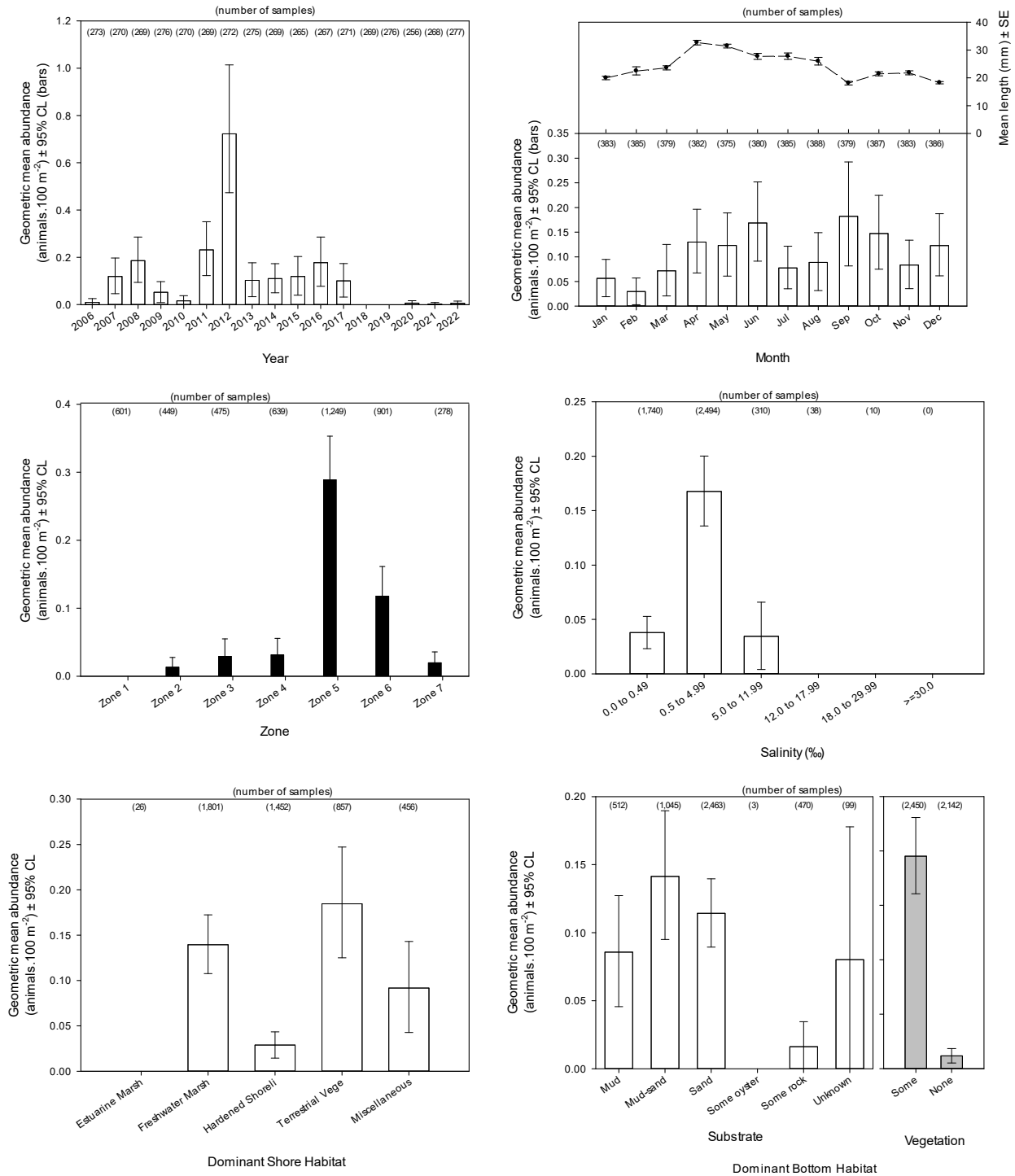


Figure 3.22 Relative abundance of sailfin molly collected with 21.3 m seines (water depths ≤ 1.8 m) in the lower St. Johns River. Box: average relative abundance; error bars: 95% CI.

Spatial and temporal trends in relative abundance with SAV recovery periods

The yearly abundance of the sailfin molly for any sections of the mainstem did not vary between the successful SAV recovery period and the background period ($p_T = 0.36$, $p_F = 1.00$) nor the successful SAV recovery period and the recent period ($p_T = 1.00$, $p_F = 0.05$). Additionally, the yearly abundance in the estuarine and transition sections did not vary between the background period and the recent period ($p_E = 1.00$, $p_T = 0.12$). The only groupwise differences of yearly abundance of the sailfin molly occurred in the fresh region between the background period and the recent periods ($p_F = 0.04$). (Figure 3.23) (Table 3.1).

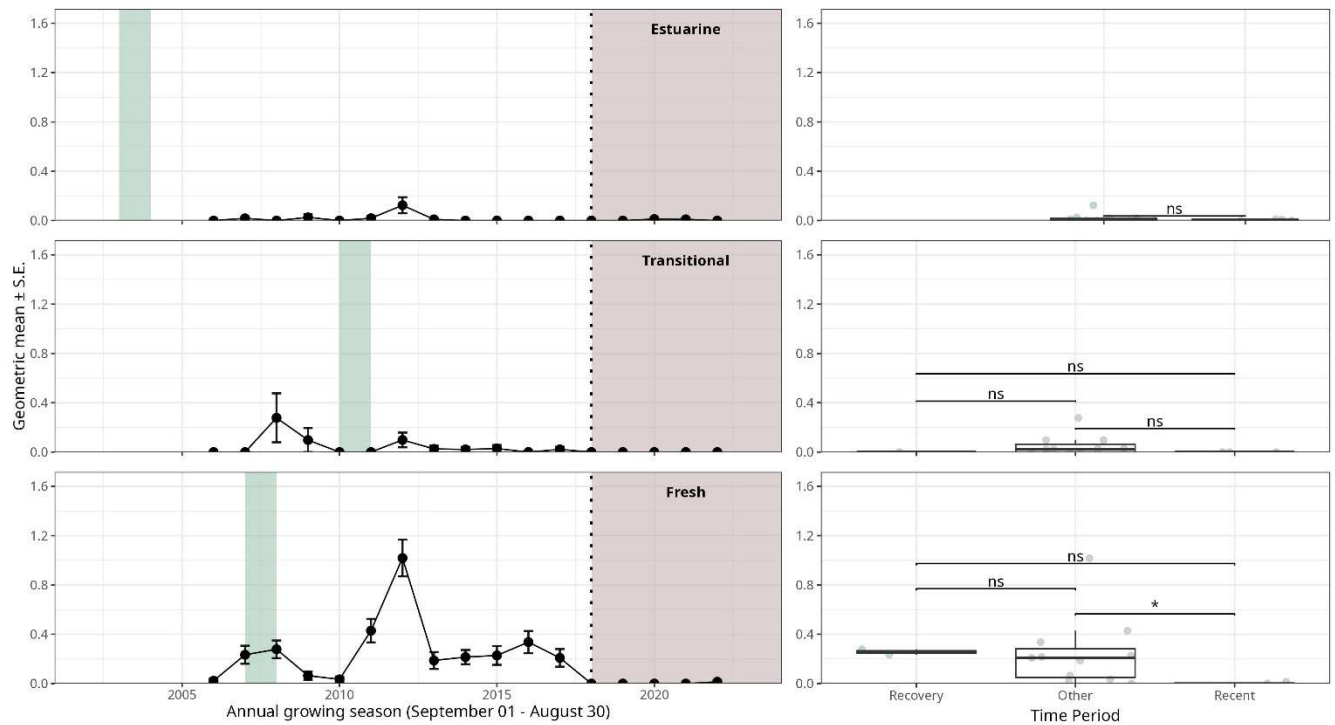


Figure 3.23 Relative abundance with standard error of sailfin molly collected with 21.3 m seines (water depths ≤ 1.8 m) within the estuarine, transitional, and freshwater regions of the lower St. Johns River throughout long-term temporal periods of SAV abundance (recovery, recent, and other). The background colors represent the selected periods for groupwise comparisons (Recovery Period = green, Recent Period = brown). Statistical significance between temporal periods is indicated with asterisks (* = $p < 0.05$, ** = $p < 0.01$, *** = $p < 0.001$, ns = $p > 0.05$).

Pinfish, *Lagodon rhomboides*

Habitat characteristics and relative abundance

Pinfish is an ecologically and recreationally important sparid found in marine and estuarine waters from Massachusetts to Texas (Bigelow 1953, Caldwell 1957). It is one of the most abundant resident species in estuaries of the northeastern Gulf of Mexico (Hoesel and Jones 1963, Ogren and Brusher 1977). Densities of pinfish have been found to be positively correlated to seagrass and drift algae (Rydene and Matheson 2003, Faletti et al. 2019). Studies have shown that predation by pinfish plays a role in the organization of seagrass macro benthic faunal assemblages (Buzas et al. 1976, Young and Young 1977). Pinfish are a major link between primary and secondary production as individuals >60 mm standard length (SL) consume and digest seagrasses and encrusting epiphytes (Stoner 1980, Weinstein et al. 1982, Montgomery and Targett 1992). Pinfish represent a large percentage of the offshore movement of nearshore nutrients and carbon to reef fish stocks in the Gulf of Mexico (Nelson et al. 2013). Pinfish of all sizes are commonly targeted by anglers for use as bait.

Pinfish were most abundant in the study area between the months of April and July (Figure 3.24). Within the nearshore habitat sampled with 21.3 m seines, pinfish were most abundant in salinities ranging from 5.0–17.99 and were most abundant in Zones 3 and 7. Pinfish were commonly collected on both vegetated and unvegetated bottom habitats (Figure 3.24).

Lagodon rhomboides (Pinfish) in 21.3-m seines

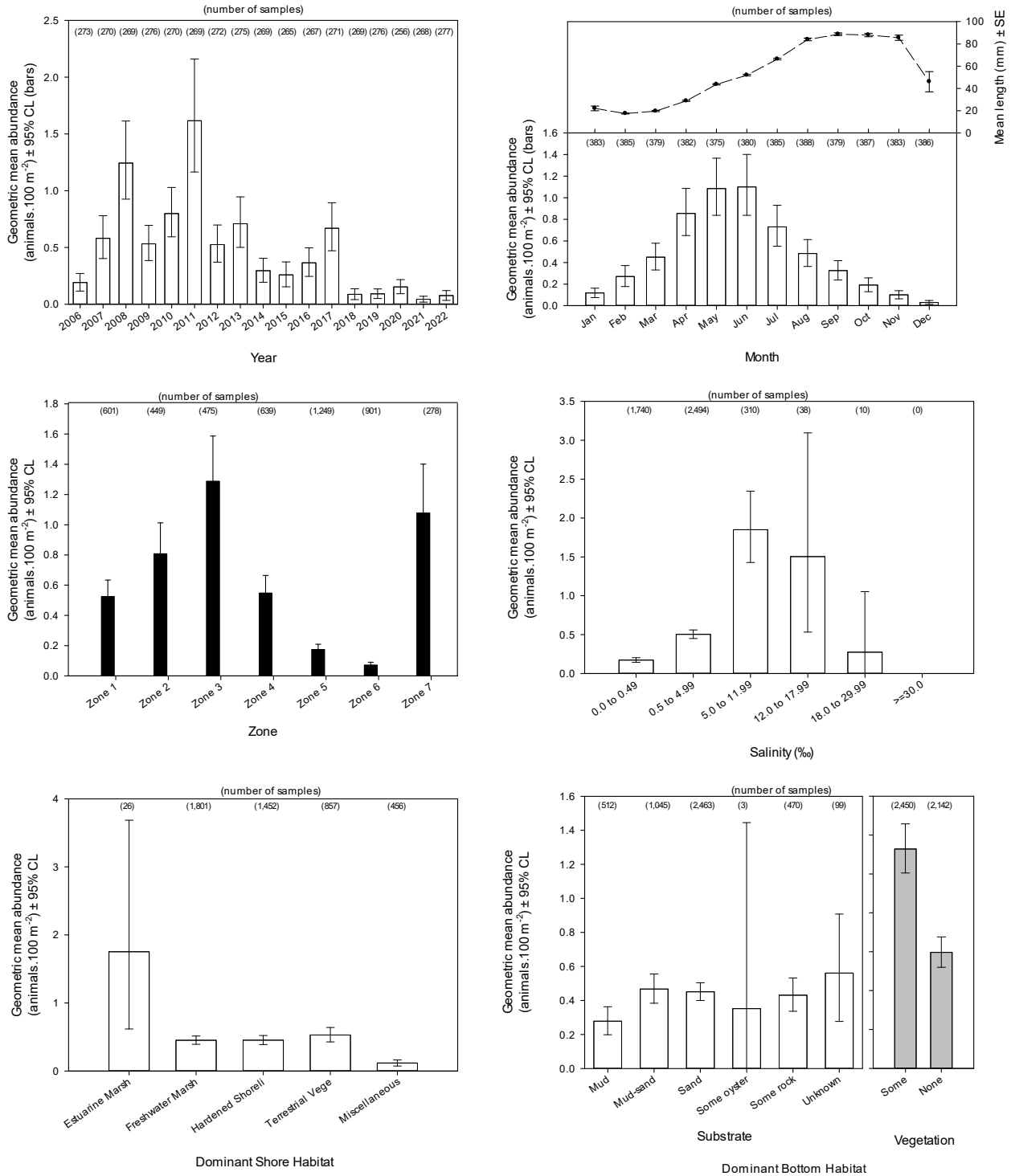


Figure 3.24 Relative abundance of pinfish collected with 21.3 m seines (water depths ≤ 1.8 m) in the lower St. Johns River. Box: average relative abundance; error bars: 95% CI.

Spatial and temporal trends in relative abundance with SAV recovery periods

The yearly abundance of the pinfish for any sections of the mainstem did not vary between the successful SAV recovery period and the background period ($p_T = 0.50$, $p_F = 0.51$). The yearly abundance in the transitional and fresh sections did not vary between the background period and the recent period ($p_T = 0.20$, $p_F = 0.73$). Additionally, the yearly abundance in the fresh region did not vary between the background period and the recent periods ($p_F = 0.14$). The only groupwise differences of yearly abundance of the pinfish occurred in the estuarine region between the background period and the recent periods ($p_F < 0.01$) and in the transitional region between the successful SAV recovery period and the recent periods ($p_T = 0.04$). (Figure 3.25) (Table 3.1).

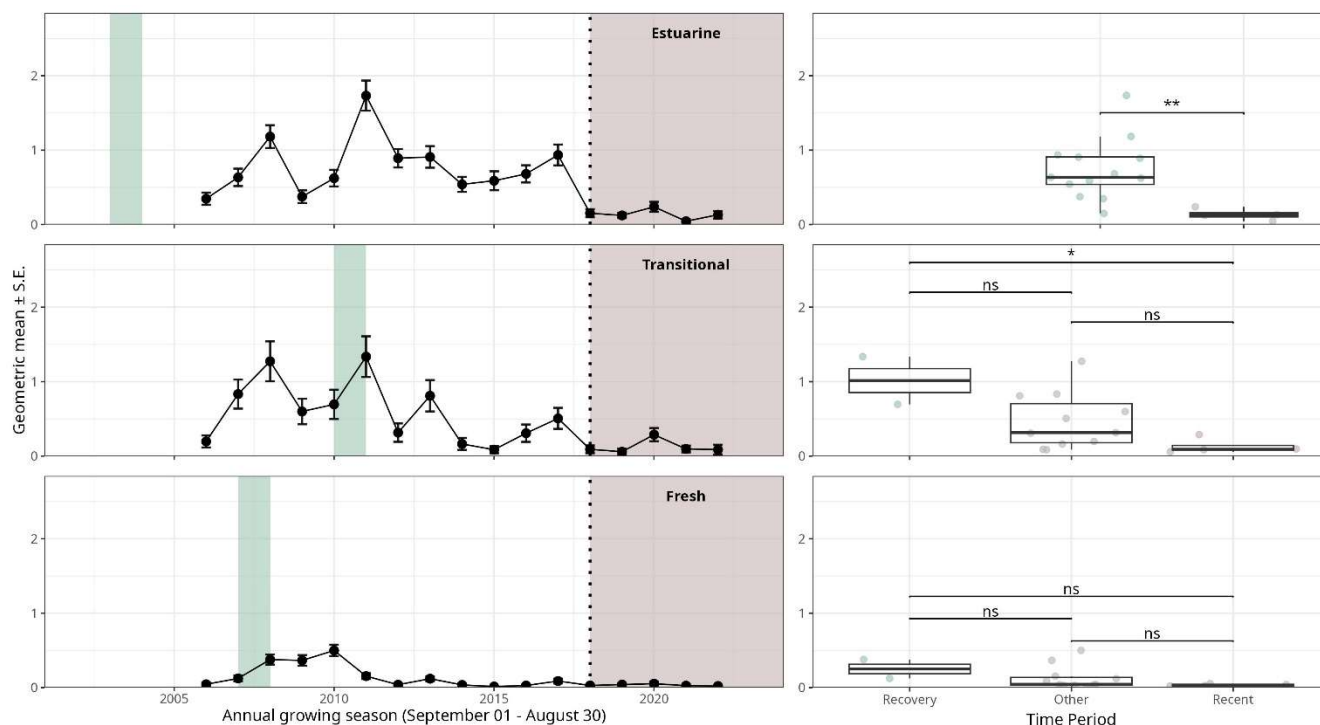


Figure 3.25 Relative abundance with standard error of pinfish collected with 21.3 m seines (water depths ≤ 1.8 m) within the estuarine, transitional, and freshwater regions of the lower St. Johns River throughout long-term temporal periods of SAV abundance (recovery, recent, and other). The background colors represent the selected periods for groupwise comparisons (Recovery Period = green, Recent Period = brown). Statistical significance between temporal periods is indicated with asterisks (* = $p < 0.05$, ** = $p < 0.01$, *** = $p < 0.001$, ns = $p > 0.05$).

Tilapia, *Oreochromis/Sarotherodon* complex

Habitat characteristics and relative abundance

Due to hybridization and difficulties with identification to the species level at different sizes, all specimens of the genera *Tilapia spp.*, *Oreochromis spp.*, and *Sarotherodon spp.* captured were combined into a single complex for analysis for this report. Tilapia were introduced into Florida in the 1960s and can be found extensively in tropical/sub-tropical regions of the US, Central and South America, Africa, and Eurasia. However, their native range is typically represented in parts of Africa and the Middle East. Tilapia are widespread and have abundantly populated Florida's canals, ponds, rivers, streams, lakes, and springs. Sensitivity to salinity varies greatly between species, and some species of tilapia can fully tolerate seawater in marine environments. The most common food consumed by tilapia are green algae, diatoms, plankton, and small invertebrates living in/on bottom detritus (FWC 2024).

Tilapia were most abundant in the study area between the months of May and September with a peak abundance in July (Figure 3.26). They were most commonly collected in Zones 5–7, typically in salinities less than 4.99. Tilapia were most abundantly collected on vegetated bottom habitats (Figure 3.26).

Oreochromis/Saratherodon species (Tilapias) in 21.3-m seines

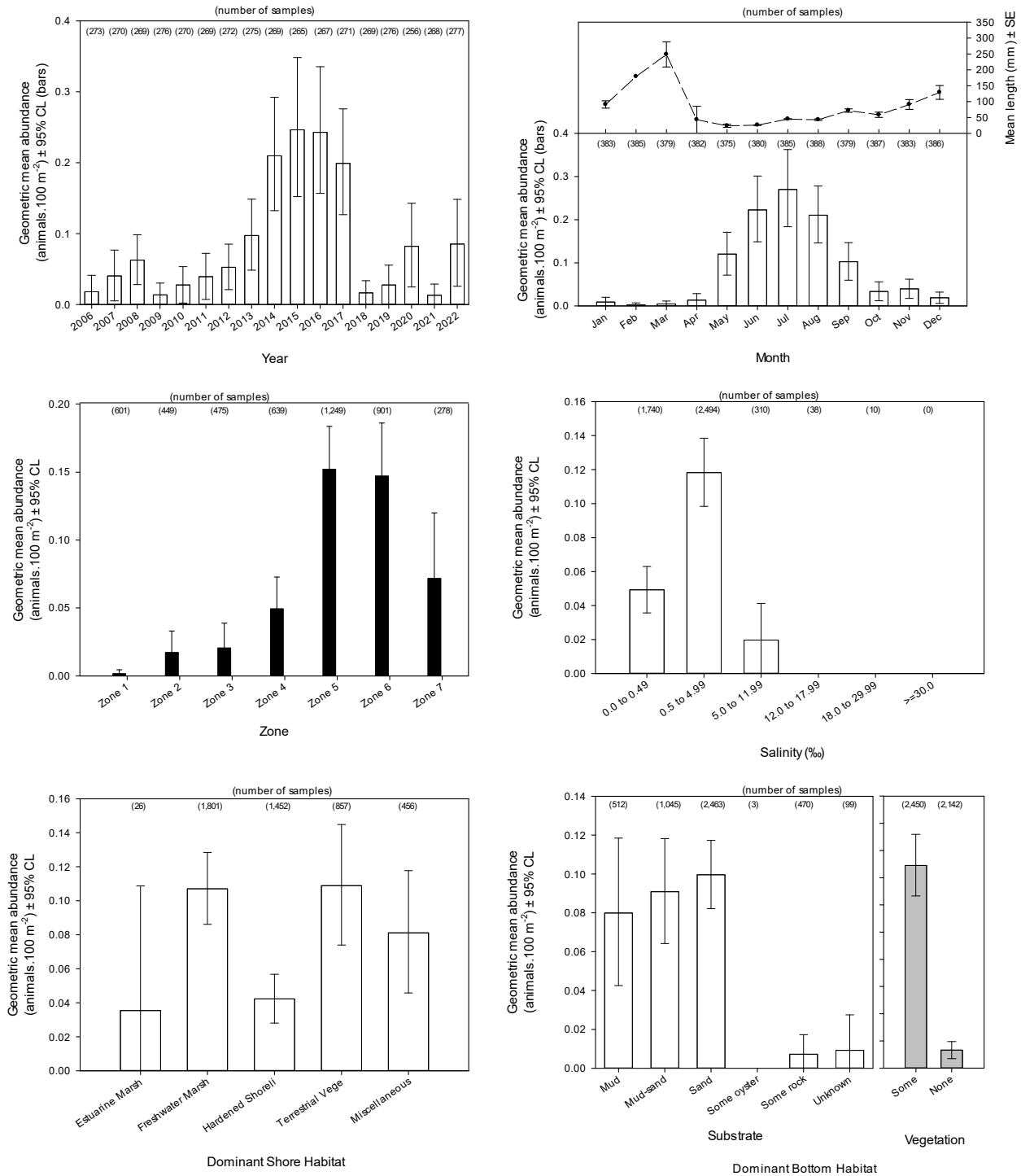


Figure 3.26 Relative abundance of tilapia collected with 21.3 m seines (water depths ≤ 1.8 m) in the lower St. Johns River. Box: average relative abundance; error bars: 95% CI.

Spatial and temporal trends in relative abundance with SAV recovery periods

Despite some fluctuations, the average yearly abundance within each region did not vary among any of the monitoring periods in any Zone of the study area for tilapia (Figure 3. 27) (Table 3.1).

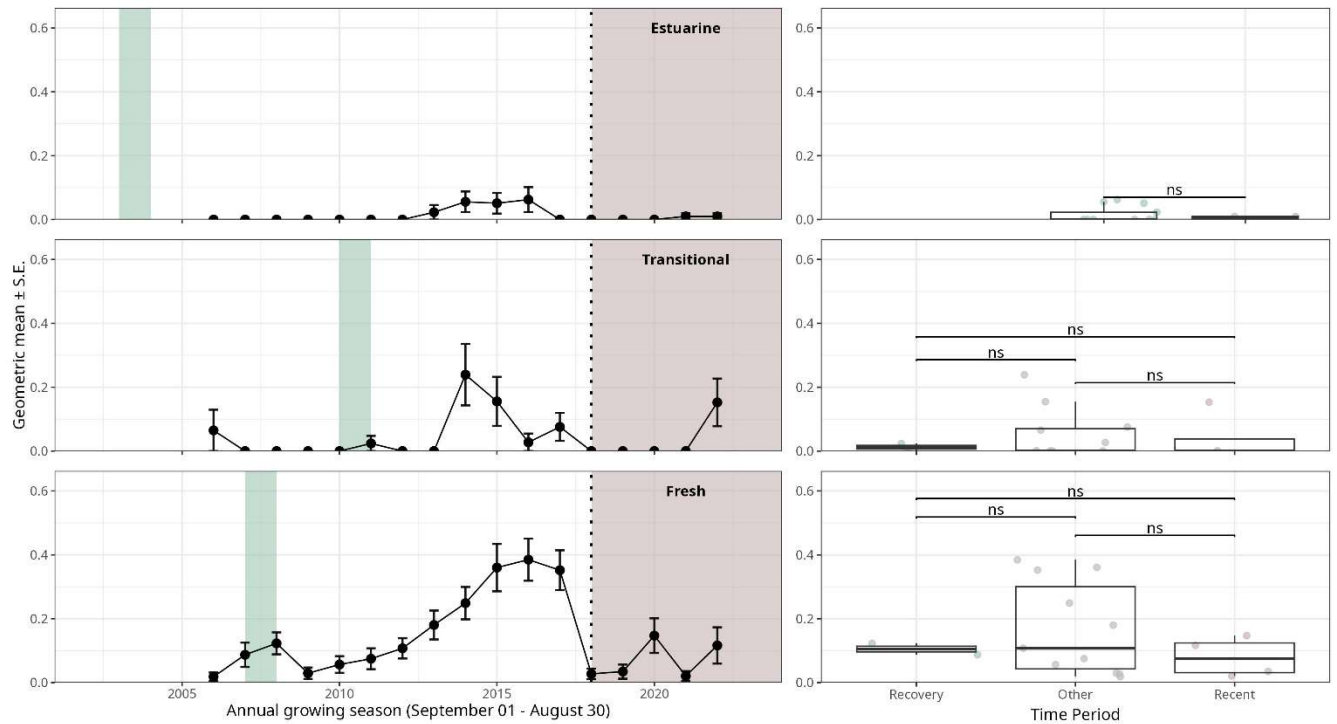


Figure 3.27 Relative abundance with standard error of tilapia collected with 21.3 m seines (water depths ≤ 1.8 m) within the estuarine, transitional, and freshwater regions of the lower St. Johns River throughout long-term temporal periods of SAV abundance (recovery, recent, and other). The background colors represent the selected periods for groupwise comparisons (Recovery Period = green, Recent Period = brown). Statistical significance between temporal periods is indicated with asterisks (* = $p < 0.05$, ** = $p < 0.01$, *** = $p < 0.001$, ns = $p > 0.05$).

Assessment of Relationships Between SAV Recovery Periods and Abundances of Selected
Fish And Macroinvertebrates

Species	Zone	Time period comparison		
		Recovery - Other	Other - Recent	Recovery - Recent
White Shrimp	Estuarine	-	0.09	-
	Transitional	1.00	1.00	1.00
	Fresh	1.00	1.00	1.00
Blue Crab	Estuarine	-	0.21	-
	Transitional	1.00	1.00	1.00
	Fresh	0.29	0.95	1.00
Gizzard Shad	Estuarine	-	0.39	-
	Transitional	1.00	0.11	0.91
	Fresh	1.00	0.61	0.75
Threadfin Shad	Estuarine	-	0.07	-
	Transitional	1.00	0.55	1.00
	Fresh	0.28	0.22	1.00
Golden Shiner	Estuarine	-	0.40	-
	Transitional	0.23	0.01	1.00
	Fresh	1.00	0.01	0.51
Rainwater Killifish	Estuarine	-	0.01	-
	Transitional	1.00	0.01	0.33
	Fresh	0.86	0.02	0.02
Eastern Mosquitofish	Estuarine	-	0.11	-
	Transitional	0.49	0.01	1.00
	Fresh	1.00	0.07	0.63
Bluefin Killifish	Estuarine	-	0.18	-
	Transitional	0.46	0.03	1.00
	Fresh	1.00	0.01	0.32
Seminole Killifish	Estuarine	-	0.00	-
	Transitional	1.00	0.01	0.09
	Fresh	1.00	0.04	0.04
Least Killifish	Estuarine	-	0.11	-
	Transitional	1.00	0.11	1.00
	Fresh	1.00	0.01	0.46
Sailfin Molly	Estuarine	-	1.00	-
	Transitional	0.36	0.12	1.00
	Fresh	1.00	0.04	0.05
Pinfish	Estuarine	-	0.00	-
	Transitional	0.50	0.20	0.04
	Fresh	0.51	0.73	0.14
Tilapia	Estuarine	-	0.89	-
	Transitional	1.00	1.00	1.00
	Fresh	1.00	1.00	1.00

Table 3.1. P values of Bonferroni-corrected Dunn's tests of relative abundance between groups for each species of the study. P values below the alpha of 0.05 are in bold.

Discussion

Throughout the survey it is evident that of the selected species there are both resident species (higher abundance in all months) as well as more seasonally abundant species (higher abundances in select months). Despite this, none of the species showed a significant increase in relative abundance on an annual basis since the most recent SAV die-off. The species that decreased in relative abundance between the recent SAV die-off period and past, higher SAV abundance time periods were more resident species, such as the golden shiner, rainwater killifish, eastern mosquitofish, bluefin killifish, seminole killifish, least killifish, sailfin molly, and pinfish. FWC collected these species predominantly on vegetated bottom habitats. The reduction of SAV as a structure would then disperse these individuals that would previously congregate on vegetated bottom. A cursory investigation into the community structure of the freshwater regions by the FWC has observed a shift in fisheries assemblages to more pelagic species, which are less reliant on SAV during the majority of their life history.

The species that did not differ between the three time periods of successful SAV recovery were white shrimp, blue crab, gizzard shad, threadfin shad, and tilapia. These species can utilize a variety of habitats and are also more seasonal residents within the study area, so the loss of SAV was not as detrimental to their assemblages. Any herbivory stress caused by these species would have stayed constant over time, and when SAV beds were healthy and abundant, the impact that these species made on SAV were minimal. However, when the SAV bed abundances were lower and recovering, the same amount of stress to the SAV by these species could have caused noticeable harm. Additionally, it is possible that their grazing efforts could contribute to reduced canopy height, especially in areas that are too shallow for large grazers such as manatees (*Trichechus manatus latirostris*). Further investigation into the specific biomass of SAV that these individual species consume is needed.

The last aerial synoptic surveys for manatees occurred in 2021/2022 and Gowan et al. (2023) estimated a 95% CI of 20–130 individuals in the LSJR, which has stayed constant since the initial synoptic survey in 2011/2012. It is important to note that the report highlights the high variability in manatee estimates for this region because of the water's color and various depths (Gowan et al. 2023). White et al. 2002, observed manatee distribution in our Estuarine region was correlated with season and high concentrations of *V. americana*. Dr. Pinto at Jacksonville University has continued annual aerial and aquatic sighting surveys, which is posted on their on the Manatee Research Center Online (MaRCO) website (<https://www.ju.edu/marco/>). Over the years, areas near Mandarin Point and Fleming Island continue to have a high number of manatee sightings, which Section 1 describes as having long beds of SAV.

Despite the large effect of cooters (*Pseudemys spp.*) on SAV biomass in other systems and evidence of intense grazing by cooters in Silver Glen Spring and Lake George, the FIMS data contained too few observations of cooters to allow for robust analysis (Harwell and Havens 2003, Adler et al. 2018, Timbs and Kolterman 2023).

CONCLUSIONS

Severity of Post-Irma Die-off

The post-Hurricane Irma die-off of SAV was unprecedented within the study period, surpassing previous declines in both scale and persistence. SAV canopy heights and bed widths have remained markedly lower in the years following the storm compared to earlier recovery periods. In all Zones, canopy heights remained near historic lows throughout the post-Irma period. These findings highlight that SAV resilience observed in earlier recovery phases, such as 2002–2004 and 2006–2008, has diminished during of the post-Irma period.

In Zones 2 and 3, SAV bed widths returned to near pre-Irma levels during the recent period, suggesting a partial recolonization of the littoral Zone. However, this recovery has not been uniform across all Zones. Zone 1 exhibited minimal increases in bed width, consistent with its poor canopy height recovery. Additionally, bed widths in Zones 4, 5, and 6 have been volatile during the recent period and declined from 2022 to 2023, the final years of the study period.

Data from the recovery periods indicate that increases in canopy height frequently occur when bed widths are robust. During the recovery periods of Zones 2-5, bed widths were already near study period maximums before canopy heights began to rise. This suggests that the expansion of SAV beds provides a foundation for subsequent vertical growth. Wider beds may facilitate canopy height recovery by stabilizing sediments, reducing erosion, and enhancing nutrient cycling within the SAV ecosystem. As the storm caused bed widths to fall precipitously and recovery has been slow, more substantial increases of bed widths may be required before canopy heights increase.

Light Availability in Freshwater Zones

In freshwater sections (Zones 5 and 6), light availability during the recent period was substantially reduced compared to recovery periods, primarily due to increased water depth and elevated water color driving higher diffuse attenuation coefficients (K_d). During the recovery periods, lower water levels and decreased color contributed to much higher irradiance at the benthic surface, fostering SAV growth. Conversely, the elevated water levels and sustained high color during the recent period impeded light availability, potentially limiting SAV recovery.

Salinity Stress in Estuarine Zones

In estuarine Zones, the salinity regime during the recent period appears to have caused greater physiological stress on *V. americana*, the dominant SAV species. The SSI, which incorporates the intensity, frequency, and duration of high-salinity events, indicates that SAV beds in Zones 1–3 were exposed to higher levels of episodic salinity stress during the recent period compared to recovery periods. While there were no differences in mean salinity between the periods, maximum salinity values were substantially higher during the recent period, reflecting acute stress events. These high-salinity events, combined with elevated light requirements for SAV in brackish waters, may have contributed to reduced bed widths and canopy heights in these regions. However, the temporal resolution of available salinity data limits precise attribution of salinity stress to observed SAV declines, emphasizing the need for finer-scale salinity data in the future.

Limited Role Chlorophyll and Nutrients

Chlorophyll *a*, while important to water quality, was not a differentiating factor between the recovery and recent periods in any LSJR Zone. Chlorophyll *a* concentration varied inconsistently across Zones and periods, with no clear pattern distinguishing recovery and recent conditions. Similarly, TN remained stable or showed minor variations that did not correlate with SAV recovery or decline. TP was lower during the recovery period than the recent period but it is unclear how this affected SAV as it did not coincide with decreased Chlorophyll *a*. Lower TP during the recovery period may have contributed to lower epiphyte loads on SAV and reduced algal mats in the littoral Zones but these phenomena are not measured in SJRWMD ambient data. These results suggest that while nutrient-driven algal blooms may have localized impacts, they were not primary drivers of the broad-scale SAV trends observed in the LSJR.

Nekton Community Dynamics and Herbivory

The relative abundance of herbivorous species associated with vegetated habitats, such as pinfish, have declined significantly in recent years. Meanwhile, generalist species that graze on SAV such as white shrimp, blue crab, and tilapia have remained stable. Due to the severely depressed SAV biomass relative to previous die-offs, a stable background population of these generalists may contribute to reduced canopy height in the wake of Hurricane Irma, particularly in areas inaccessible to larger grazers like manatees. We were unable to quantify the abundance of herbivorous turtles and manatees, two primary species of interest. The relationship between nekton and SAV warrants further investigation to quantify herbivory impacts.

ACKNOWLEDGEMENTS

We gratefully acknowledge the contributions of numerous individuals and teams, past and present, who made this study possible. Special thanks are extended to Anabelle Baggs for her dedication and expertise in coordinating field work and maintaining the extensive SAV dataset used in this analysis. Thanks are also owed to the SJRWMD Bureau of Water Resources Information (WRI) and the Palatka field crew, without whom annual monitoring would not be possible. We also wish to thank Anna Diaz, our intern, for her valuable assistance with data processing and preliminary analyses. We are deeply appreciative of the Environmental Sciences (ES) staff who generously volunteered their time and expertise to support various aspects of this project. Your collective efforts have been instrumental in advancing our understanding of submerged aquatic vegetation dynamics in the Lower St. Johns River. Additionally, we thank the field staff of the Jacksonville Florida Fish and Wildlife Conservation Commission's Fish and Wildlife Research Institute's Fisheries Independent Monitoring (FIM) program for their continued dedication to field sampling and data collection

APPENDIX A ANNUAL VARIABILITY OF SAV ABUNDANCE BY ZONE

Zone 1

From 2002 to 2004, the first three years of the study period, mean canopy height rose 8-fold from 2.1 ± 0.8 cm to 16.9 ± 3.6 cm ($p < 0.001$, Figure A.1). Increases occurred at multiple sites within the Zone but were most pronounced on the east bank of the river between Beauclerc Bluff and Goodby's Creek (Figure A.2). In 2005, canopy heights became more variable, but the mean did not change ($p = 0.982$). In 2006, canopy height fell to 6.6 ± 1.4 cm ($p < 0.001$), less than half the previous mean. Canopy height continued to generally decline over the next five years to a mean of 1.2 ± 0.5 cm in 2011. Monitoring was paused from 2012–2014 and there are no SAV data. 2015 canopy height was 2.7 ± 0.6 cm and rose to 8.7 ± 1.0 cm the next year ($p = 0.008$) before falling again to 1.2 ± 0.5 cm ($p = 0.001$) in 2017. After Hurricane Irma there were no year-over-year changes in the mean until 2023, when canopy height dropped to a near study-period-low of 0.6 ± 0.6 cm ($p = 0.043$). The declines from 2022 to 2023 may be influenced by monitoring limitations as three stations north of Goodby's Creek that historically maintained SAV beds, including small beds in 2022, were not monitored in 2023.

Mean bed width rose over 5-fold from 8.2 ± 4.8 meters in 2002 to 44.7 ± 11.0 m in 2004 ($p < 0.001$), coinciding with the increase in canopy height. Mean bed width remained stable through 2006 ($p = 0.921$) but fell to 17.9 ± 6.5 m in 2007 ($p < 0.001$). The decline continued through 2009 when SAV disappeared from all but two sites in the Zone and mean bed width was 1.5 ± 1.4 m ($p < 0.001$, Figure A.3). By 2011, bed width partially recovered to 12.9 ± 5.0 m ($p = 0.004$). When monitoring resumed in 2015, mean bed width was 33.1 ± 9.9 m and increased the following year to a study period high of 52.7 ± 10.2 m ($p = 0.001$). Bed width fell almost 10-fold to 5.7 ± 3.3 m ($p < 0.001$) between the 2016 and 2017 monitoring, prior to Hurricane Irma, and did not change after the storm in 2018 ($p = 0.900$). Bed width fluctuated from 2018–2023, reaching a post-Irma high of 14.8 ± 7.9 m in 2022 ($p < 0.001$). In 2023, SAV was only found at a single site in the Zone and the mean fell to 0.5 ± 0.5 m ($p < 0.001$).

Percent occurrence followed a near identical temporal pattern as canopy height and bed width, rising consecutively from 2002–2004, before falling in 2009. Then 2016 was the only year when SAV was observed at 100% of monitoring sites. SAV was observed less frequently in the northern, downstream sites as they approach salinities beyond the physiological limits of the freshwater plants that inhabit the river.

Period Delineation

- Recovery Period (September 2002 – August 2004)
- Recent Period (September 2017 – August 2023)

September 2002 through August 2004 was selected as the recovery period due to consecutive bed width and percent occurrence increases from 2002 to 2003 and 2003 to 2004 and the large canopy height increase between 2002 and 2003. September 2017 through August 2023 was selected as the recent post die-off scenario. Mean Canopy height and bed width did not differ between the start of the recovery period and the start of the recent period ($p_{CH} = 0.99$,

$p_{BW} = 0.99$) though percent occurrence was lower in 2017. By the end of the recovery period, mean canopy height was 7 times greater than the highest mean canopy height during the recent period and bed width was 3 times higher. Despite starting from similar standing stocks, the 2002–2004 period exhibited substantial recovery while the recent period did not.

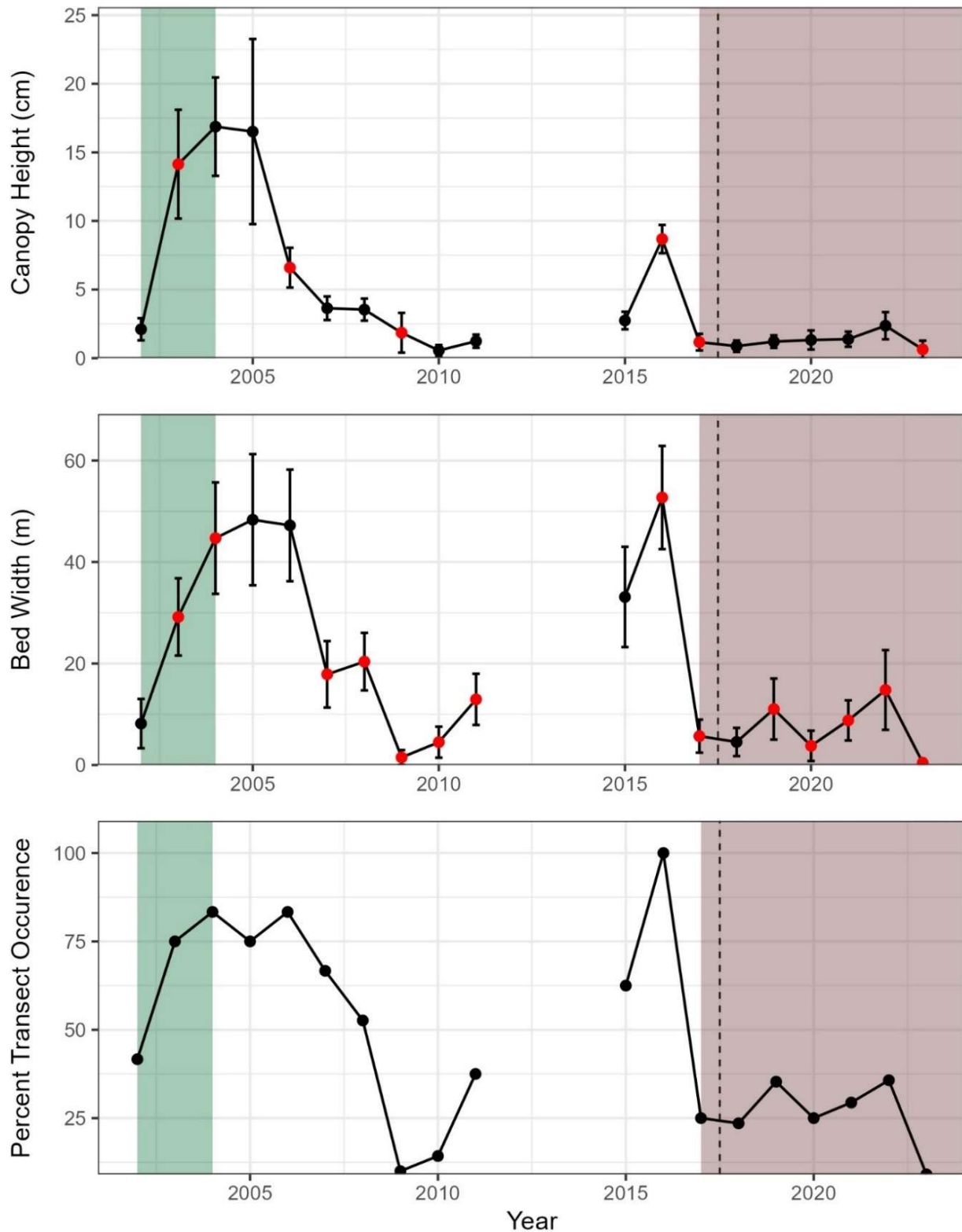


Figure A.1 Time series of annual mean SAV canopy height, bed width, and percent occurrence within Zone 1 of the Lower St. Johns River from 2002–2023. Error bars depict the standard error, and red points indicate a statistically significant change ($p < 0.05$) from the previous year in the generalized linear model. The background colors represent the selected periods for groupwise comparisons (Recovery Period = green, Recent Period = brown).

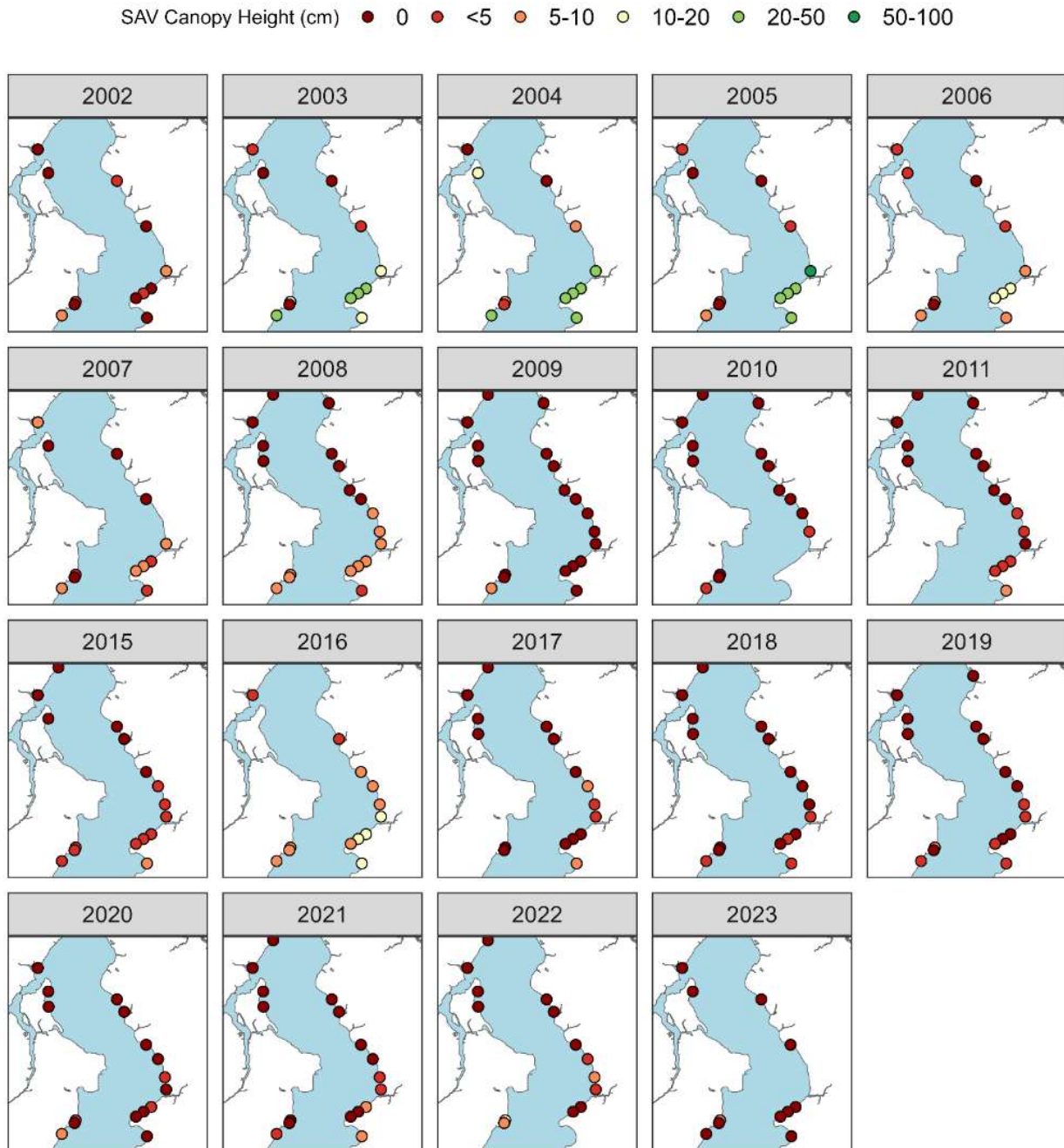


Figure A.2 Map of SAV canopy height at each transect over the study period in Zone 1.

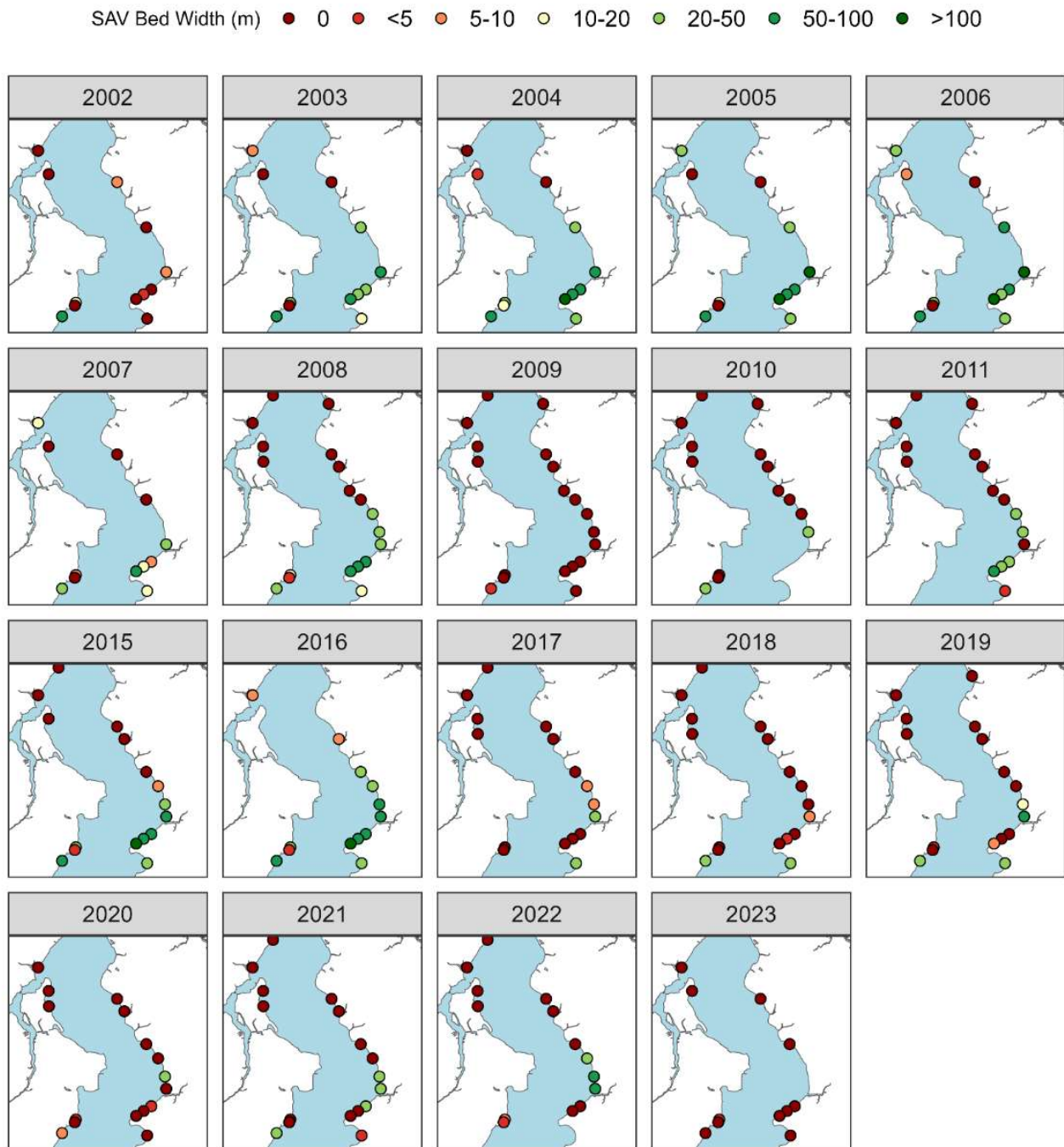


Figure A.3 Map of SAV bed width at each transect over the study period in Zone 1.

Zone 2

From 2002 to 2004 mean canopy height rose from 6.0 ± 0.7 cm to 28.5 ± 3.1 cm ($p < 0.001$, Figure A.4), the only consecutive increase in the study period. It dropped approximately 40% in 2005 ($p < 0.001$) before rebounding in 2006 ($p < 0.001$). By 2007, mean canopy height declined to 4.9 ± 0.4 cm ($p < 0.001$) and did not increase over the next two years ($p = 0.496$, $p = 0.340$). No sites in this section were monitored in 2010, but the mean doubled in 2011 to 10.9 ± 1.7 cm ($p < 0.001$). No sites in this section were monitored from 2012–2014. In 2015, mean canopy height was 7.8 ± 1.1 cm and gradually declined to 2.9 ± 0.79 in 2018 ($p < 0.001$). The mean did not change through the end of the study period in 2023 ($p = 0.496$).

Mean bed width in 2002 was 70.2 ± 20.8 m. Over the next two years, it rose by over 30 m to a study period maximum of 103.3 ± 21.8 m ($p = 0.034$) in 2004, before generally declining over time to 60.5 ± 11.4 m in 2011 ($p < 0.001$). In 2015, bed width was 74.0 ± 17.5 m and did not change in 2016 ($p = 0.996$). Bed width began to decline in 2017 ($p < 0.001$), the same year as the extreme decrease downstream in Zone 1, though not as severe. Bed width declined again following Hurricane Irma to a study period low of 14.5 ± 5.6 m in 2018. By 2020, the mean had increased by over 40 m ($p < 0.001$) to 57.4 ± 17.0 m, and it was not different in 2023 ($p = 0.638$).

Percent occurrence increased from 90.9% in 2002 to 100% in 2003 and remained there through 2007. It then dropped for two consecutive years in 2008 and 2009, two years in which mean bed width also fell. Percent occurrence was again at 100% from 2015 through 2017. By 2018, it fell to a study period low of 63.6% and it rebounded slowly over the next 5 years, only reaching 100% in 2023, a year with a low sample size in this area that omitted sites which had no SAV the previous year.

Period Delineation

- Recovery Period (September 2002 – August 2004)
- Recent Period (September 2018 – August 2023)

September 2002 through August 2004 was selected as the recovery period due to the rises in canopy height, bed width, and percent occurrence during this time. Mean canopy height did not vary between the start of the recovery period and the start of the recent period ($p = 0.085$). However, starting bed width was 5 times higher ($p < 0.001$), and starting percent occurrence was 27% greater during the recovery period, indicating a more advantageous starting scenario in the recovery period. Canopy height increased to a study period high during the recovery period ($p < 0.001$), while it did not change during the recent period ($p = 0.78$). During the first two years of the recent period, bed width increased at a greater rate than the recovery period, though the increases ceased after 2020. At the end of the recovery period, canopy height and bed width were both higher than the end of the recent period ($p < 0.001$, $p < 0.001$). Percent occurrence was 100% at the end of both periods.

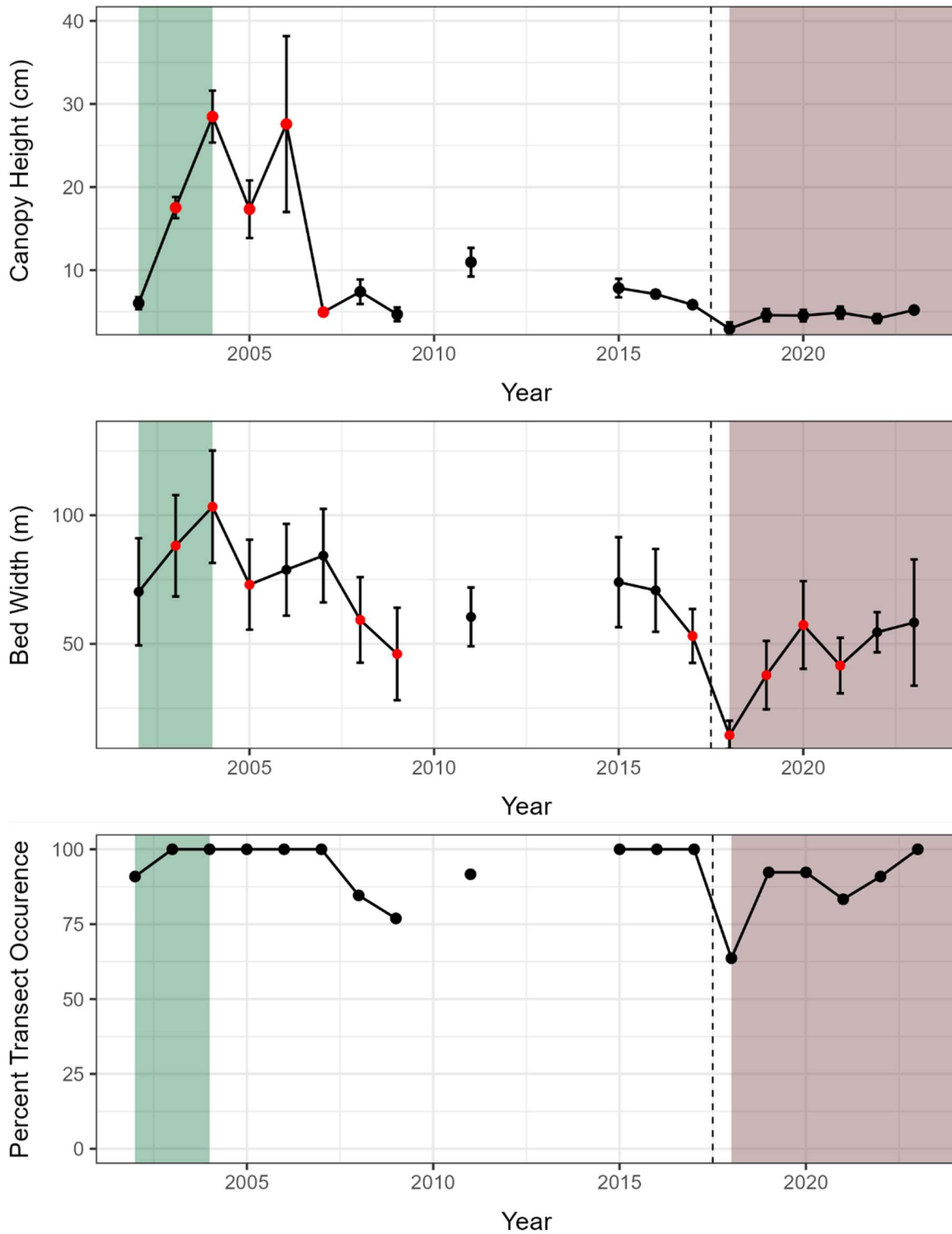


Figure A.4 Time series of annual mean SAV canopy height, bed width, and percent occurrence within Zone 2 of the Lower St. Johns River from 2002–2023. Error bars depict the standard error, and red points indicate a statistically significant change ($p < 0.05$) from the previous year in the generalized linear model. The background colors represent the selected periods for groupwise comparisons (Recovery Period = green, Recent Period = brown).

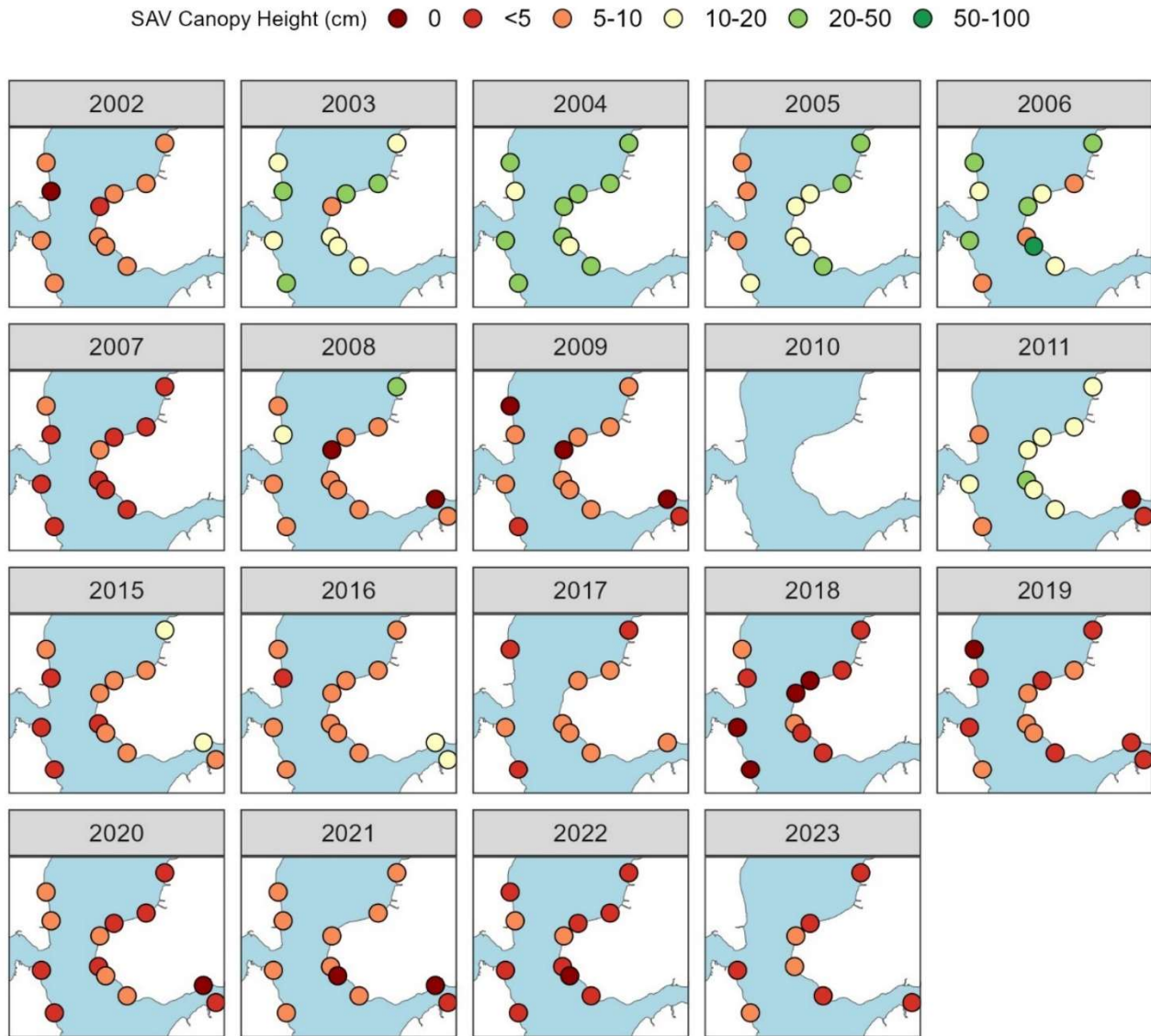


Figure A.5 Map of SAV canopy height at each transect over the study period in Zone 2.

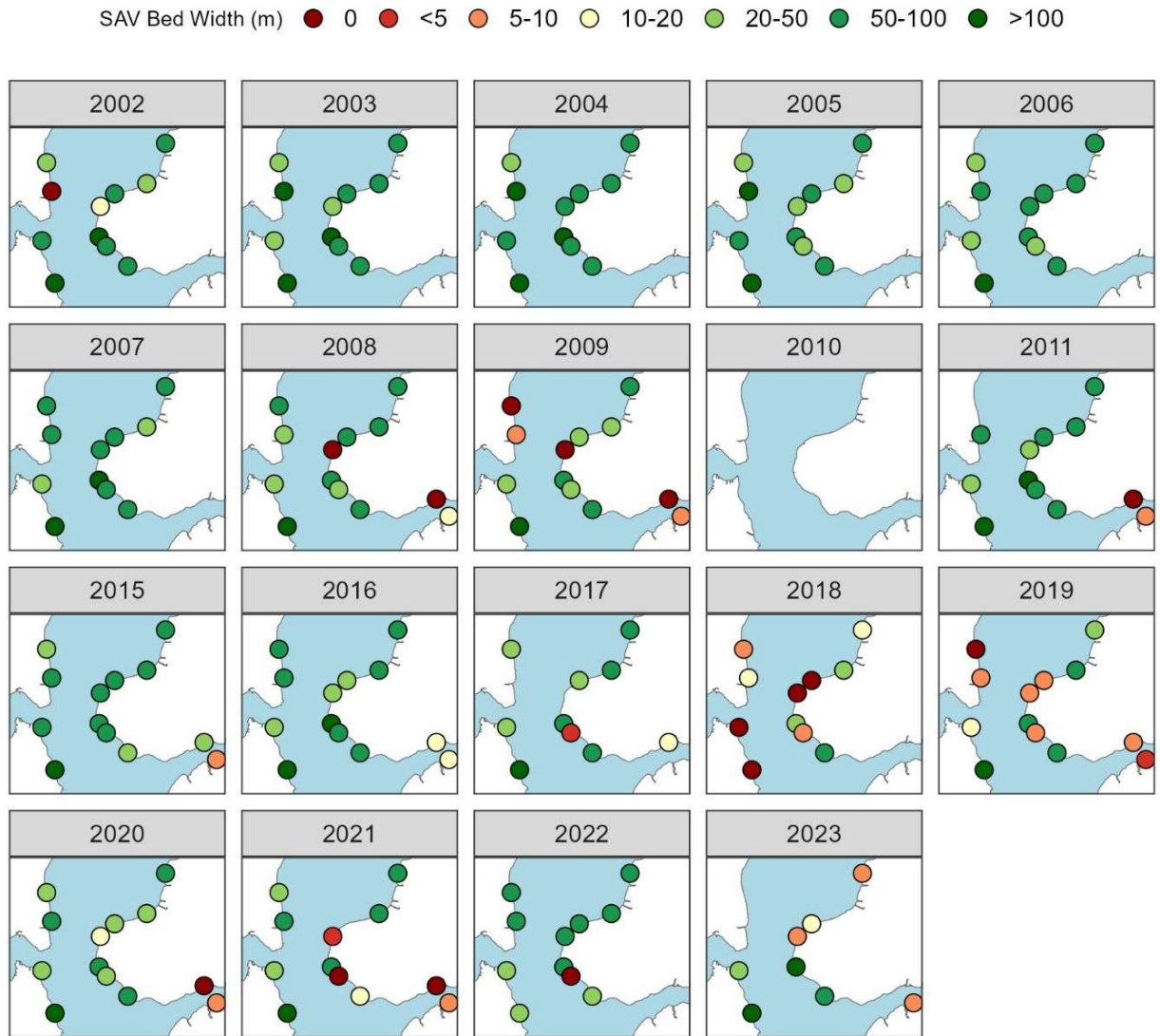


Figure A.6 Map of SAV bed width at each transect over the study period in Zone 2.

Zone 3

Only four sites were monitored annually in Zone 3 from 2002 to 2007 (Figures A.8, A.9). Similarly to Zones 1 and 2, mean canopy height rose rapidly from 6.3 ± 0.8 cm in 2002 to 54.5 ± 20.1 cm in 2004 ($p < 0.001$, Figure A.7). Canopy height fell in 2005 ($p < 0.001$) and again in 2007 to 7.5 ± 2.5 cm ($p < 0.001$), mirroring the pattern in Zone 2. Sample size roughly tripled after 2008, and canopy height remained low through 2009 before rising slightly in 2011 to 14.9 ± 1.5 cm ($p < 0.001$). In 2015, the mean had not changed ($p = 0.999$) and remained stable in 2016 ($p = 0.999$). In 2017, prior to Hurricane Irma, canopy height dropped by over 50% to 6.6 ± 2.1 cm ($p < 0.001$), and it did not rise for the rest of the study period ($p = 0.94$).

Mean bed width did not change year-over-year during the first half of the study period ($p = 0.394$), and it was 104.5 ± 10.8 m in 2011, the last year before the data gap. When monitoring resumed in 2015, bed width had fallen to 79.3 ± 8.6 m ($p < 0.001$). Despite a fall in canopy height during the same year, bed width remained stable through 2017 ($p = 0.501$) before decreasing to a study-period low of 32.7 ± 8.7 m in 2018 ($p < 0.001$), one year after the decline in canopy height. Over the next 3 years, bed width recovered to 83.2 ± 8.1 m in 2021, approximately 20 meters below the means of the first half of the study period, and did not change for the rest of the study period ($p = 0.937$).

Percent occurrence was 100% every year of the study period except for 2018 when SAV disappeared from two sites, the northern-most site on the western bank and the southern-most site on the same bank, just south of the mouth of Black Creek. This was the same year as the drop in bed width.

Period Delineation

- Recovery Period (September 2002 – August 2004)
- Recent Period (September 2018 – August 2023)

September 2002 through August 2004 was selected as the recovery period due to the rapid increase in mean canopy height during this time. Although canopy height declined in 2017, 2018 was selected as the start of the recent period due to the drop in bed width this year.

The recovery and recent scenarios in this section occur during the same years and are of similar patterns to those of Zone 2 immediately downstream. The recovery period began with very low canopy heights, but high bed widths. During this time canopy heights rose rapidly ($p < 0.001$), and bed widths did not increase ($p = 0.305$). Also, like in Zone 2, the recent post-decline period had low canopy heights and low bed widths, with bed widths increasing ($p < 0.001$) but no changes in canopy heights ($p = 0.08$).

Again, as in Zone 2, mean canopy height was equal at the start of the two periods ($p = 0.893$), but the recent period mean bed width started at roughly one third of the mean at start of the recovery period ($p < 0.001$). These results indicate a more severe die-off preceding the recent period than the recovery period.

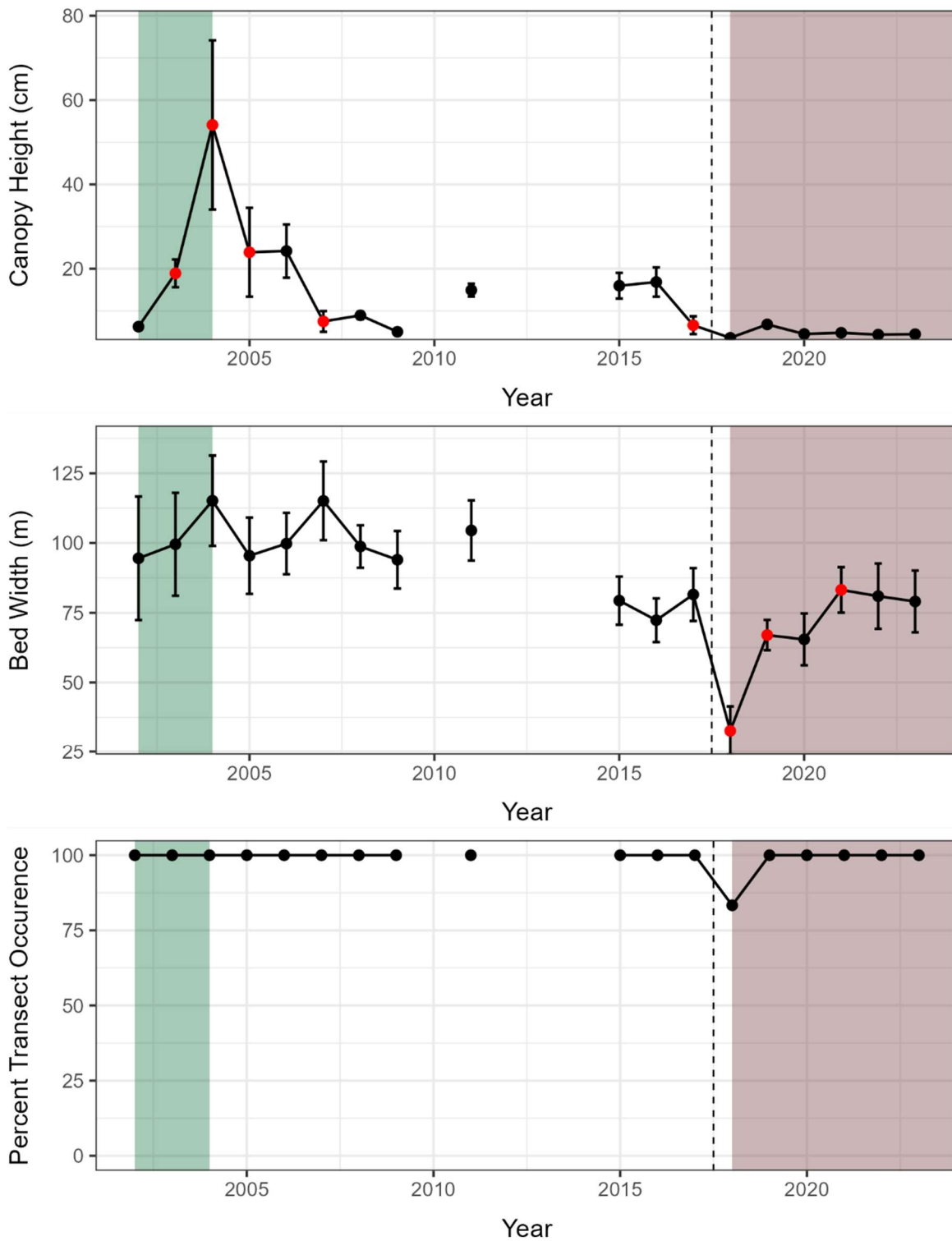


Figure A.7 Time series of annual mean SAV canopy height, bed width, and percent occurrence within Zone 3 of the Lower St. Johns River from 2002–2023. Error bars depict the standard error, and red points indicate a statistically significant change ($p < 0.05$) from the previous year in the generalized linear model. The background colors represent the selected periods for groupwise comparisons (Recovery Period = green, Recent Period = brown).

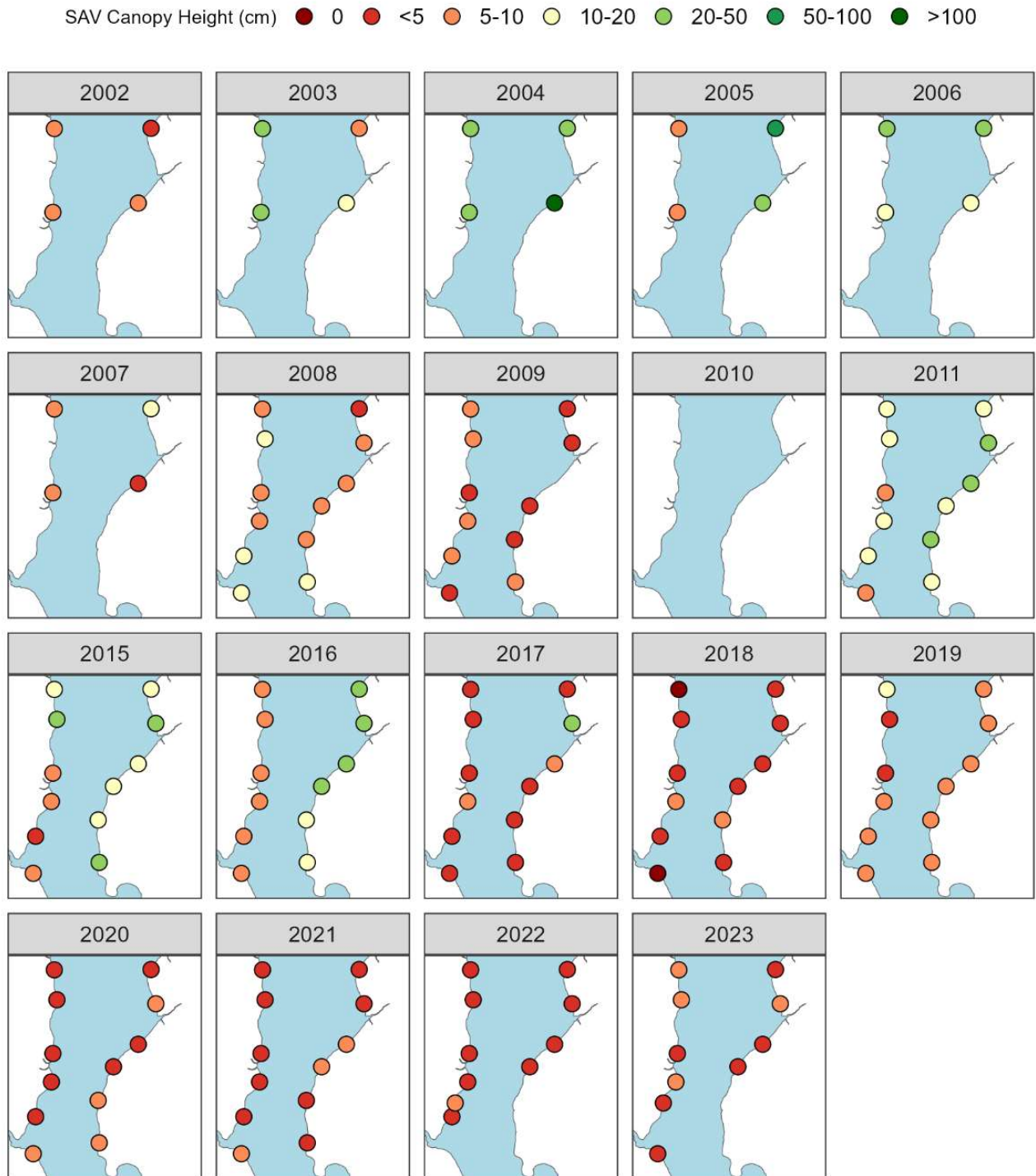


Figure A.8 Map of SAV canopy height at each transect over the study period in Zone 3.

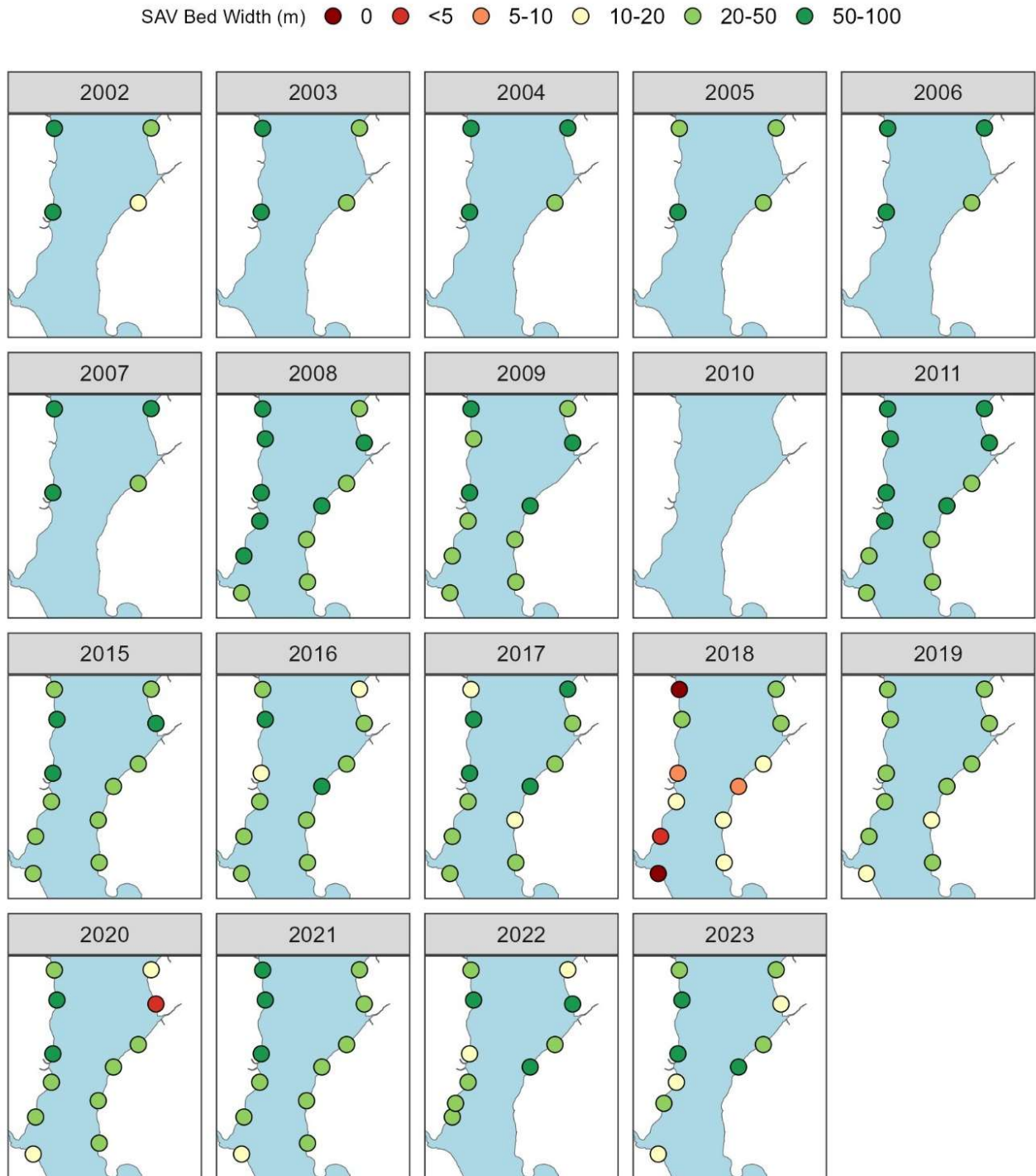


Figure A.9 Map of SAV bed width at each transect over the study period in Zone 3.

Zone 4

From 2002–2007 only four sites were monitored in this Zone (Figures A.11, A.12). Mean canopy height in 2002 was 8.7 ± 1.5 cm and did not change in 2003 ($p = 0.999$, Figure A.10). The mean briefly rose to a study period high of $46.6 \text{ cm} \pm 22.5$ in 2004 ($p < 0.001$), concurrent with increases in the downstream sections, before it fell to 17.7 ± 7.7 cm in 2005 ($p < 0.001$). Canopy height remained low through 2008 ($p = 0.952$), when monitoring effort increased. In 2009 the mean fell to 3.7 ± 0.3 cm ($p < 0.001$) and increased consecutively in 2010 ($p < 0.001$) and 2011 ($p < 0.001$) to 32.1 ± 5.5 cm. No sites were monitored from 2012 to 2014. Mean canopy height in 2015 was 34.4 ± 0.7 cm and did not vary year-to-year through 2017 ($p = 0.912$), marking a departure from the pattern observed in Zones 1, 2, and 3, where canopy height declined in 2017. Following Hurricane Irma, the mean fell almost 90% to 3.9 ± 1.0 cm in 2018 ($p < 0.001$) and did not vary through the rest of the study period ($p = 0.529$).

During the first half of the study period, bed width did not follow a similar pattern to canopy height in this region, with no year-to-year increases in bed width that coincided with increases in canopy height. At the start of the study period, mean bed width was 40.1 ± 11.2 m and did not vary year-to-year until it increased to 55.0 ± 13.3 m in 2007 ($p = 0.002$). It then dropped approximately 40% in 2008 ($p < 0.001$), when new sites were introduced. It rebounded to 61.8 ± 19.3 m in 2009 ($p < 0.001$), the same year as a decline in mean canopy height. Bed width did not rise year-to-year in 2010 ($p = 0.804$) or 2011 ($p = 0.732$), but it finished the two-year period at 71.6 ± 5.5 m, an overall increase from 2009 ($p = 0.002$). No sites were monitored from 2012 to 2014. Bed width was 68.2 ± 15.2 m in 2017 and fell to 20.8 ± 5.7 m in 2018 after Irma ($p < 0.001$). It partially rebounded to 34.7 ± 3.9 m in 2019 ($p < 0.001$), but it was unchanged through 2022 ($p = 0.750$) before dropping to a study-period low of 17.6 ± 6.5 m in 2023 ($p < 0.001$).

Percent occurrence was at 100% for most of the study period, only dropping below 100% during 2008 and 2018.

Period Delineation

- Past Recovery (September 2009 – August 2011)
- Recent Period (September 2018 – August 2023)

September 2009 through August 2011 was selected as the recovery period due to the consecutive year-to-year increases in mean canopy height during this time and the gradual increase in bed width. Though the largest single year increase in bed width occurred from 2008 to 2009, this coincided with a decline in canopy height. Another brief recovery may have occurred from 2003 to 2004, evidenced by the sharp increase in canopy height during this time. 2018 was selected as the start of the recent period due to the declines in all three metrics from the year prior. Both periods began with equally low canopy heights ($p = 0.999$), but the recovery period began with approximately triple the bed width of the recent period ($p < 0.001$). The timing of the recovery period is different from the freshwater upstream and estuarine downstream Zones, potentially indicating that this Zone has a unique combination of factors affecting SAV owing to its position in between the two regions. Just as in Zones 1–3, these data indicate a more severe die-off in the wake of Hurricane Irma than previously observed in the study period.

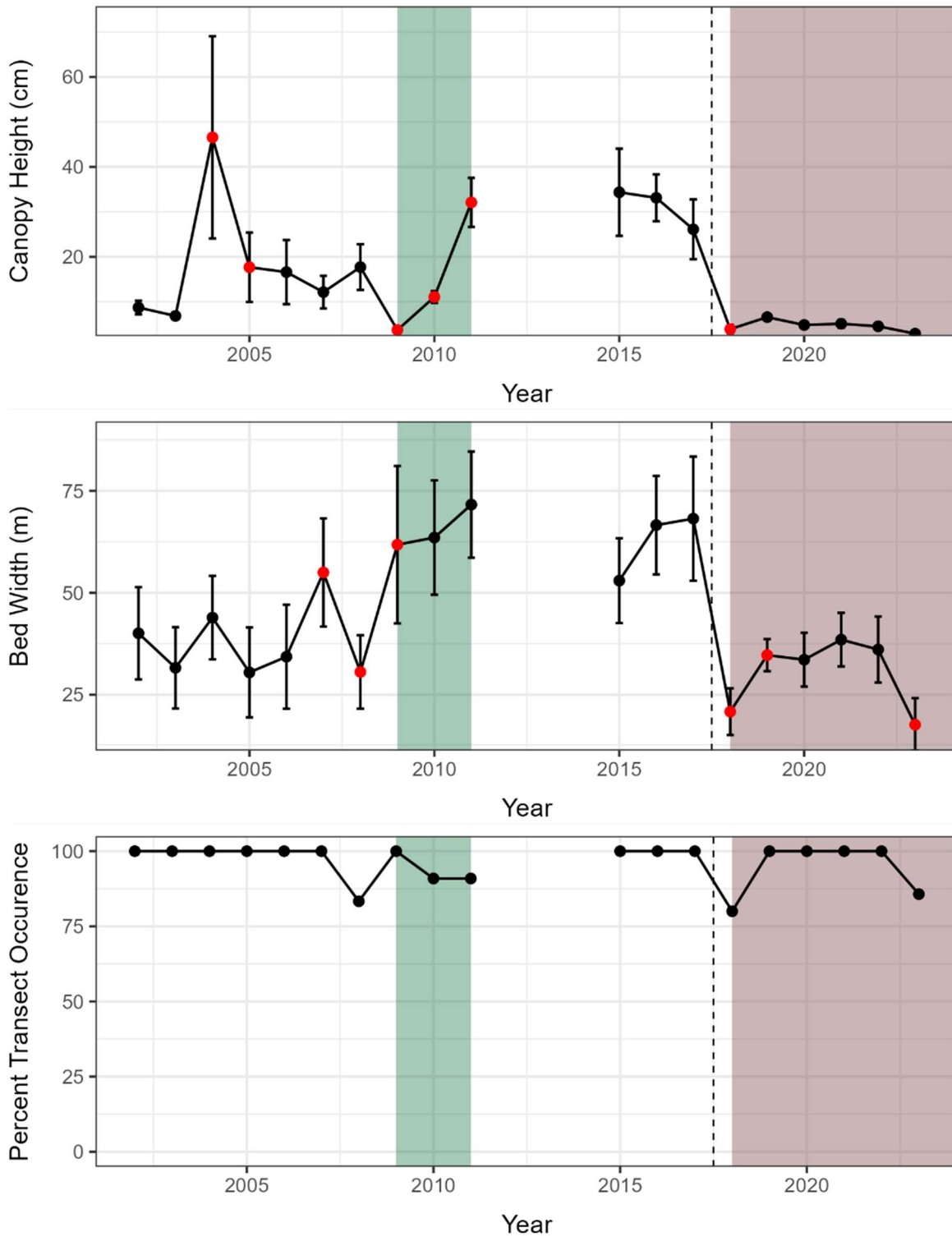


Figure A.10 Time series of annual mean SAV canopy height, bed width, and percent occurrence within Zone 4 of the Lower St. Johns River from 2002–2023. Error bars depict the standard error, and red points indicate a statistically significant change ($p < 0.05$) from the previous year in the generalized linear model. The background colors represent the selected periods for groupwise comparisons (Recovery Period = green, Recent Period = brown).

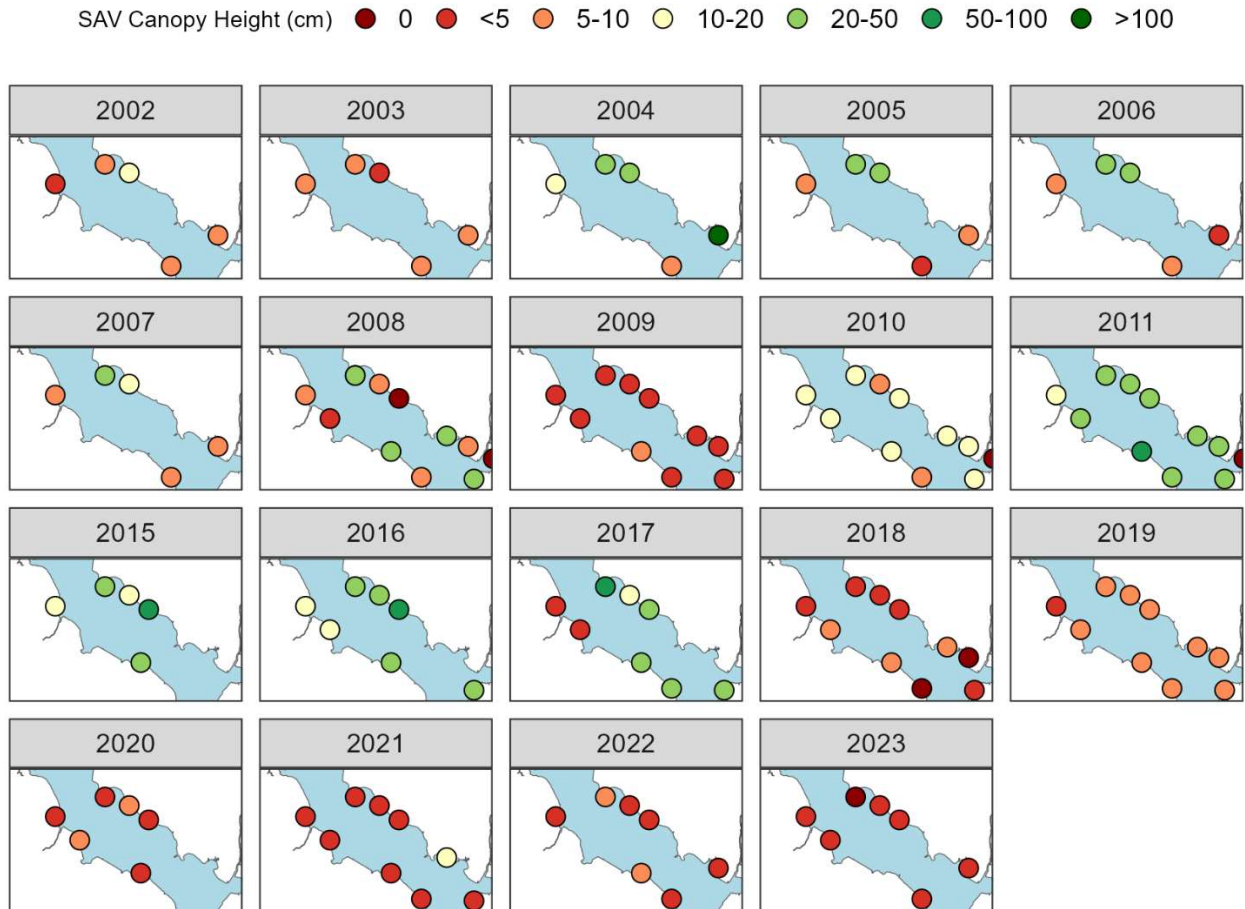


Figure A.11 Map of SAV canopy height at each transect over the study period in Zone 4.

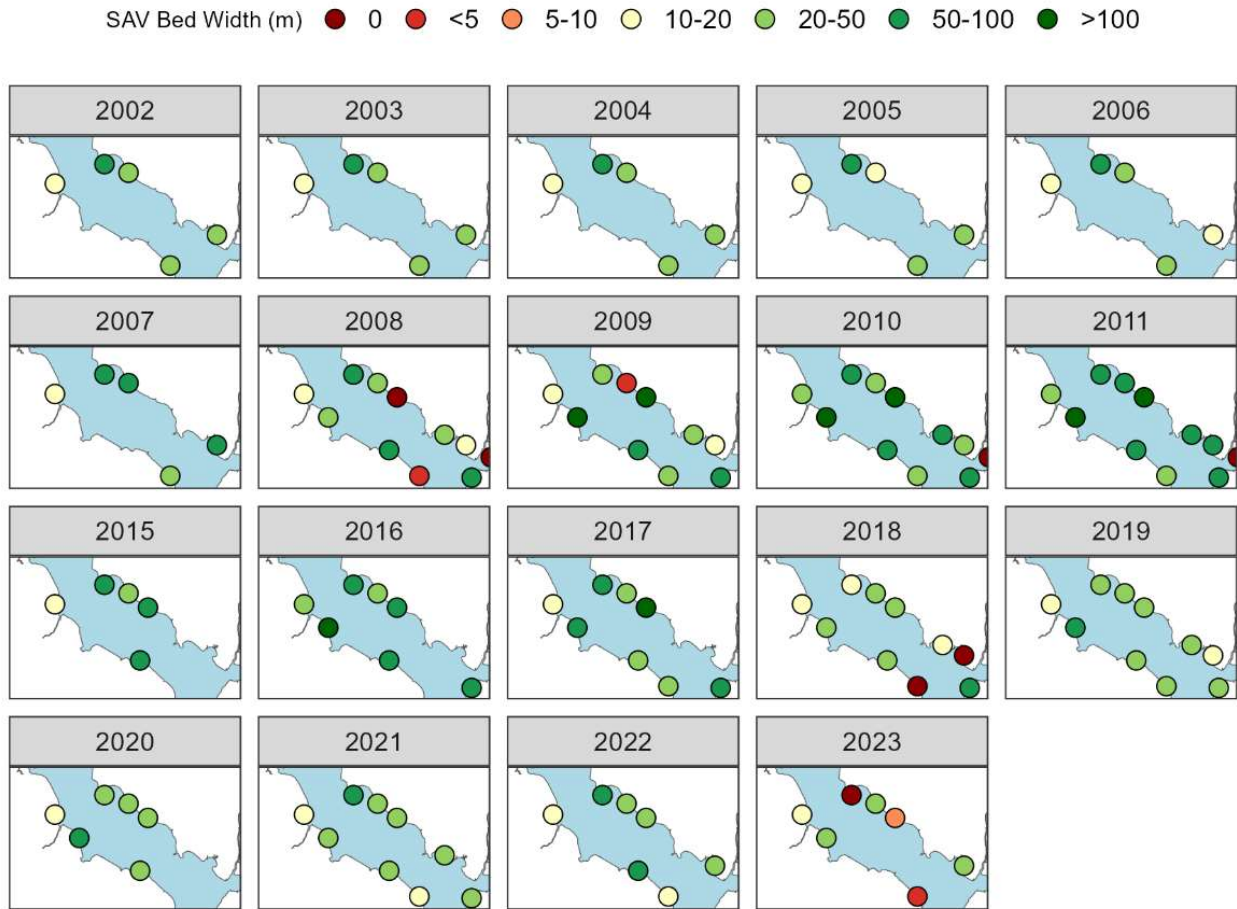


Figure A.12 Map of SAV bed width at each transect over the study period in Zone 4.

Zone 5

In 2002 mean canopy height for Zone 5 was 28.9 ± 5.1 cm (Figure A.13). It fluctuated year-to-year until 2005, when it declined to 8.9 ± 1.3 cm ($p < 0.001$), and it did not change in 2006 ($p = 0.585$). Canopy height increased in 2007 ($p < 0.001$) and continued to rise to pre-decline values in 2008 ($p < 0.001$). In the following year, the mean dropped approximately 10 cm ($p < 0.001$) before rising again to 32.3 ± 5.6 cm in 2011 ($p < 0.001$). There are no data for 2012–2016, but by 2017 canopy height was at a study period high of 44.8 ± 7.5 cm. Following Hurricane Irma in September of 2017, mean canopy height fell almost 20-fold to 2.5 ± 0.3 cm ($p < 0.001$) and did not change for the rest of the study period, though there are no data in this region for 2020.

Mean bed width followed a similar pattern as canopy height, but it was not as variable from year-to-year during the first half of the study period. From 2006 to 2007, bed width went from a 10 year low of 41.6 ± 5.2 m to a 10 year high of 62.0 ± 7.4 m ($p < 0.001$). Bed width did not change in 2008, but it declined approximately 20% in 2009 ($p = 0.002$) before rebounding to 58.4 ± 5.6 m in 2011 ($p = 0.002$). No sites were monitored in this Zone from 2012–2016, but when monitoring resumed in 2017, bed width was not different than 2011. However, in 2018 bed width dropped to a study-period low of 14.3 ± 1.5 m ($p < 0.001$). Bed width fluctuated in the following years, reaching 43.0 ± 6.1 m in 2022 before falling to 26.9 m ± 3.6 m in 2023 ($p < 0.001$).

Percent occurrence remained very high throughout the study period until 2018 with a dip in 2008 that was caused by the addition of previously unmonitored sites with no SAV. It reached a study period low of 61.5% in 2021, but it rebounded to 95.2% in the following year.

Period Delineation

- Past Recovery (September 2006 – August 2008)
- Recent Period (September 2018 – August 2023)

September 2006 through August 2008 was selected as the recovery period due to consecutive increases in annual mean canopy height after two years of low values. Additionally, bed width rose from a ten year low to a ten year high during the same period. The recent period was labeled as September 2018 through August 2023. Mean canopy height and bed width were both over 3-fold higher at the start of the recovery period than the recent period ($p < 0.001$, $p < 0.001$), indicating a more advantageous starting point for the recovery period. At the end of the recovery period, mean canopy height was over 25 cm higher than the peak mean canopy height in the recent period ($p < 0.001$). End of recovery bed width was also higher than the highest mean reached during the recent period, though the difference was not as extreme. (57.5 ± 6.3 vs 42.3 ± 6.1 m, $p < 0.001$). Percent occurrence started the recent period slightly below the recovery period and dropped well below recovery period norms in 2021, but it returned to similar values by 2023. Just as in the downstream Zones, these patterns indicate that the starting biomass for the recent period was much lower than at the start of the recovery period.

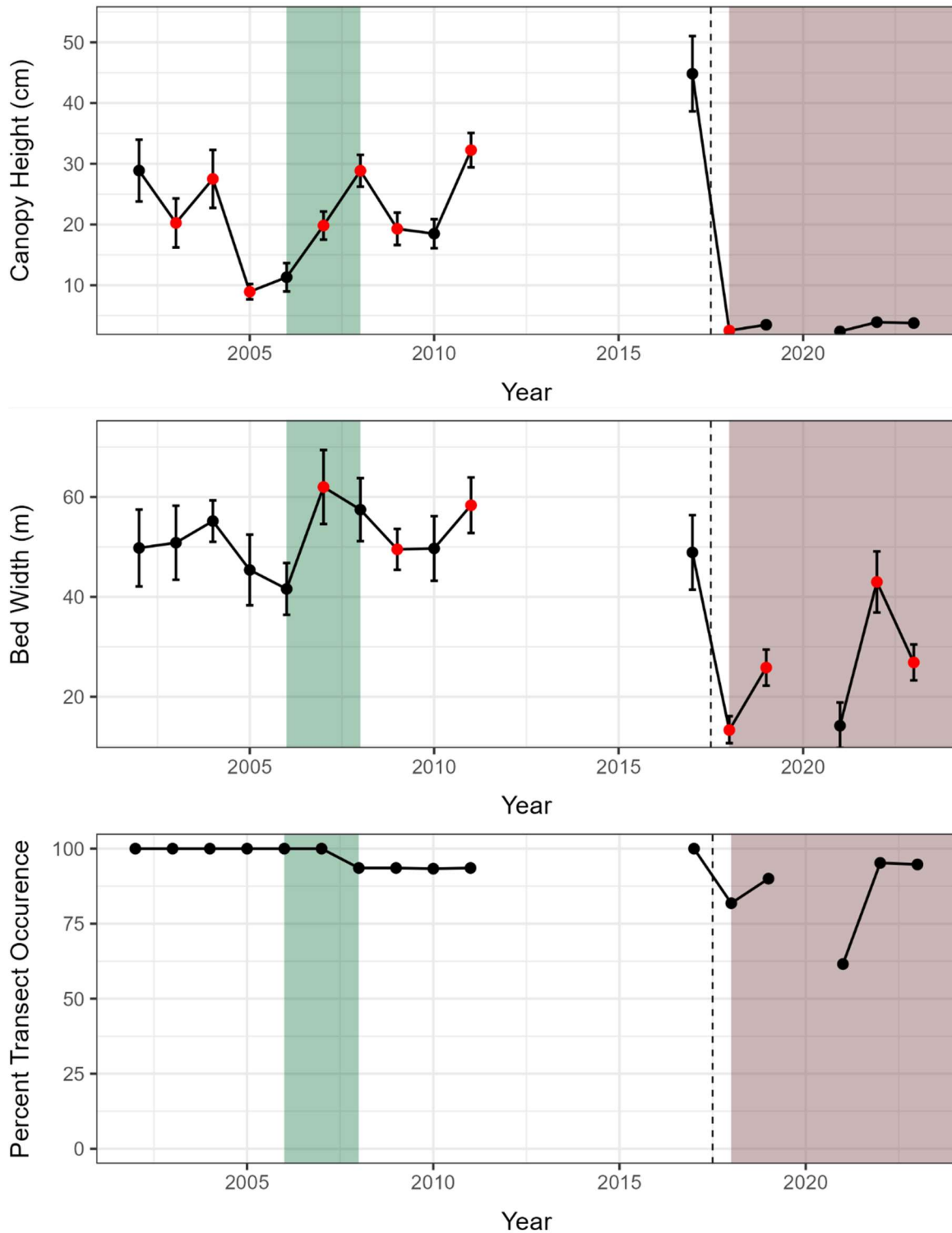


Figure A.13 Time series of annual mean SAV canopy height, bed width, and percent occurrence within Zone 5 of the Lower St. Johns River from 2002–2023. Error bars depict the standard error, and red points indicate a statistically significant change ($p < 0.05$) from the previous year in the generalized linear model. The background colors represent the selected periods for groupwise comparisons (Recovery Period = green, Recent Period = brown).

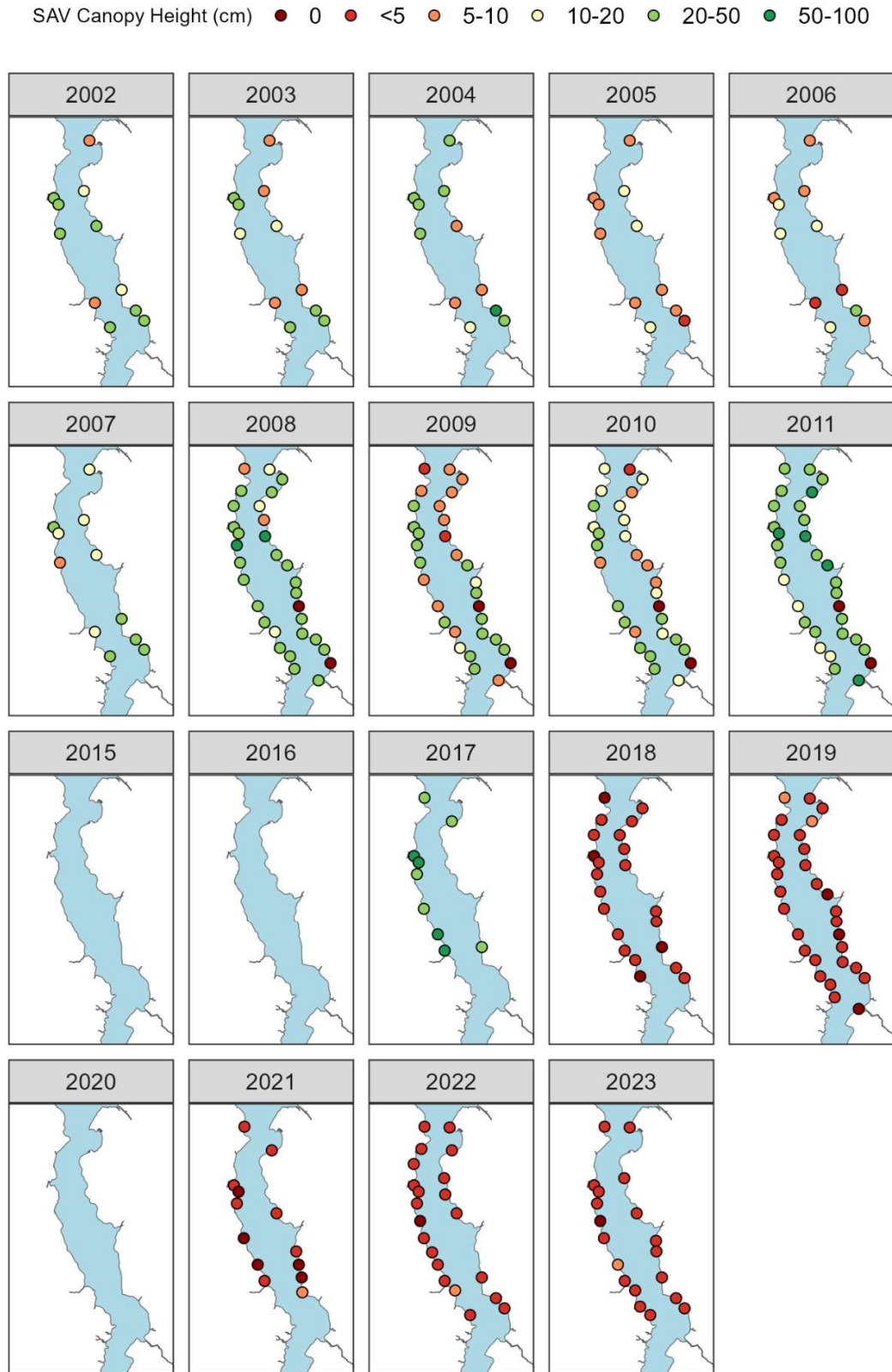


Figure A.14 Map of SAV canopy height at each transect over the study period in Zone 5.

SAV Bed Width (m) ● 0 ● <5 ● 5-10 ○ 10-20 ● 20-50 ● 50-100 ● >100

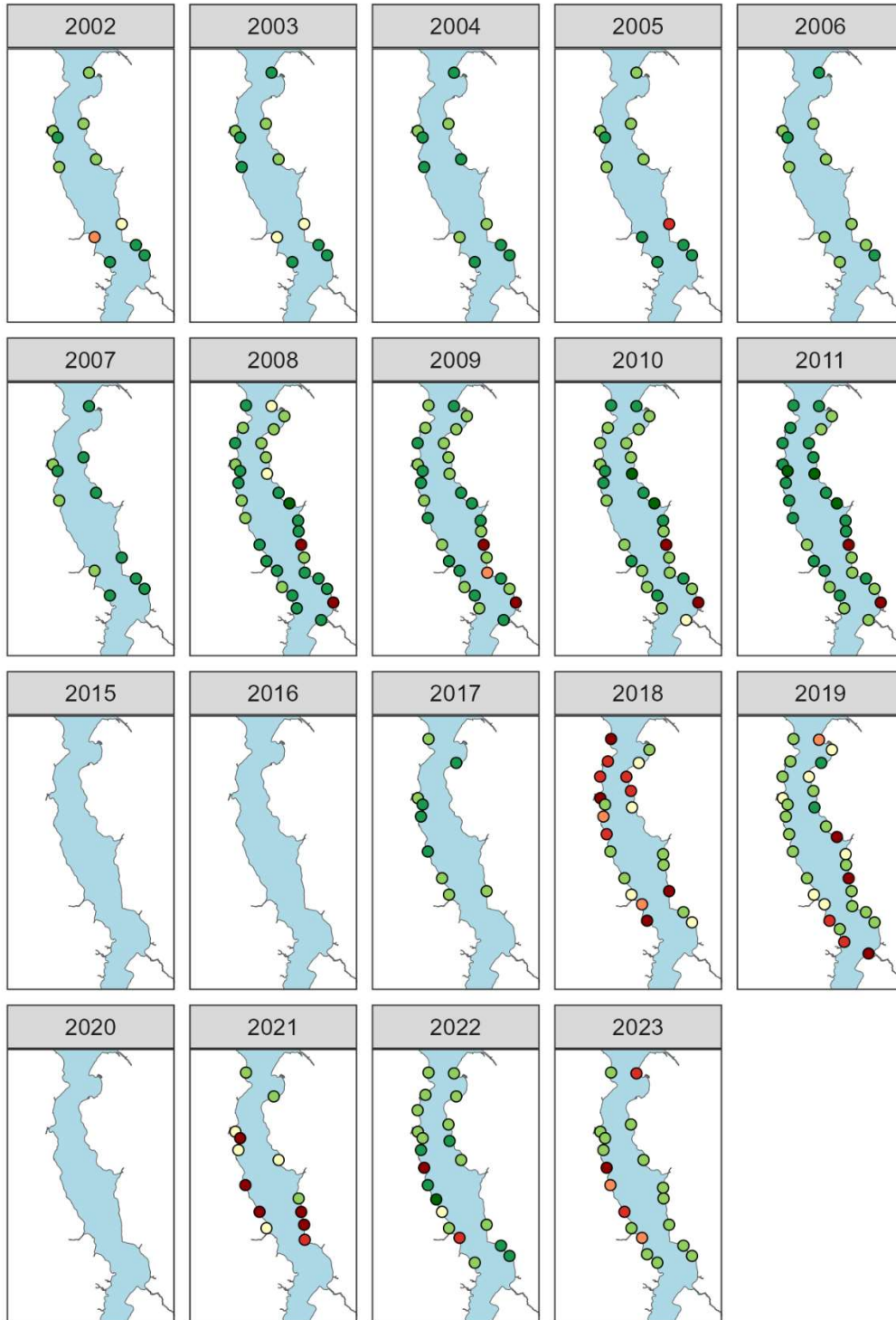


Figure A.15 Map of SAV bed width at each transect over the study period in Zone 5.

Zone 6

Mean canopy height in Zone 6 changed every year from 2002 to 2011 (Figure A.16). In 2002 it was 31.6 ± 8.0 cm, the highest of the study period. Following this high, canopy height fell for 4 consecutive years, reaching 2.9 ± 1.2 cm in 2006 ($p < 0.001$). Canopy height then rose year-to-year through 2009 to pre-decline levels, before falling slightly to 21.9 ± 3.8 cm in 2011 ($p < 0.001$). There are no data from 2012–2018. In 2019, two years after Hurricane Irma caused SAV declines throughout the rest of the LSJR, mean canopy height was 1.0 ± 0.3 cm, the lowest of the study period. Mean canopy height did not change year-to-year through the end of the study period. Canopy heights varied over time at all sites, but between 2002 and 2011 the most severe fluctuations occurred in the narrow section of the mainstem between Buffalo Bluff and Horseshoe Point (Figure A.17). Depending on the year, some sites ranged from having no SAV to over 100 cm canopy heights. Sites downstream of Rice Creek remained relatively stable during the same time period, rarely losing SAV entirely, and canopy heights typically stayed between 20 and 50 cm. However, by 2019 these sites lost all SAV or had canopy heights below 5 cm.

Bed width varied less over time than canopy height but varies spatially within the region (Figure A.18). As the littoral shelf contracts upstream there is less habitable area for SAV. As a result, bed widths are generally limited to below 20 m south of the Palatka Bridge. Mean bed width was 16.8 ± 6.8 m in 2002 and did not change in 2003 ($p = 0.45$) or 2004 ($p = 0.99$). It began falling in 2005 ($p = 0.002$) and continued to a 10-year low in 2006 of 5.1 ± 2.3 m ($p = 0.018$), coinciding with the lowest mean canopy height of the same timeframe. In 2007 bed width rebounded to 23.3 ± 13.5 m ($p < 0.001$) and did not vary in 2008 ($p = 0.23$). Bed width subsequently fell and was 14.4 ± 2.7 m in 2011. When monitoring resumed in 2019, bed width was at a study period low of 3.9 ± 1.5 m. By 2023 it had increased slightly to 8.0 ± 3.2 m ($p < 0.001$).

Percent occurrence followed roughly the same pattern as the other two variables. It was 75.0% in 2002, fell to 37.5% in 2005, then recovered in 2007, only fluctuating slightly through 2011. In 2019, the percent occurrence was 37.5% and rose to 62.5% by 2023, the end of the study period.

Period Delineation

- Past Recovery (September 2006 – August 2008)
- Recent Lack of Recovery (September 2018 – August 2023)

The selected recovery period for this section is September 2006 – August 2008, the same as in the J–K section. Canopy height increased during each year of this period from a study-low, and bed width more than quadrupled during the first year and remained high during the second. Starting points for all three SAV metrics were similar between the two periods. Mean canopy height did not differ ($p = 0.94$), mean bed width was only slightly higher in the recovery scenario (5.1 ± 2.3 m vs 3.9 ± 1.5 m, $p = 0.04$), and percent occurrence was comparable (40% vs 37.5%). In the two-year window of the recovery period, canopy height increased over 7-fold to 21.5 cm ($p < 0.001$) and in the four sampling years of the recent scenario, it only marginally increased from 2019 to a maximum of 3.4 ± 0.5 cm in 2022 ($p =$

0.001). Zone 6 and Zone 1 are the only two Zones where SAV was in a similar state at the start of the recovery and recent periods.

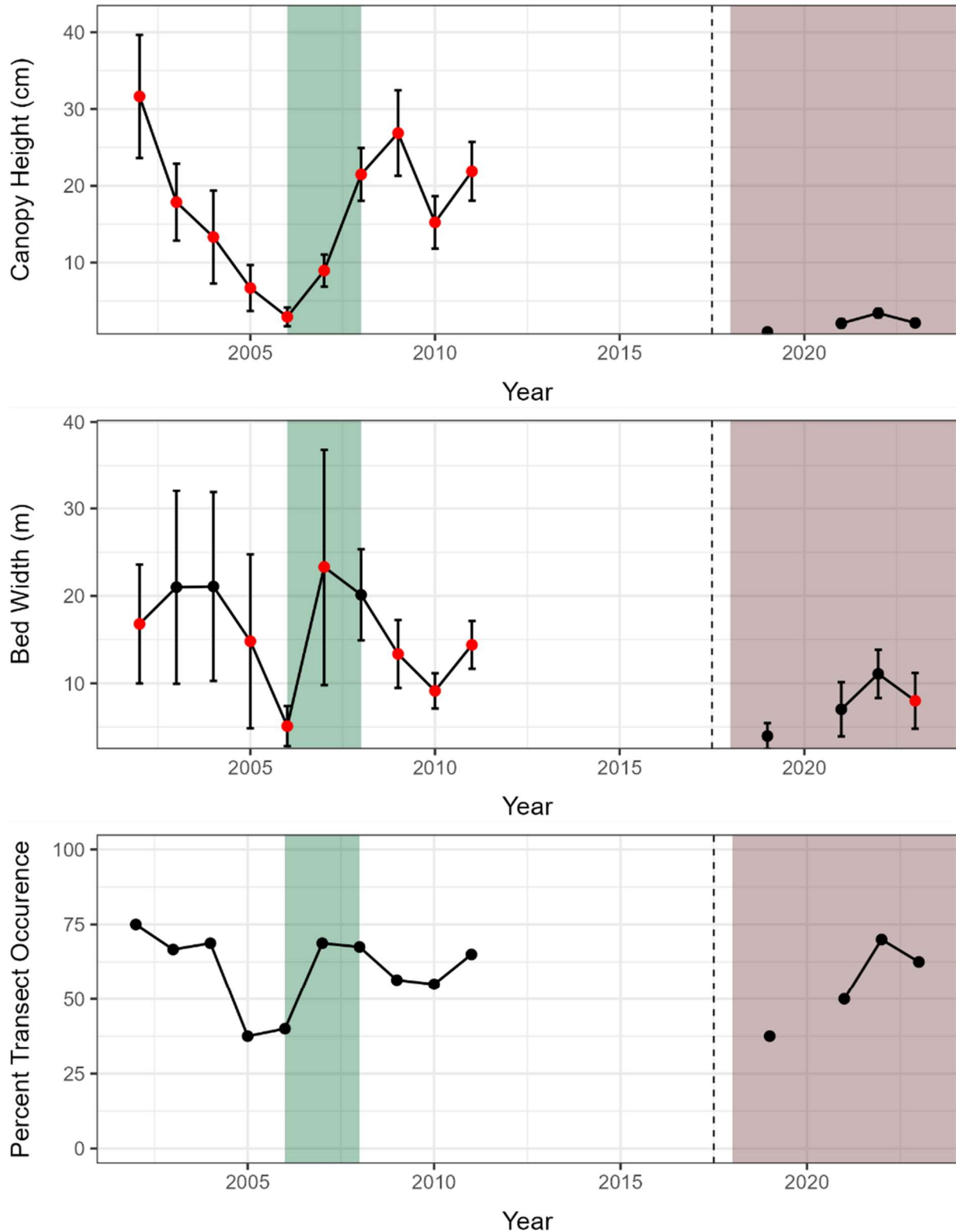


Figure A.16 Time series of annual mean SAV canopy height, bed width, and percent occurrence within Zone 6 of the Lower St. Johns River from 2002–2023. Error bars depict the standard error, and red points indicate a statistically significant change ($p < 0.05$) from the previous year in the generalized linear model. The background colors represent the selected periods for groupwise comparisons (Recovery Period = green, Recent Period = brown).

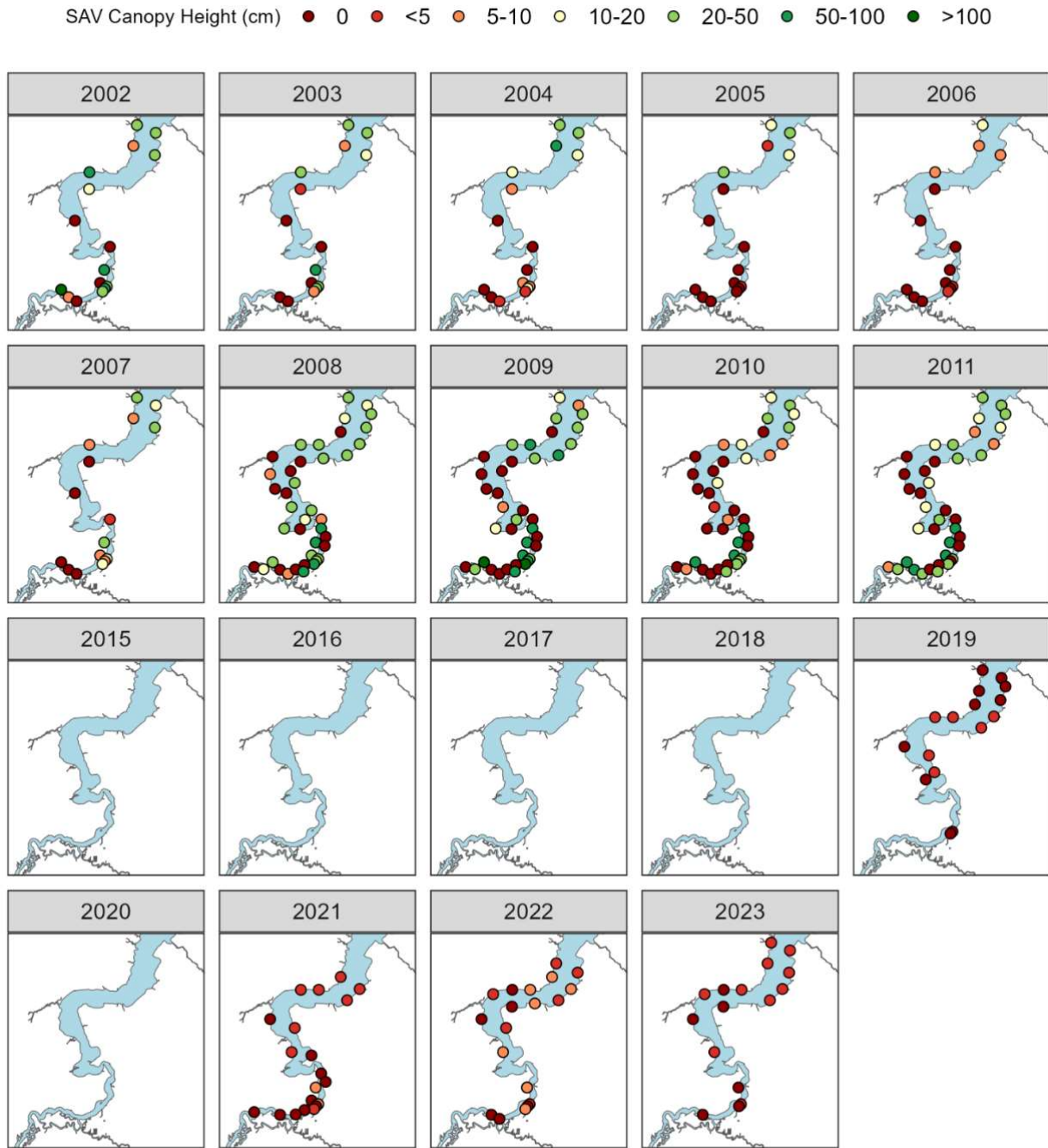


Figure A.17 Map of SAV canopy height at each transect over the study period in Zone 6.

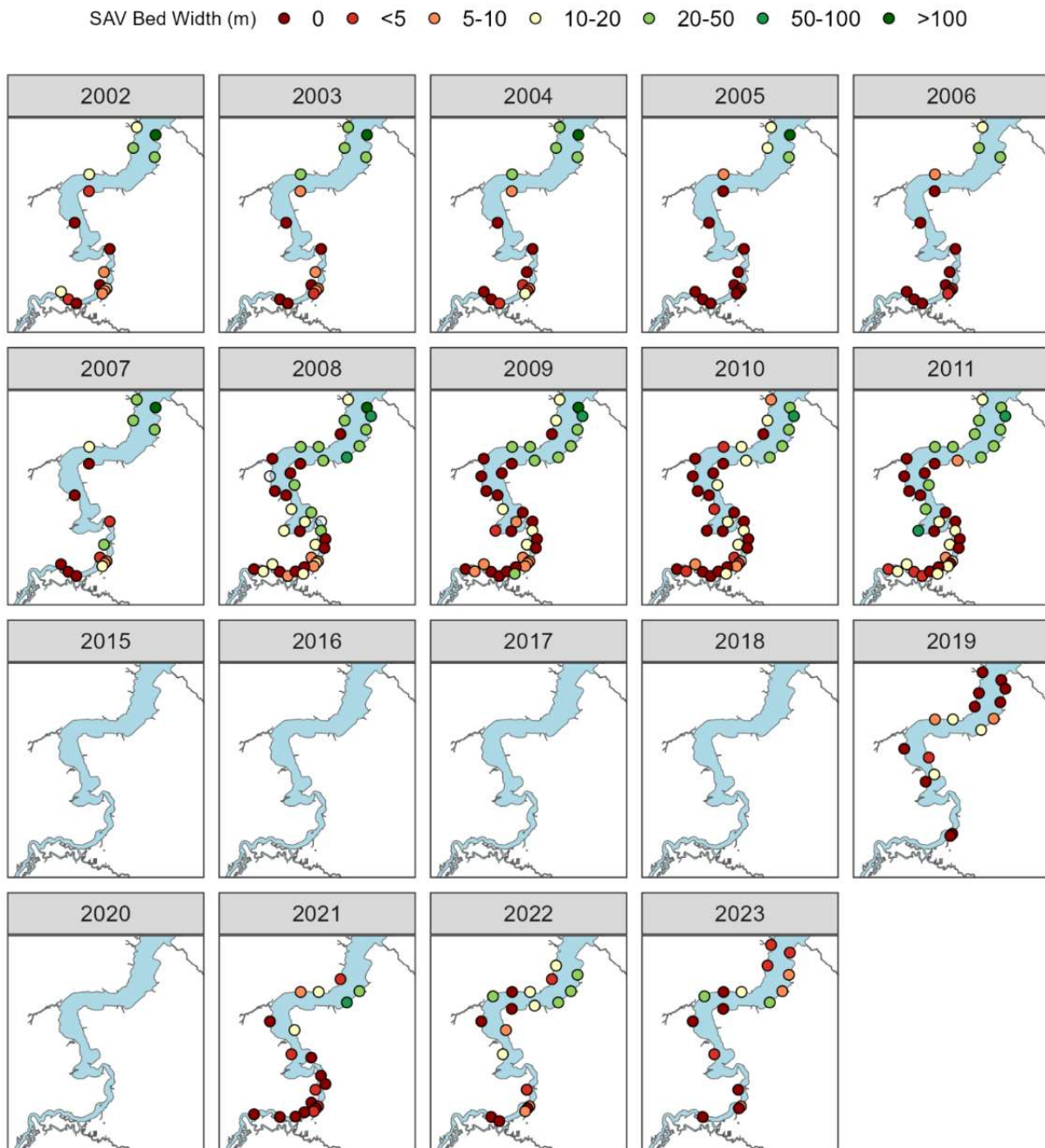


Figure A.18 Map of SAV bed width at each transect over the study period in Zone 6.

REFERENCES

- Adler, J. M., S. C. Barry, G. R. Johnston, C. A. Jacoby, and T. K. Frazer. 2018. An aggregation of turtles in a Florida spring yields insights into effects of grazing on vegetation. *Freshwater Science* **37**:397-403.
- Bates, D., M. Mächler, B. Bolker, and S. Walker. 2015. Fitting Linear Mixed-Effects Models Using lme4. *Journal of Statistical Software* **67**:1 - 48.
- Bennett, M., and K. Conway. 2010. An overview of North America's diminutive freshwater fish fauna. *Ichthyological Exploration of Freshwaters* **21**:63-72.
- Bigelow, H. B. 1953. Fishes of the Gulf of Maine. *Fishery Bulletin* **53**:577.
- Bornette, G., and S. Puijalon. 2011. Response of aquatic plants to abiotic factors: a review. *Aquatic sciences* **73**:1-14.
- Boschung, H. T., Jr., and R. L. Mayden. 2004. *Fishes of Alabama*. Smithsonian Books, Washington, D.C.
- Buzas, M. A., D. K. Young, and M. W. Young. 1976. Species densities of macrobenthos associated with seagrass: A field experimental study of prédation.
- Caldwell, D. K. 1957. The biology and systematics of the pinfish, *Lagodon rhomboides* (Linnaeus). *Bulletin of the Florida State Museum, Biological Sciences* **2**:77-173.
- Carpenter, K. E. 2002a. The living marine resources of the Western Central Atlantic. Volume 1: Introduction, molluscs, crustaceans, hagfishes, sharks, batoid fishes and chimaeras. .
- Carpenter, K. E. 2002b. The living marine resources of the Western Central Atlantic. Volume 2: Bony fishes part 1 (*Acipenseridae* to *Grammatidae*).
- Chamberlain, R. H. 2012. Predicted changes in *Vallisneria americana* habitat suitability indices using modeled salinity and light conditions in the lower St. Johns River, Florida. St. Johns Water Management District.
- Connelly, C. R., E. Bolles, D. Culbert, J. DeValerio, M. Donahoe, K. Gabel, R. Jordi, J. McLaughlin, A. Neal, S. Scalera, E. Toro, and J. Walter. 2014. Florida residents guide to mosquito control: Integrated pest management for mosquito reduction around homes and neighborhoods. University of Florida Institute of Food and Agricultural Sciences, Gainesville, FL.
- Davis, C. D. 2009. A Generalized Food Web for Lake Pontchartrain in Southeastern Louisiana.
- De Cicco, L. A., R. M. Hirsch, D. Lorenz, W. Watkins, R. Bailey, and K. White. 2023. dataRetrieval: R packages for discovering and retrieving water data available from U.S. federal hydrologic web services. U.S. Geological Survey.
- Dennison, W. C., R. J. Orth, K. A. Moore, J. C. Stevenson, V. Carter, S. Kollar, P. W. Bergstrom, and R. A. Batiuk. 1993. Assessing Water Quality with Submersed Aquatic Vegetation. *Bioscience* **43**:86-94.
- Dobberfuhr, D. R. 2007. Light limiting thresholds for submerged aquatic vegetation in a blackwater river. *Aquatic Botany* **86**:346-352.
- Doering, P. H., R. H. Chamberlain, and J. M. McMunigal. 2001. Effects of simulated saltwater intrusions on the growth and survival of wild celery, *Vallisneria americana*, from the Caloosahatchee estuary (South Florida). *Estuaries* **24**:894-903.
- Dunn, A. E., D. R. Dobberfuhr, and D. A. Casamatta. 2008. A Survey of Algal Epiphytes from *Vallisneria americana* Michx. (Hydrocharitaceae) in the Lower St. Johns River, Florida. *Southeastern Naturalist* **7**:229-244.

- Durant, D. F., J. V. Shireman, and G. R.D. 1979. The American Midland Naturalist **102**:127-133.
- Faletti, M. E., D. H. Chacin, J. A. Peake, T. C. MacDonald, and C. D. Stallings. 2019. Population dynamics of Pinfish in the eastern Gulf of Mexico (1998-2016). PloS one **14**.
- Farfante, I. P. 1969. Western Atlantic Shrimps of the Genus *Penaeus*.
- Forward, R. B., Jr., R. A. Tankersley, D. Blondel, and D. Rittschof. 1997. Metamorphosis of the blue crab *Callinectes sapidus*: effects of humic acids and ammonium. Marine Ecology Progress Series **157**:277-286.
- Fraser, M. W., B. C. Martin, H. L. Wong, B. P. Burns, and G. A. Kendrick. 2023. Sulfide intrusion in a habitat forming seagrass can be predicted from relative abundance of sulfur cycling genes in sediments. Science of The Total Environment **864**:161144.
- French, G. T., and K. A. Moore. 2003. Interactive effects of light and salinity stress on the growth, reproduction, and photosynthetic capabilities of *Vallisneria americana* (wild celery). Estuaries **26**:1255-1268.
- Froese, R., and D. Pauly. 2018. FishBase Database.
- FWC. 2024. Florida Fish and Wildlife Conservation Commission.
- Gallegos, C. L. 2005. Optical water quality of a blackwater river estuary: the Lower St. Johns River, Florida, USA. Estuarine, Coastal and Shelf Science **63**:57-72.
- Goldberg, N., and T. Trent. 2020. Patterns in submerged aquatic vegetation in the Lower St. Johns River, Florida, from 2001 to 2019. Journal of Aquatic Plant Management **58**:000-000.
- Gowan, T. A., H. H. Edwards, A. M. Krzystan, J. Martin, and J. A. Hostetler. 2023. 2021-2022 Statewide Abundance Estimates for the Florida Manatee. Florida Fish and Wildlife Conservation Commission, Fish and Wildlife Research Institute.
- Harwell, M. C., and K. E. Havens. 2003. Experimental studies on the recovery potential of submerged aquatic vegetation after flooding and desiccation in a large subtropical lake. Aquatic Botany **77**:135-151.
- Hasler-Sheetal, H., and M. Holmer. 2015. Sulfide intrusion and detoxification in the seagrass *Zostera marina*. PloS one **10**:e0129136.
- Hassan-Williams, C., T. H. Bonner, and C. Thomas. 2007. Reproduction, Growth and Food Habits of Seminole Killifish, *Fundulus seminolis*, from Two Central Florida Lakes., Texas State University-San Marcos.
- Haynes, K. E., Idris A.; Fearnhead, Pau. 2017. changepoint.np: Methods for Nonparametric Changepoint Detection. R Package Documentation **2.2**.
- Hendrickson, J., and J. Konwinski. 1998. Seasonal Nutrient Import-Export Budgets for the Lower St. Johns River, Florida. St. Johns River Water Management District.
- Hildebrand, S., and W. C. Schroeder. 1928. Fishes of Chesapeake Bay.
- Hoese, H. D., and R. S. Jones. 1963. Seasonality of larger animals in a Texas turtle grass community.
- Juárez, B., S. A. Stockton, K. A. Serafin, and A. Valle-Levinson. 2022. Compound flooding in a subtropical estuary caused by Hurricane Irma 2017. Geophysical Research Letters **49**:e2022GL099360.
- Kemp, M., R. Batleson, P. Bergstrom, V. Carter, C. L. Gallegos, W. Hunley, L. Karrh, E. W. Koch, J. M. Landwehr, K. A. Moore, L. Murray, M. Naylor, N. B. Rybicki, J. Court Stevenson, and D. J. Wilcox. 2004. Habitat requirements for submerged aquatic

- vegetation in Chesapeake Bay: Water quality, light regime, and physical-chemical factors. *Estuaries* **27**:363-377.
- Kirk, J. T. O. 2010. *Light and Photosynthesis in Aquatic Ecosystems*. 3 edition. Cambridge University Press, Cambridge.
- Koch, M. S., S. A. Schopmeyer, M. Holmer, C. J. Madden, and C. Kyhn-Hansen. 2007. *Thalassia testudinum* response to the interactive stressors hypersalinity, sulfide and hypoxia. *Aquatic Botany* **87**:104-110.
- Lacoul, P., and B. Freedman. 2006. Environmental influences on aquatic plants in freshwater ecosystems. *Environmental Reviews* **14**:89-136.
- Lenth, R. V. 2023. emmeans: Estimated Marginal Means, aka Least-Squares Means. R Package Documentation **1.8.6**.
- Magley, W., and D. Joyner. 2008. Total Maximum Daily Load for Nutrients for the Lower St. Johns River. Florida Department of Environmental Protection.
- Michael Kemp, W., R. Batleson, P. Bergstrom, V. Carter, C. L. Gallegos, W. Hunley, L. Karrh, E. W. Koch, J. M. Landwehr, K. A. Moore, L. Murray, M. Naylor, N. B. Rybicki, J. Court Stevenson, and D. J. Wilcox. 2004. Habitat requirements for submerged aquatic vegetation in Chesapeake Bay: Water quality, light regime, and physical-chemical factors. *Estuaries* **27**:363-377.
- Miller, R. R. 1960. Systematics and biology of the Gizzard Shad (*Dorosoma cepedianum*) and related fishes. U.S. Fish and Wildlife Service.
- Mills, D., and G. Vevers. 1989. *The Tetra encyclopedia of freshwater tropical aquarium fishes*. Tetra Press, New Jersey.
- Montgomery, J. L. M., and T. E. Targett. 1992. The nutritional role of seagrass in the diet of the omnivorous pinfish *Lagodon rhomboides* (L.). *Journal of Experimental Marine Biology and Ecology* **158**:37-57.
- Moore, K. 2012. St. Johns River Water Supply Impact Study Appendix 9.B. Submerged Aquatic Vegetation (SAV) in the Lower St. Johns River and the Influences of Water Quality Factors on SAV., St. Johns River Water Management District.
- Moore, K. A., R. L. Wetzel, and R. J. Orth. 1997. Seasonal pulses of turbidity and their relations to eelgrass (*Zostera marina* L.) survival in an estuary. *Journal of Experimental Marine Biology and Ecology* **215**:115-134.
- Morris, L., and D. Dobberfuhl. 2009. Appendix 9. A. Submerged Aquatic Vegetation Patterns in the Lower St. Johns River Basin. St. Johns River Water Management District.
- Mundahl, N. D. 1991. Sediment processing by gizzard shad, *Dorosoma cepedianum* (Lesueur), in Acton Lake, Ohio, U.S.A. *Journal of Fish Biology* **38**:565-572.
- Murdy, E. O., R. S. Birdsong, and J. A. Musick. 1997. *Fishes of Chesapeake Bay*.
- Nelson, J. A., C. D. Stallings, W. M. Landing, and J. Chanton. 2013. Biomass Transfer Subsidizes Nitrogen to Offshore Food Webs. *Ecosystems* **16**:1130-1138.
- Neundorfer, J. V., and W. M. Kemp. 1993. Nitrogen versus phosphorus enrichment of brackish waters: responses of the submersed plant *Potamogeton perfoliatus* and its associated algal community. *Marine Ecology Progress Series* **94**:71-82.
- Ogren, L. H., and H. A. Brusher. 1977. *The Distribution and Abundance of Fishes Caught with a Trawl in the St. Andrew Bay System, Florida*.
- Olmi, E. 1994. Vertical migration of blue crab *Callinectes sapidus megalopae*: implications for transport in estuaries. *Marine Ecology Progress Series* **113**:39-54.

- Orth, R. J., T. J. B. Carruthers, W. C. Dennison, C. M. Duarte, J. W. Fourqurean, K. L. Heck, A. R. Hughes, G. A. Kendrick, W. J. Kenworthy, and S. Olyarnik. 2006. A global crisis for seagrass ecosystems. *Bioscience* **56**:987-996.
- Page, L. M., and B. M. Burr. 2011. *Peterson Field Guide to Freshwater Fishes of North America North of Mexico*. Houghton Mifflin Harcourt.
- Pattillo, M. E., T. E. Czapla, D. M. Nelson, and M. E. Monaco. 1997. Distribution and abundance of fishes and invertebrates in Gulf of Mexico estuaries, Volume II: Species life history summaries.
- R Development Core Team. R: A Language and Environment for Statistical Computing. R Foundation for Statistical Computing, Vienna, Austria.
- R Development Core Team. 2010. R: A language and environment for statistical computing. R Foundation for Statistical Computing, Vienna, Austria.
- Rigby, R. A., and D. M. Stasinopoulos. 2005. Generalized additive models for location scale and shape (GAMLSS). *Journal of the Royal Statistical Society: Series C (Applied Statistics)* **54**:507-554.
- Robins, R. H. 2018. Fishes in the Fresh Waters of Florida: An Identification Guide and Atlas Fisheries **44**:552-552.
- Rohde, F. C., R. G. Arndt, D. G. Lindquist, and J. F. Parnell. 1994. *Freshwater fishes of the Carolinas, Virginia, and Delaware*. University of North Carolina Press, Chapel Hill, NC.
- Rout, N. P., and B. P. Shaw. 2001. Salt Tolerance in Aquatic Macrophytes: Ionic Relation and Interaction. *Biologia Plantarum* **44**:95-99.
- Rydene, D., and R. Matheson. 2003. Diurnal Fish Density in Relation to Seagrass and Drift Algae Cover in Tampa Bay, Florida. *Gulf of Mexico Science* **21**:35-58.
- Sagan, J. J. 2002. Distribution of submerged aquatic vegetation within the St. Johns River estuary, North Florida, U.S.A., St. Johns River Water Management District, Palatka, FL.
- Sagan, J. J. 2003. Assessment of Littoral Zone Periphyton Biomass in the Lower St. Johns River: A Pilot Study. A report for the St. Johns River Water Management District. . St. Johns River Water Management District.
- Sagan, J. J. 2007a. SAV Monitoring Project: Interim Reports I–V. Interim reports associated with quarterly sampling and groundtruth surveys for the St. Johns River Water Management District. Palatka, FL.
- Sagan, J. J. 2007b. A summary of submerged aquatic vegetation (SAV) status within the lower St. Johns River: 1996–2007. Report prepared for: St. Johns River Water Management District, Palatka, Florida.
- Sagan, J. J. 2009. A summary of submerged aquatic vegetation (SAV) status within the lower St. Johns River: 1996–2007. St. Johns River Water Management District, Palatka, FL.
- Smith, K. N. 1993. *Manatee Habitat and Human-related Threats to Seagrass in Florida: A Review*. Florida Department of Environmental Protection.
- Steele, P., and T. Bert. 1994. Population ecology of the blue crab, *Callinectes sapidus* Rathbun, in a subtropical estuary: Population structure, aspects of reproduction, and habitat partitioning. 1-24.
- Stevenson, J. C., and N. M. Confer. 1978. *Summary of Available Information on Chesapeake Bay Submerged Vegetation*. U.S. Fish and Wildlife Service.

- Stoner, A. 1980. Feeding ecology of *Lagodon rhomboides* (Pisces, Sparidae): Variation and Functional responses. *Fishery Bulletin- National Oceanic and Atmospheric Administration* **78**:337-352.
- Takoukam, A. K., D. G. E. Gomes, M. V. Hoyer, L. W. Keith-Diagne, R. K. Bonde, and R. Francis-Floyd. 2021. African manatee (*Trichechus senegalensis*) habitat suitability at Lake Ossa, Cameroon, using trophic state models and predictions of submerged aquatic vegetation. *Ecology and Evolution* **11**:15212-15224.
- Tankersley, R., M. Cl, M. Sigala, and K. Kachurak. 1998. Migratory Behavior of Ovigerous Blue Crabs *Callinectes sapidus*: Evidence for Selective Tidal-Stream Transport. *Biological Bulletin* **195**.
- Timbs, R., and D. Kolterman. 2023. Herbivory impacts *Vallisneria americana* recovery in the lower St. Johns River, Florida. *Journal of Aquatic Plant Management* **61**:63-65.
- Timbs, R., and S. Russo. 2023. Lower St. Johns River SAV Dashboard. St Johns River Water Management District.
- Verdi, R. J., S. A. Tomlinson, and R. L. Marella. 2006. Drought of 1998-2002: impacts on Florida's hydrology and landscape. Report 1295.
- Weinstein, M. P., J. K. L. Heck, P. E. Giebel, and J. E. Gates. 1982. The Role of Herbivory in Pinfish (*Lagodon Rhomboides*): A Preliminary Investigation. *Bulletin of Marine Science* **32**:791-795.
- White, A. Q., G. F. Pinto, and A. P. Robison. 2002. Seasonal distribution of manatees, *Trichechus manatus latirostris*, in Duval County and adjacent waters, Northeast Florida. *Florida Scientist* **65**:208-221.
- Whitehead, P. J. P. 1985. *FAO Species Catalogue. Vol. 7. Clupeoid fishes of the world (suborder Clupeoidei). An annotated and illustrated catalogue of the herrings, sardines, pilchards, sprats, shads, anchovies and wolf-herrings.*
- Williams, A. B. 1984. *Shrimps, Lobsters, and Crabs of the Atlantic Coast of the Eastern United States, Maine to Florida.* Smithsonian Institution Press.
- Wolcott, D. L., and M. C. d. Vries. 1994. Offshore megalopae of *Callinectes sapidus*: depth of collection, molt stage and response to estuarine cues. *Marine Ecology Progress Series* **109**:157-163.
- Wuellner, M., B. D. S. Graeb, M. Ward, and D. W. Willis. 2008. Review of gizzard shad population dynamics at the northwestern edge of its range. *Balancing fisheries management and water uses for impounded river systems*:637-653.
- Young, D. K., and M. W. Young. 1977. *Community structure of the macrobenthos associated with seagrass of the Indian River estuary, Florida.* University of South Carolina Press.
- Zimmerman, R. C. 2003. A biooptical model of irradiance distribution and photosynthesis in seagrass canopies. *Limnology and Oceanography* **48**:568-585.